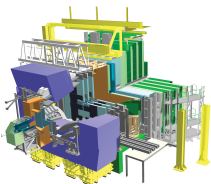


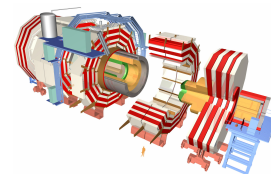
The Upgrade Programme of the LHC Detectors

CERN Academic Training Lectures 3/3

Werner Riegler, CERN



W. Riegler, CERN



Outline

Lecture 1: Overview of experiment and machine goals,
some overall numbers and facts

Lecture 2: LHCb and CMS upgrade plans,
with excursion into DAQ/Trigger and photon detectors

Lecture 3: ALICE and ATLAS upgrade plans,
with excursions into Silicon and Micropattern Gas Detectors

Bonus: Brainstorming on detectors for a FHC (100TeV)

Excursion to Silicon Detectors

Thanks to Petra Riedler

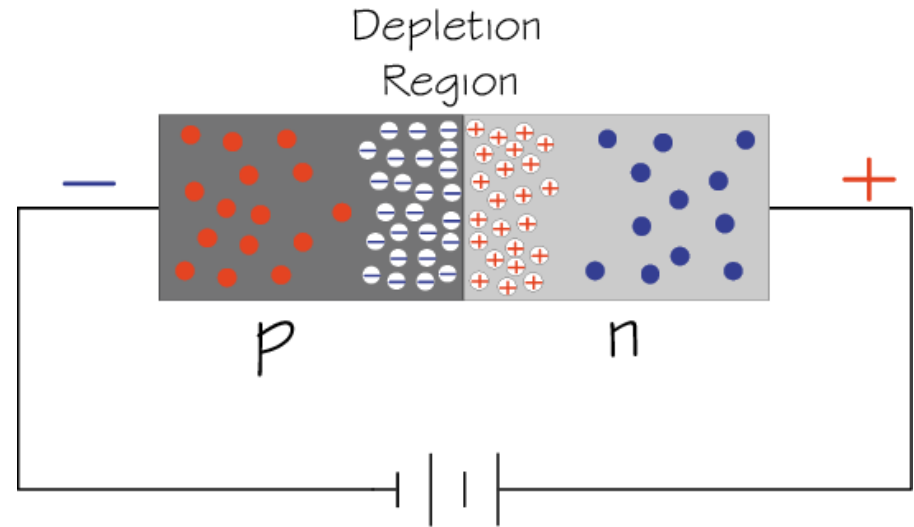
Si-Diode used as a Particle Detector

At the p-n junction the charges are depleted and a zone free of charge carriers is established.

By applying a voltage, the depletion zone can be extended to the entire diode → highly insulating layer.

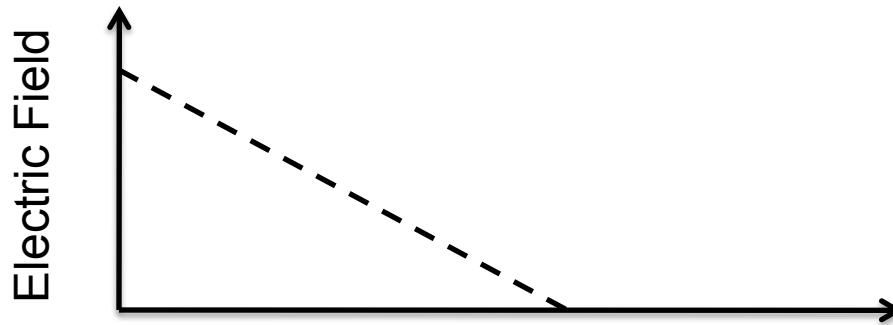
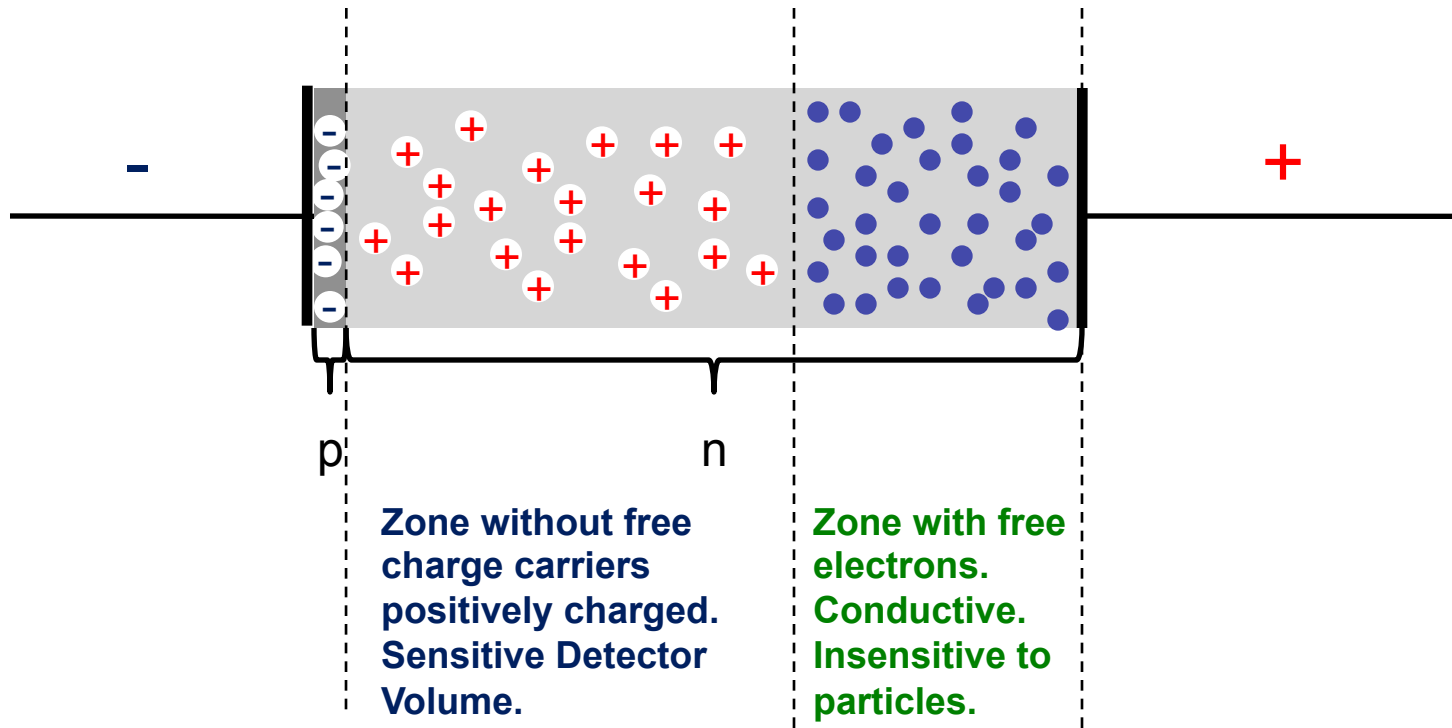
An ionizing particle produces free charge carriers in the diode, which drift in the electric field and induce an electrical signal on the metal electrodes.

As silicon is the most commonly used material in the electronics industry, it has one big advantage with respect to other materials, namely highly developed technology.

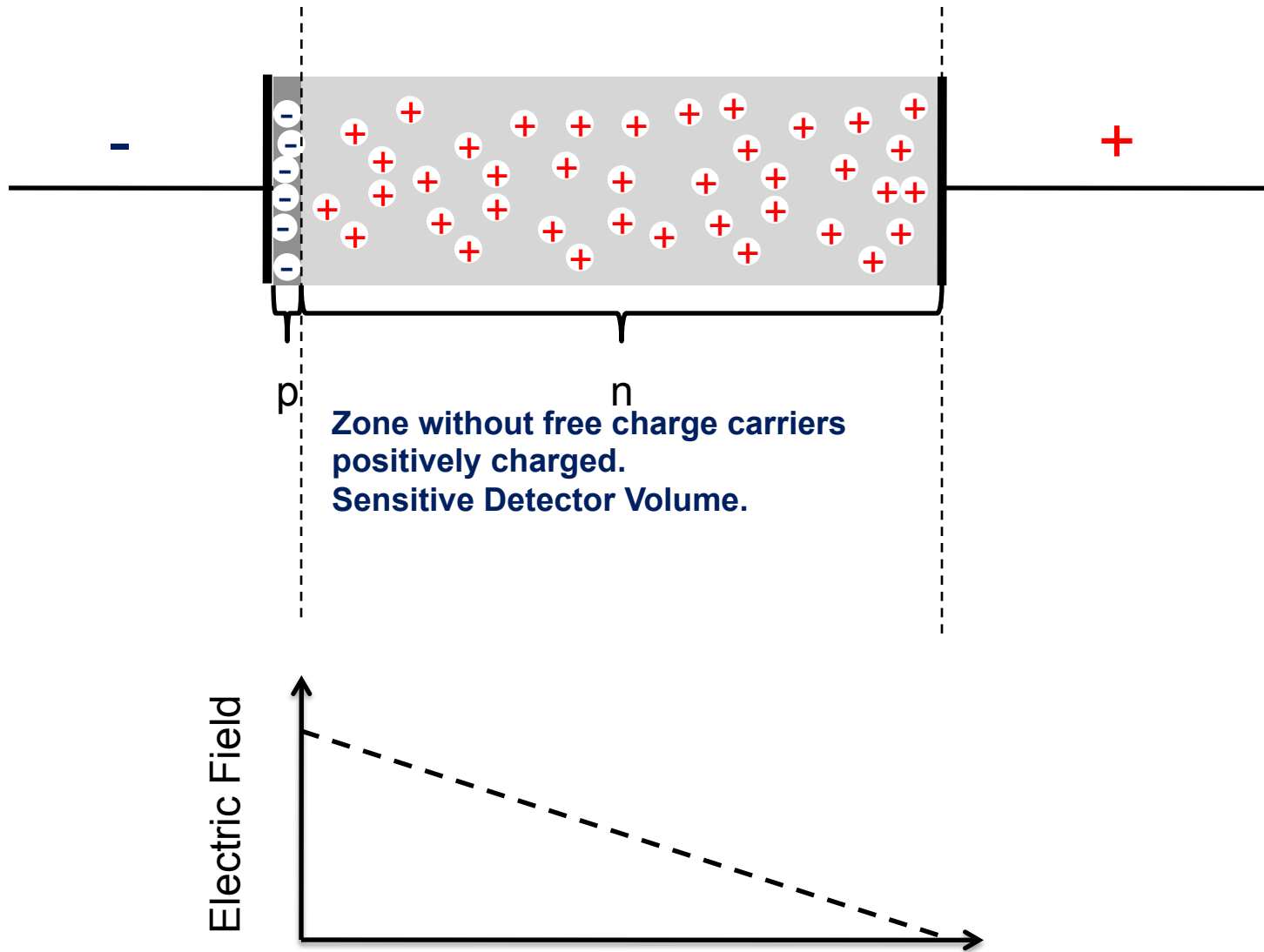


- Electron
- ⊕ Positive ion from removal of electron in n-type impurity
- ⊖ Negative ion from filling in p-type vacancy
- Hole

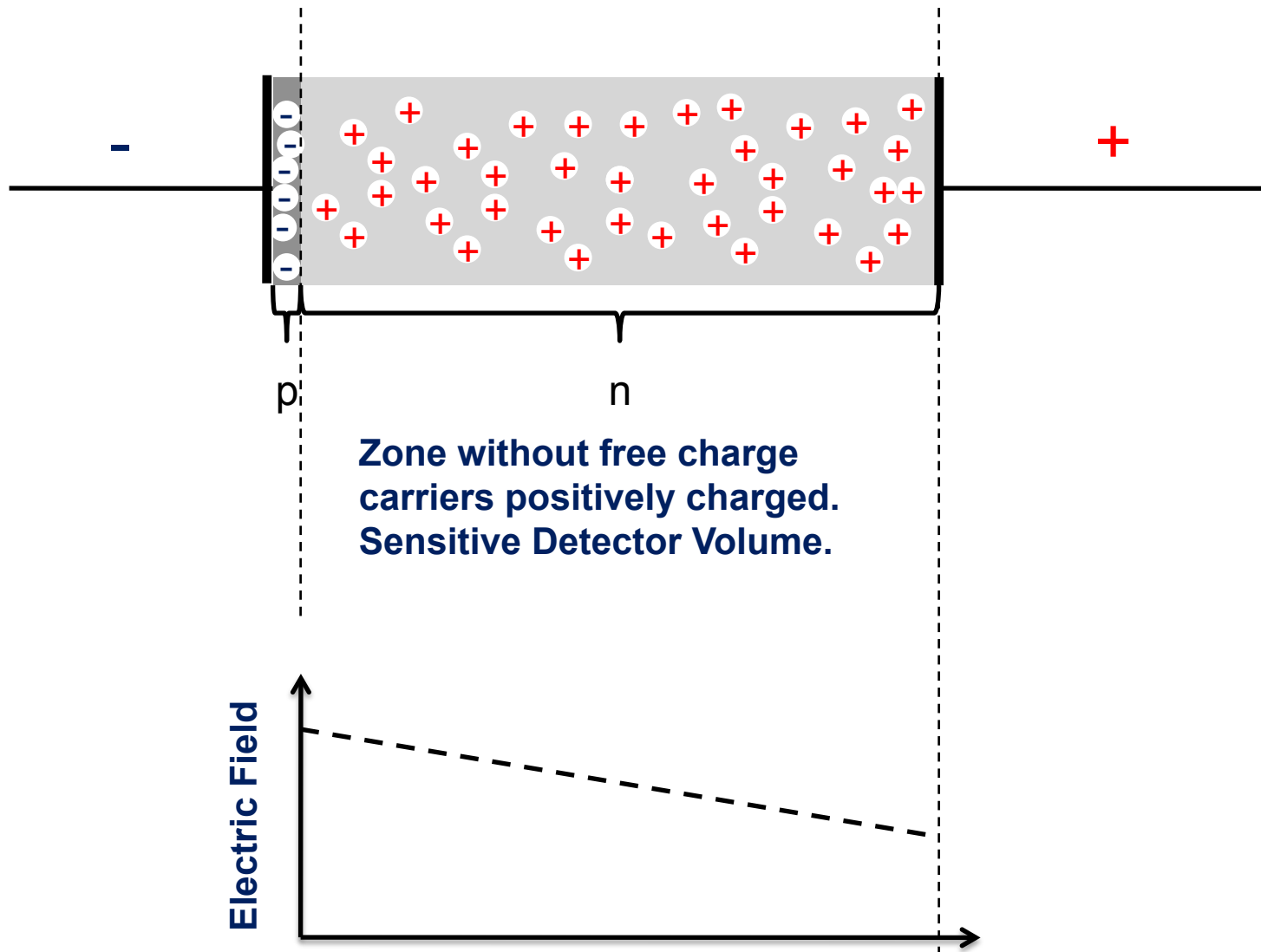
Under-Depleted Silicon Detector



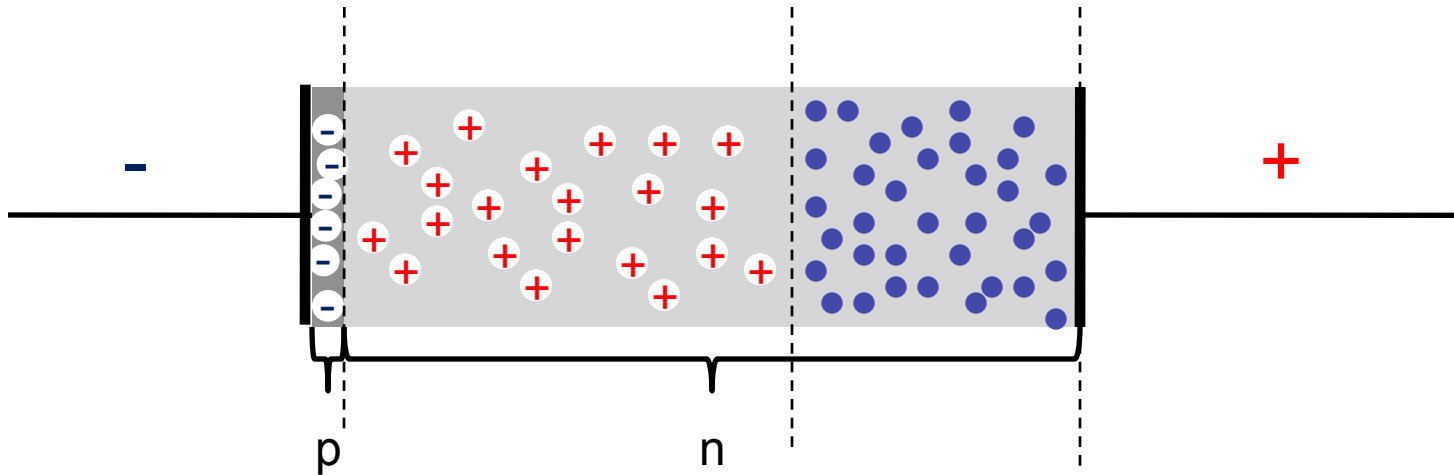
Fully-Depleted Silicon Detector



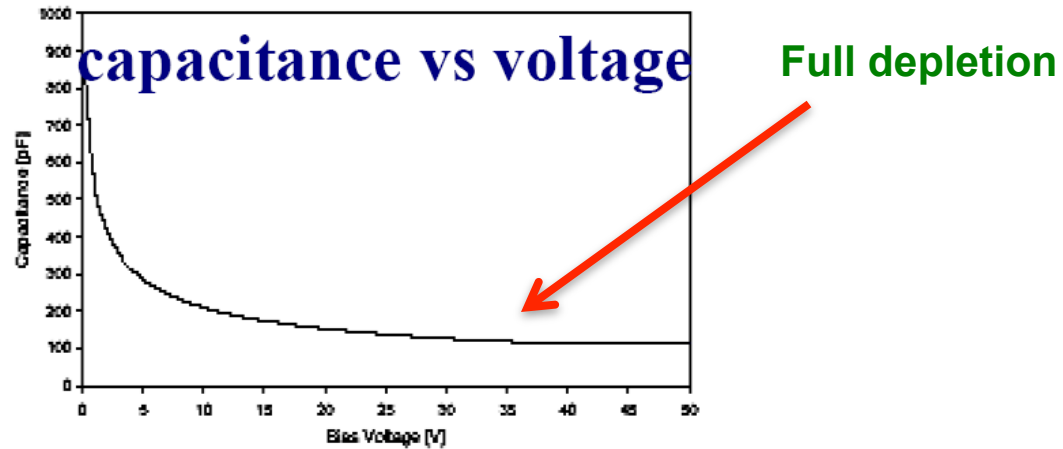
Over-Depleted Silicon Detector



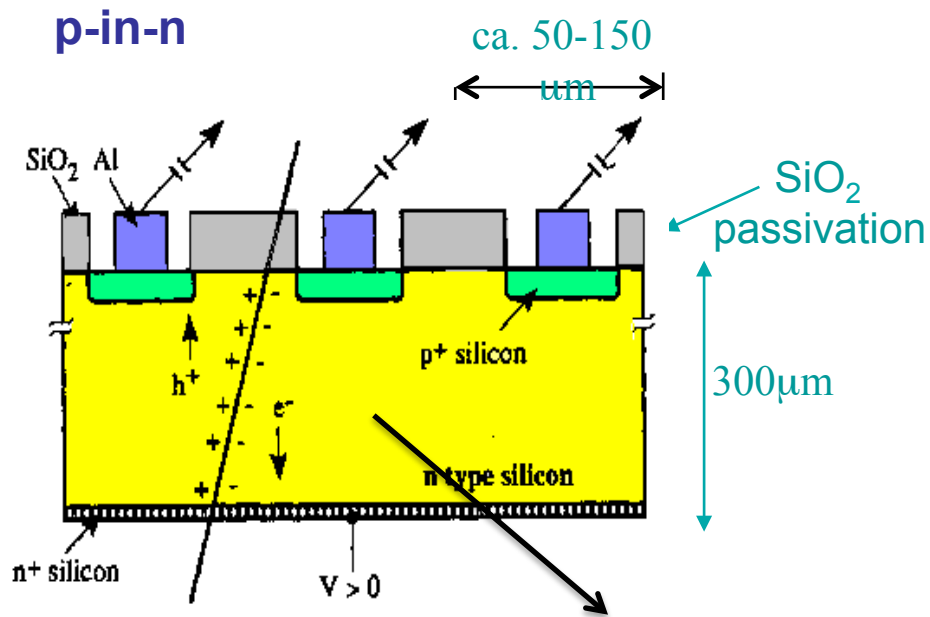
Depletion Voltage



The capacitance of the detector decreases as the depletion zone increases.



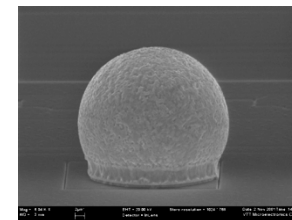
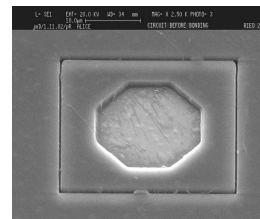
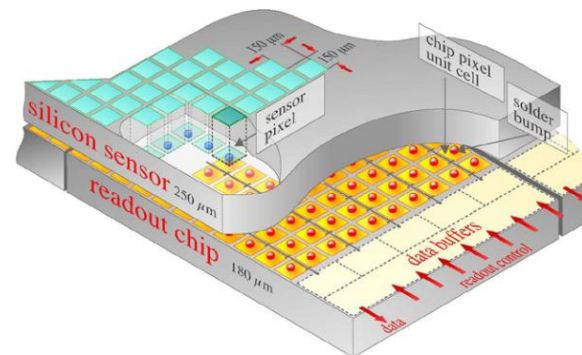
Silicon Sensor



Fully depleted zone

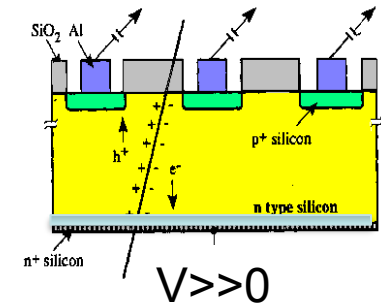
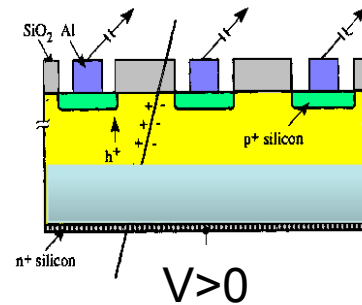
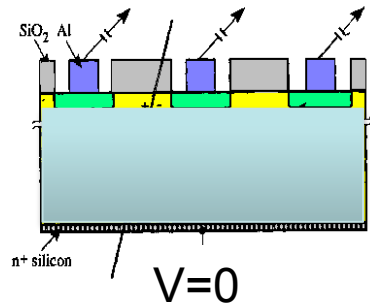
N (e-h) = 11 000/100 μm

Position Resolution down to ~ 5 μm !



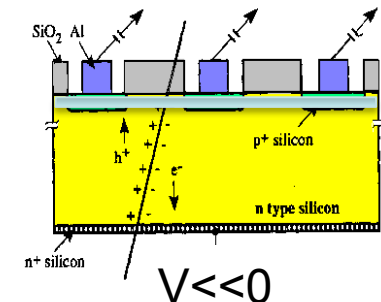
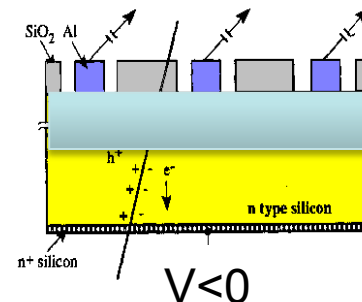
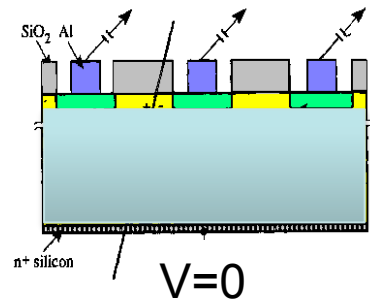
Silicon Sensor before Irradiation

p(strips)-in-n



→ depletion grows from the segmented side

n(strips)-in-p



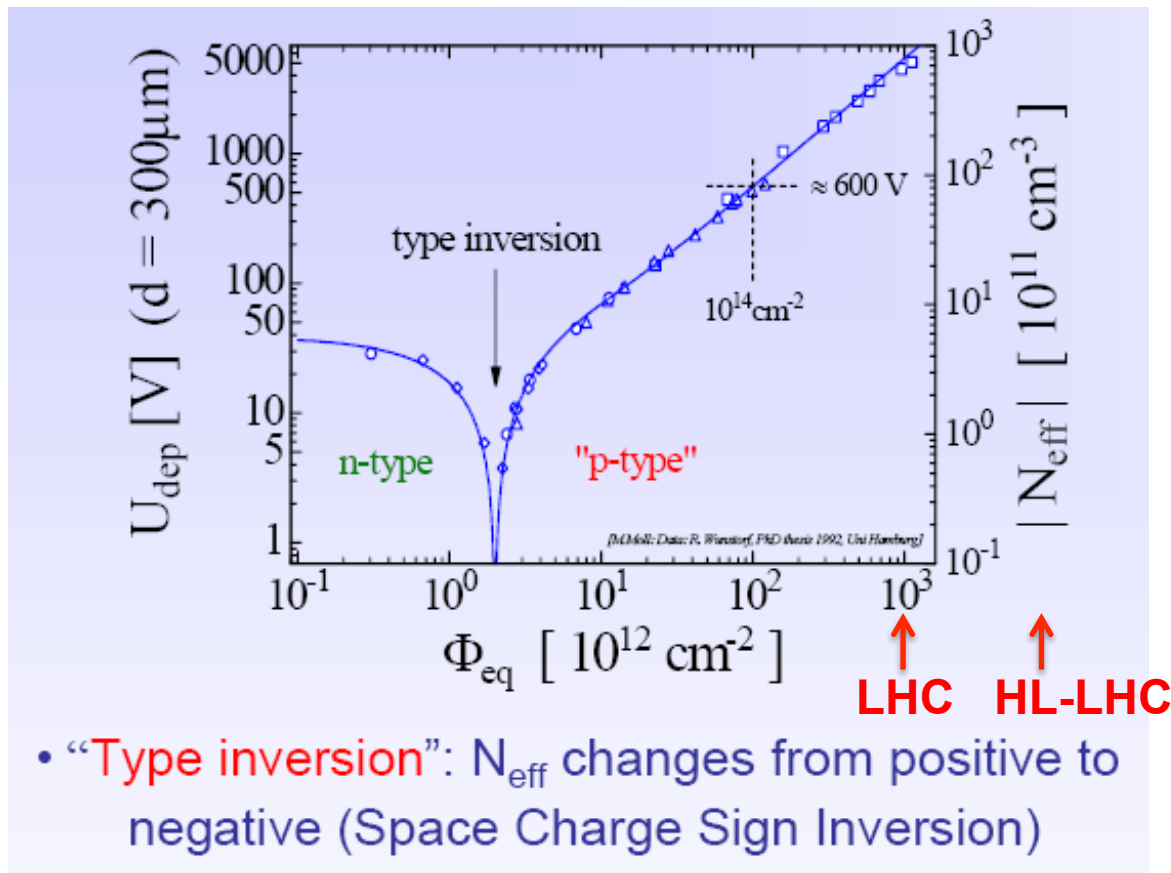
- depletion grows from the un-segmented side
- This detector does not work properly unless it is fully depleted.
- For partial depletion the ,charge collection' is very inefficient and the ,cluster size' is increasing.

Radiation Effects, Type Inversion

Type inversion ! An n-type Si detector becomes a p-type Si detector !

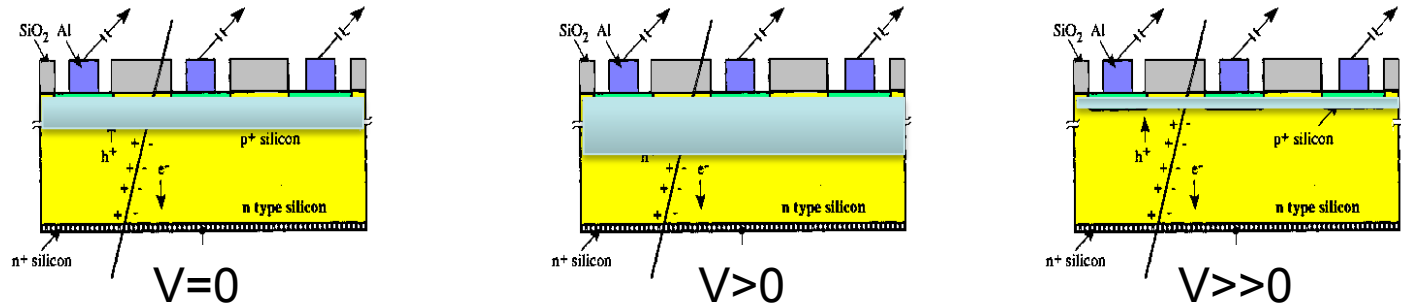
More voltage is needed to fully deplete the detector.

It might happen that the full depletion voltage becomes larger than the breakdown voltage
→ have to work in under depleted regime.



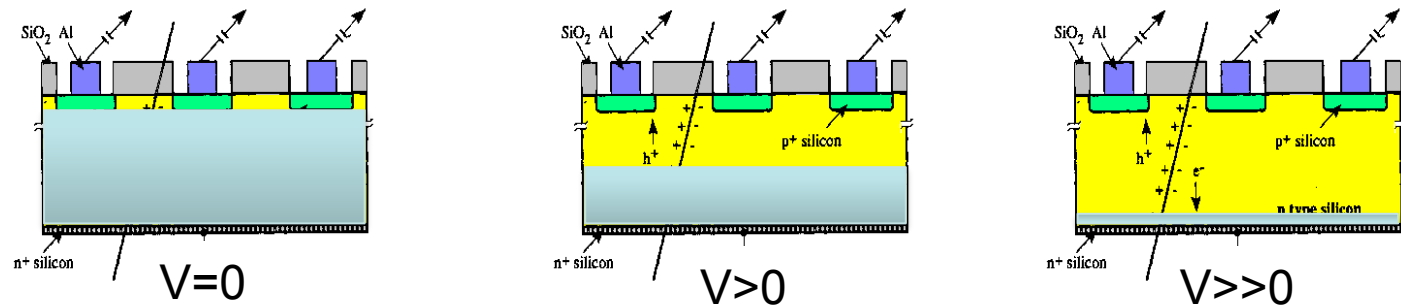
Silicon Sensor after Irradiation and type inversion

p(strips)-in-n



→ depletion grows now from the unsegmented side !

n(strips)-in-p



- depletion now grows from the segmented side
- Can work in under depleted mode

For high radiation environment, where one might not reach full depletion after some time, n-in-p detectors are preferred.

Until recently, p-bulk material was not available in a quality that is sufficient for these detectors. n⁺-in-n strips were used were therefore used up to now for high radiation environment. Additional complication for n⁺-in-n: mask processing on both sensor sides.

n^+ -in-n and p-in-n sensors

double sided processing

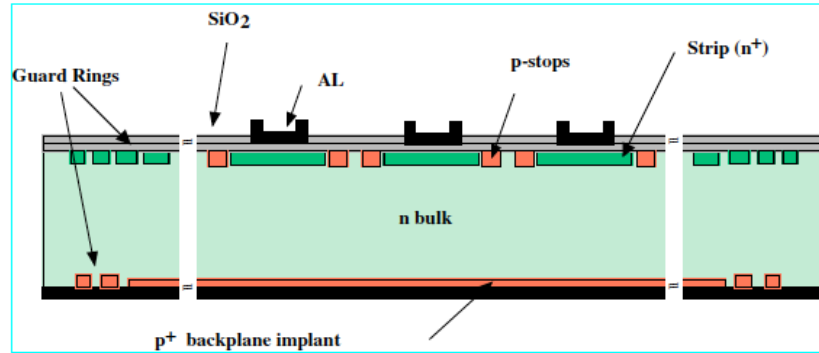


Figure 3.10: Schematic cross section of a n-in-n detector.

single sided processing

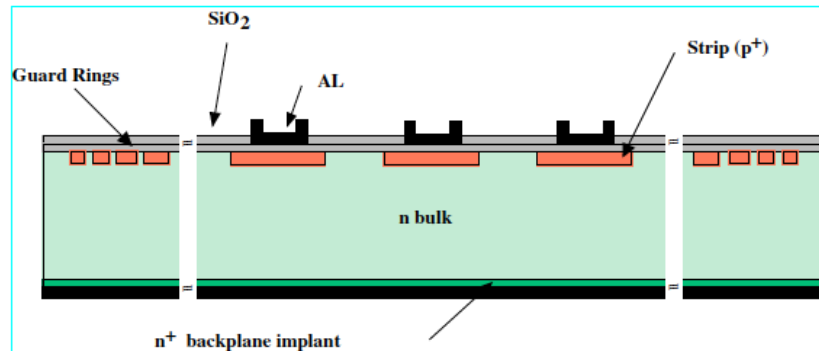


Figure 3.11: Schematic cross section of a p-in-n detector.

from P. Riedler

Radiation Effects 'Aging'

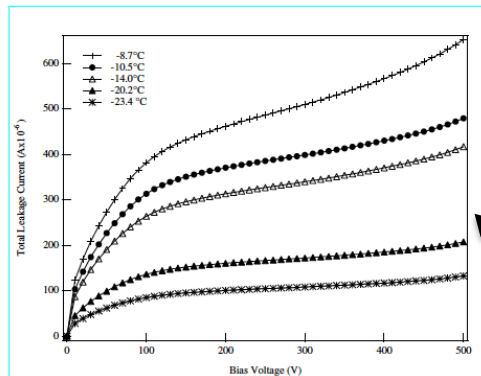
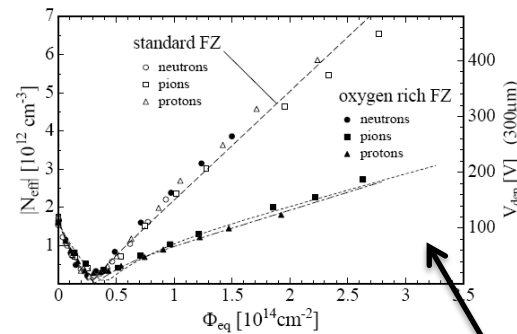
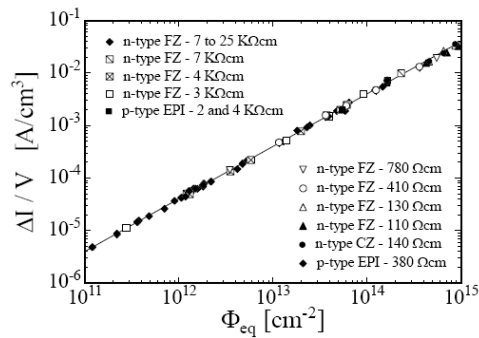
- Two general types of radiation damage
 - "Bulk" damage due to physical impact within the crystal
 - "Surface" damage in the oxide or Si/SiO₂ interface
- Cumulative effects
 - Increased leakage current (increased shot noise)
 - Silicon bulk type inversion (n-type to p-type)
 - Increased depletion voltage
 - Increased capacitance
- Sensors can fail from radiation damage
 - Noise too high to effectively operate
 - Depletion voltage too high to deplete
 - Loss of inter-strip isolation (charge spreading)
- Signal/noise ratio is the quantity to watch

Radiation Effects 'Aging'

Increase of leakage current

Increase of depletion voltage

Decrease of charge collection efficiency due to under-depletion and charge trapping.



Use silicon material engineering to limit radiation damage

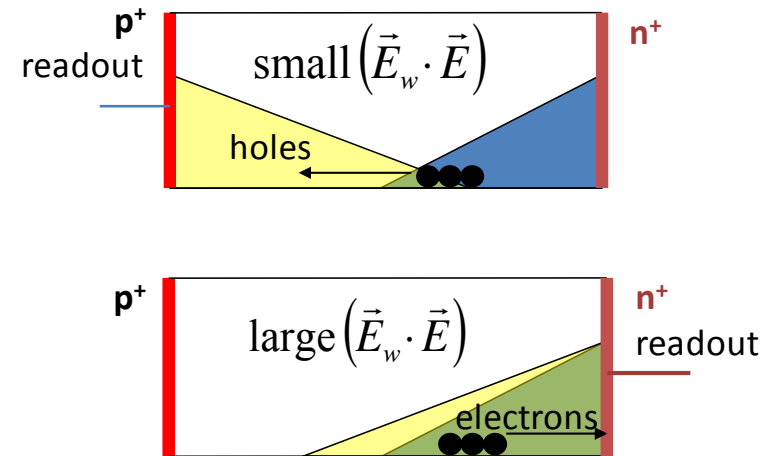
Use cooling to decrease leakage current (approx. factor two every 8 degrees)

from P. Riedler

Figure 3.17: I-V curve of detector Wedge 12-1 at various temperatures after 12 days at 25 °C.

Sensor Technology in Present Experiments

- p-in-n, n-in-p (**single sided process**)
- n-in-n (**double sided process**)
- Choice of sensor technology mainly driven by the **radiation environment**



G. Kramberger, Vertex 2012

	Fluence 1MeV n_{eq} [cm ⁻²]	Sensor type
ATLAS Pixel*	1×10^{15}	n-in-n
ATLAS Strips	2×10^{14}	p-in-n
CMS Pixels	3×10^{15}	n-in-n
CMS Strips	1.6×10^{14}	p-in-n
LHCb VELO	$1.3 \times 10^{14**}$	n-in-n, n-in-p
ALICE Pixel	1×10^{13}	p-in-n
ALICE Drift	1.5×10^{12}	p-in-n
ALICE Strips	1.5×10^{12}	p-in-n

n-side readout (n-in-n, n-in-p):

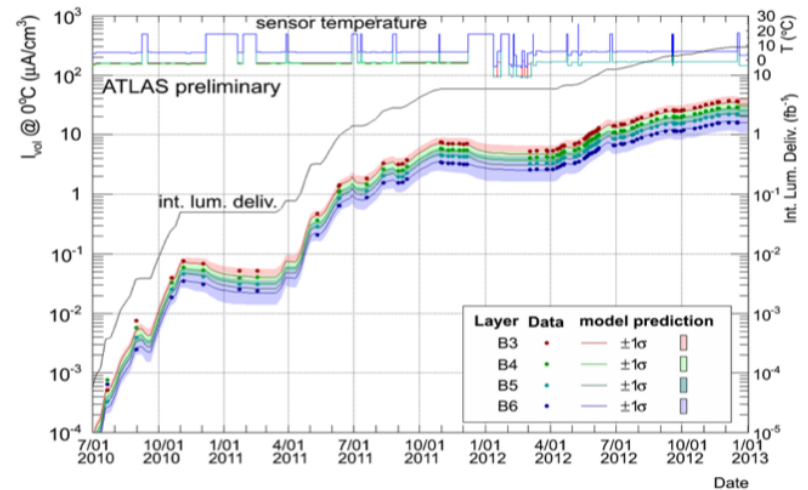
- Depletion from segmented side (under-depleted operation possible)
- Electron collection
- Favorable combination of weighting field and
- Natural for p-type material

** per year

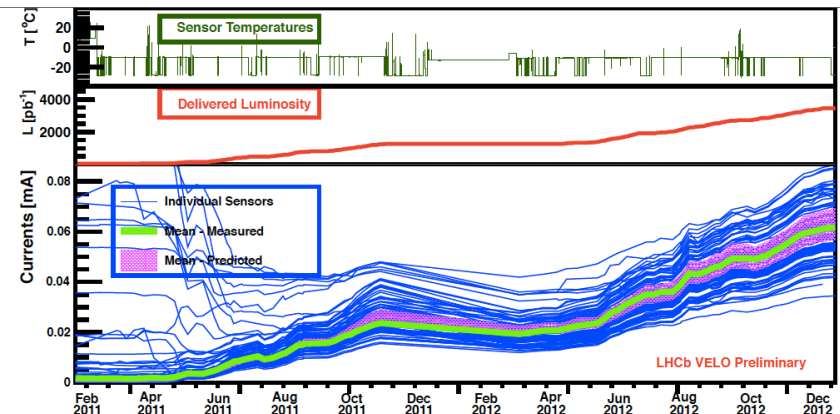
Radiation Damage Effects in Sensors

- Effects observed in ATLAS, CMS and LHCb (lower luminosity in ALICE)
- **Main challenge for the sensors is an increase in leakage current:**
 - Risk of thermal runaway -detector becomes inoperable
 - Operate sensors at low temperatures (see talk by B. Verlaet)
 - Increase in shot noise - degraded performance
- Leakage current increases with integrated luminosity in agreement with the predictions
- **Further effects:**
 - Sensor depletion voltage changes with radiation damage
 - Loss of signal due to radiation induced damage

Leakage current vs. integrated luminosity (examples)



Excellent agreement over 4 orders of magnitude, need a good knowledge of inputs ($L, flux, T$).

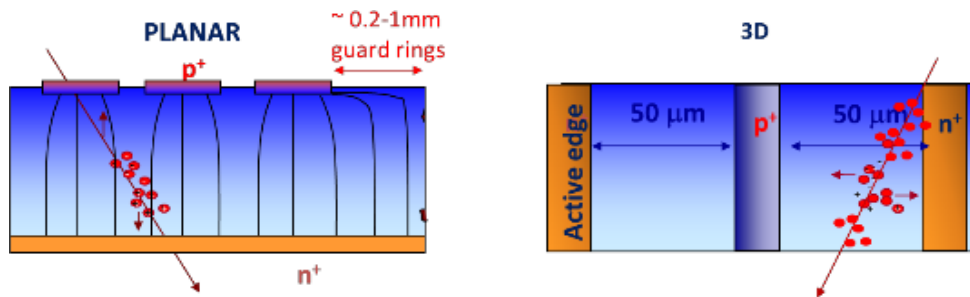


ATLAS SCT Barrel
H. Pernegger, LHCp 2013

LHCb VELO
H. Snoek, Hiroshima 2013

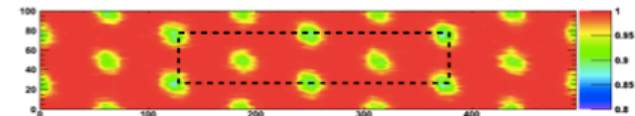
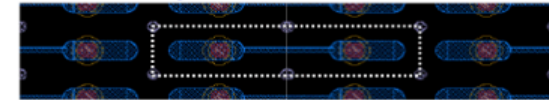
Effects will increase for HL-LHC

3D Sensors

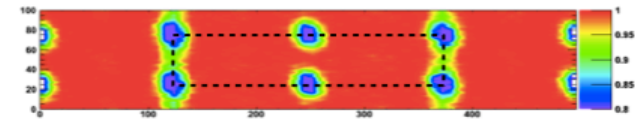


- **Both electrode types are processed inside the detector bulk**
- Max. drift and depletion distance set by electrode spacing - **reduced collection time and depletion voltage**
- **Very good performance at high fluences**
- Production time and complexity to be investigated for larger scale production
- Used in ATLAS IBL

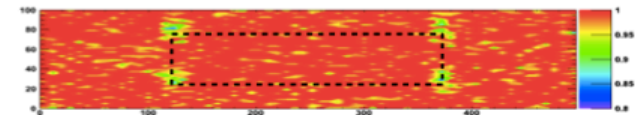
3D pixel sensors



SCC105 FBK-3D, un-irrad, HV=20V, Eff.=98.77%



SCC81 CNM-3D, n-irrad HV=160V, Eff.=97.46%



SCC34 CNM-3D, p-irrad, HV = 160V, Eff.=98.96%

ATLAS IBL Sensor (Threshold: 1600 e
 proton-irrad: $5 \times 10^{15} n_{eq}/cm^2$ with 24 MeV protons
 neutron-irrad: $5 \times 10^{15} n_{eq}/cm^2$ by nuclear reactor)

From: *Prototype ATLAS IBL Modules using the FE-I4A Front-End Readout Chip"*
 (JINST 7 (2012) P11010)

Key Sensor Issues for the Upgrades

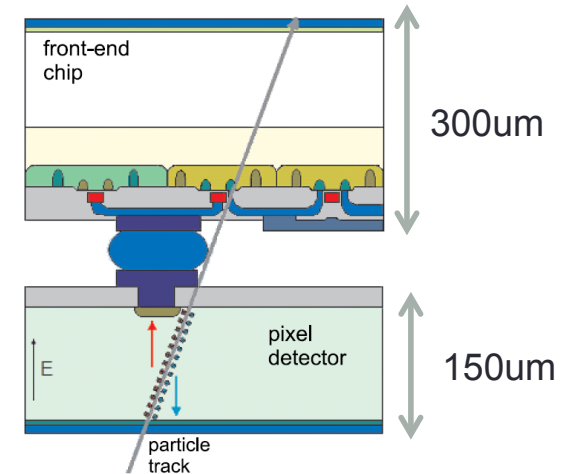
- **Radiation damage** will increase to several $10^{16} n_{eq} cm^{-2}$ for the inner regions in ATLAS and CMS
 - Example of common activities to develop radiation harder sensors within the RD50 collaboration
 - Operational requirements more demanding (low temperature and all related system aspects)
- **Increased performance:**
 - Higher granularity
 - Lower material budget
- **Control and minimize cost**
 - Large areas
 - Stable and timely production

Upgrades	Area	Baseline sensor type
ALICE ITS	10.3 m ²	CMOS
ATLAS Pixel	8.2 m ²	<i>tbd</i>
ATLAS Strips	193 m ²	n-in-p
CMS Pixel	4.6 m ²	<i>tbd</i>
CMS Strips	218 m ²	n-in-p
LHCb VELO	0.15 m ²	<i>tbd</i>
LHCb UT	5 m ²	<u>n-in-p</u>

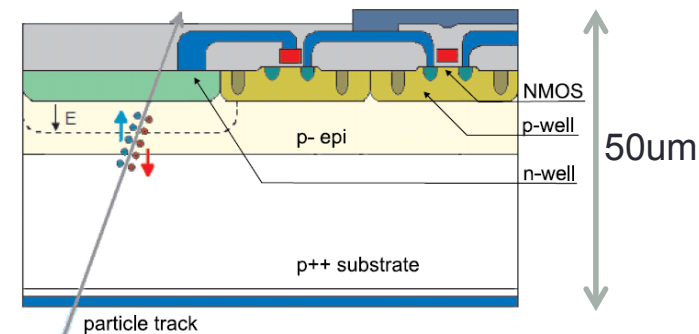
CMOS Sensors

- CMOS sensors **contain sensor and electronics combined in one chip**
 - No interconnection between sensor and chip needed
- Standard CMOS processing
 - Wafer diameter (8")
 - Many foundries available
 - Lower cost per area
 - Small cell size – high granularity
 - Possibility of stitching (combining reticles to larger areas)
- Very low material budget
- CMOS sensors installed in STAR experiment
- Baseline for ALICE ITS upgrade (and MFT, LOI submitted to LHCC)

Hybrid Pixel Detector



CMOS (Pixel) Detector



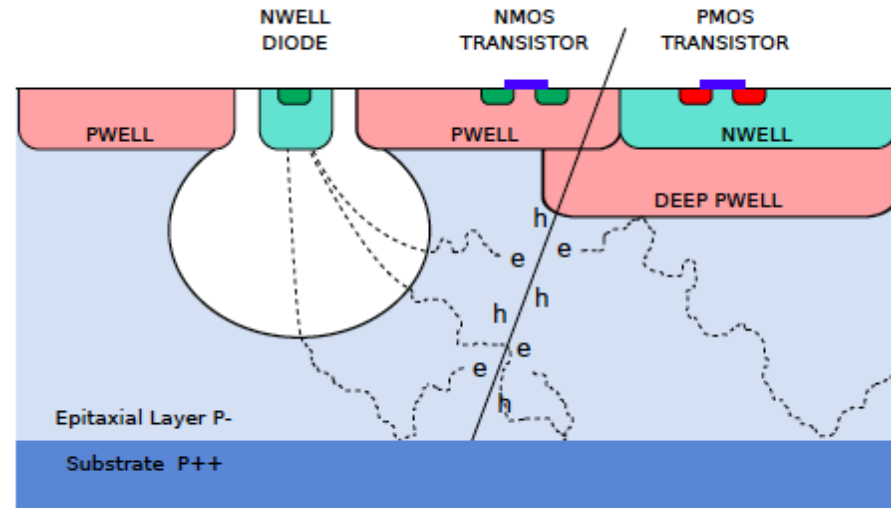
PIXEL Chip - technology

Monolithic PIXEL chip using Tower/Jazz 0.18 μm technology

- feature size 180 nm
- gate oxide < 4nm
- metal layers 6
- high resistivity epi-layer
 - thickness 18-40 μm
 - resistivity 1-6 $\text{k}\Omega\times\text{cm}$
- “special” deep p-well layer to shield PMOS transistors (allows in-pixel truly CMOS circuitry)
- Possibility to build single-die circuit larger than reticle size

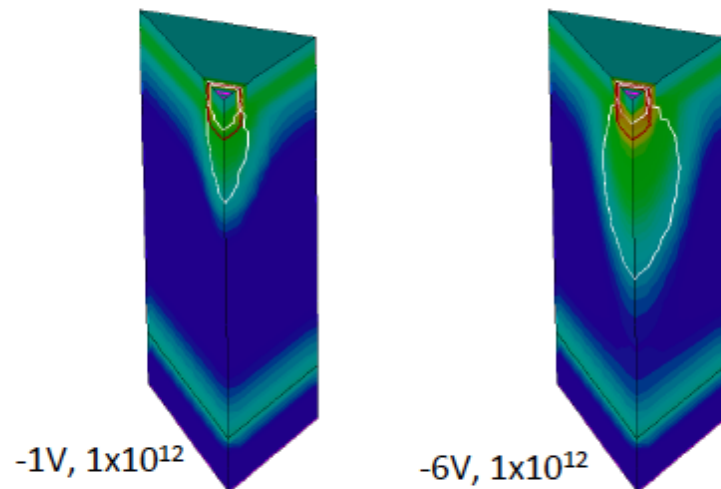
Radiation Resistance (< 10^{13} neq/cm², < 10kGy) and charge collection time (> \approx microseconds) do for the moment not allow application in high rate environments of ATLAS, CMS, LHCb.

But ! Stay tuned for developments in the near future.



Schematic cross-section of CMOS pixel sensor (ALICE ITS Upgrade TDR)

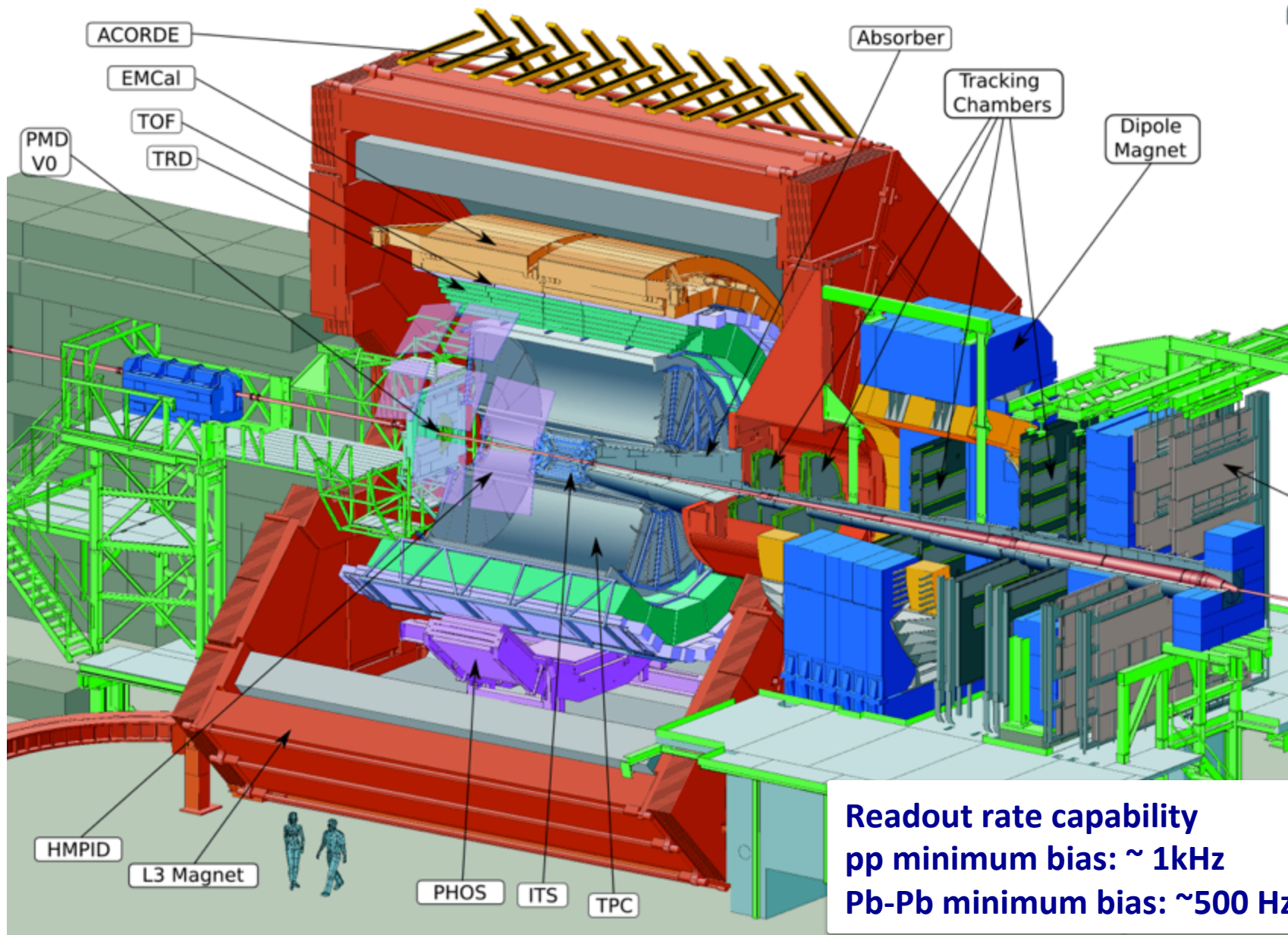
TCAD simulation of total diode reverse bias (ALICE ITS Upgrade TDR)



diode 3 μm x 3 μm square n-well with 0.5 μm spacing to p-well white line: boundaries of depletion region

The ALICE Experiment upgrade

The Current ALICE Detector



ALICE Upgrade Strategy

High precision measurements of rare probes at low p_T , which cannot be selected with a trigger, require a large sample of events recorded on tape

Target

- Pb-Pb recorded luminosity $\geq 10 \text{ nb}^{-1} \rightarrow 8 \times 10^{10} \text{ events}$
- pp (@5.5 Tev) recorded luminosity $\geq 6 \text{ pb}^{-1} \rightarrow 1.4 \times 10^{11} \text{ events}$

Gain a factor **100** in statistics over approved programme

... and significant improvement of vertexing and tracking capabilities

I. Upgrade the ALICE readout systems and online systems to

- read out all Pb-Pb interactions at a maximum rate of 50kHz (i.e. $L = 6 \times 10^{27} \text{ cm}^{-1}\text{s}^{-1}$), with a minimum bias trigger
- Perform **online data reduction** based on reconstruction of clusters and tracks (tracking used only to filter out clusters not associated to reconstructed tracks)

II. Improve vertexing and tracking at low $p_T \rightarrow$ NEW ITS

ALICE Upgrade Strategy, cont'd.

- The upgrade plans entails building

- New, high-resolution, low-material ITS
- Upgrade of TPC with replacement of MWPCs with GEMs and new pipelined readout electronics
- Upgrade of readout electronics of: TRD, TOF, Muon Spectrometer, ZDC
- Upgrade of the forward trigger detectors
- Upgrade of the online systems
- Upgrade of the offline reconstruction and analysis framework

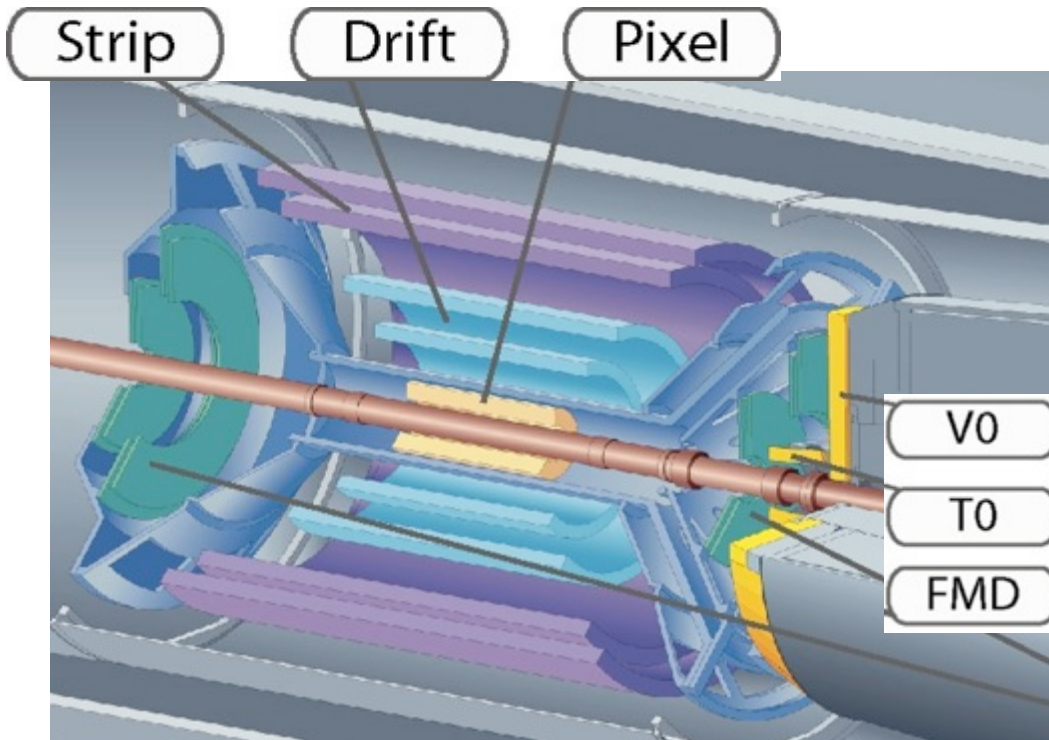
- New 5-plane silicon telescope in front of the hadron absorber covering the acceptance of the Muon Spectrometer

LoI approved
in 2012

Add. LoI
Sep 2013

- It targets 2018/19 (LHC 2nd Long Shutdown)

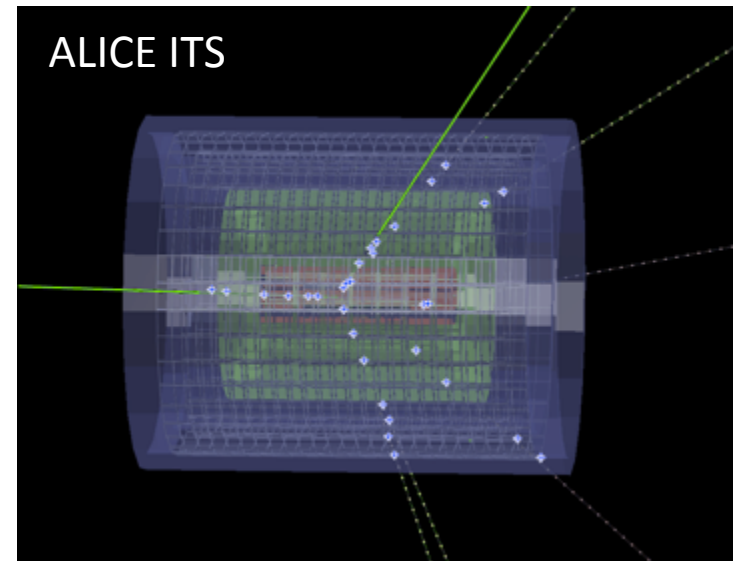
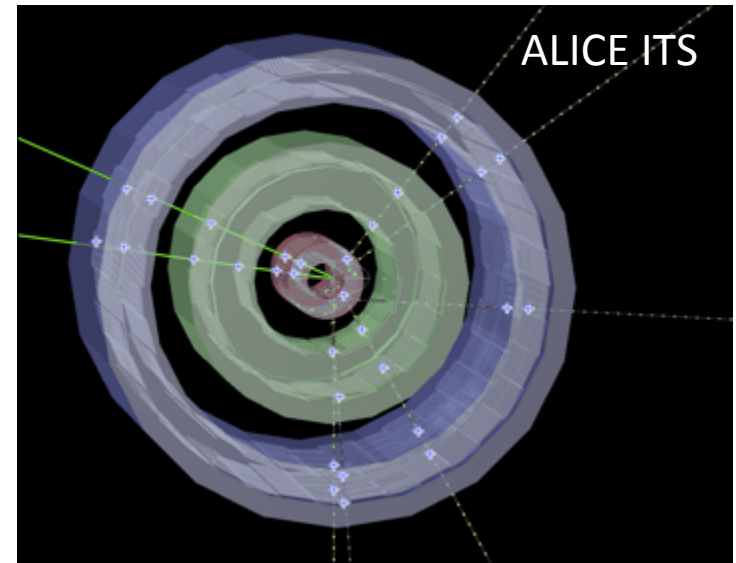
The Current ALICE Inner Tracking System



Current ITS

6 concentric barrels, 3 different technologies

- 2 layers of silicon pixel (SPD)
- 2 layers of silicon drift (SDD)
- 2 layers of silicon strips (SSD)



New ITS Design goals



1. Improve impact parameter resolution by a factor of ~ 3

- Get closer to IP (position of first layer): 39mm \rightarrow 22mm
- Reduce material budget: X/X_0 /layer: $\sim 1.14\%$ \rightarrow $\sim 0.3\%$ (for inner layers)
- Reduce pixel size
 - currently $50\mu\text{m} \times 425\mu\text{m}$
monolithic pixels \rightarrow $O(20\mu\text{m} \times 20\mu\text{m})$,

2. Improve tracking efficiency and p_T resolution at low p_T

- Increase granularity: 6 layers \rightarrow 7 layers , reduce pixel size

3. Fast readout

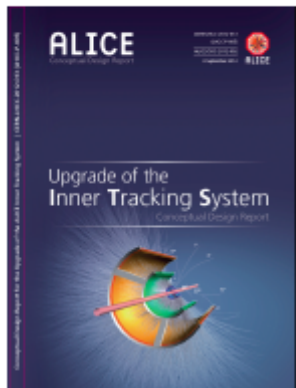
- readout of Pb-Pb interactions at > 50 kHz and pp interactions at ~ 1 MHz

4. Fast insertion/removal for yearly maintenance

- possibility to replace non functioning detector modules during yearly shutdown

New ITS Layout

25 G-pixel camera
(10.3 m²)

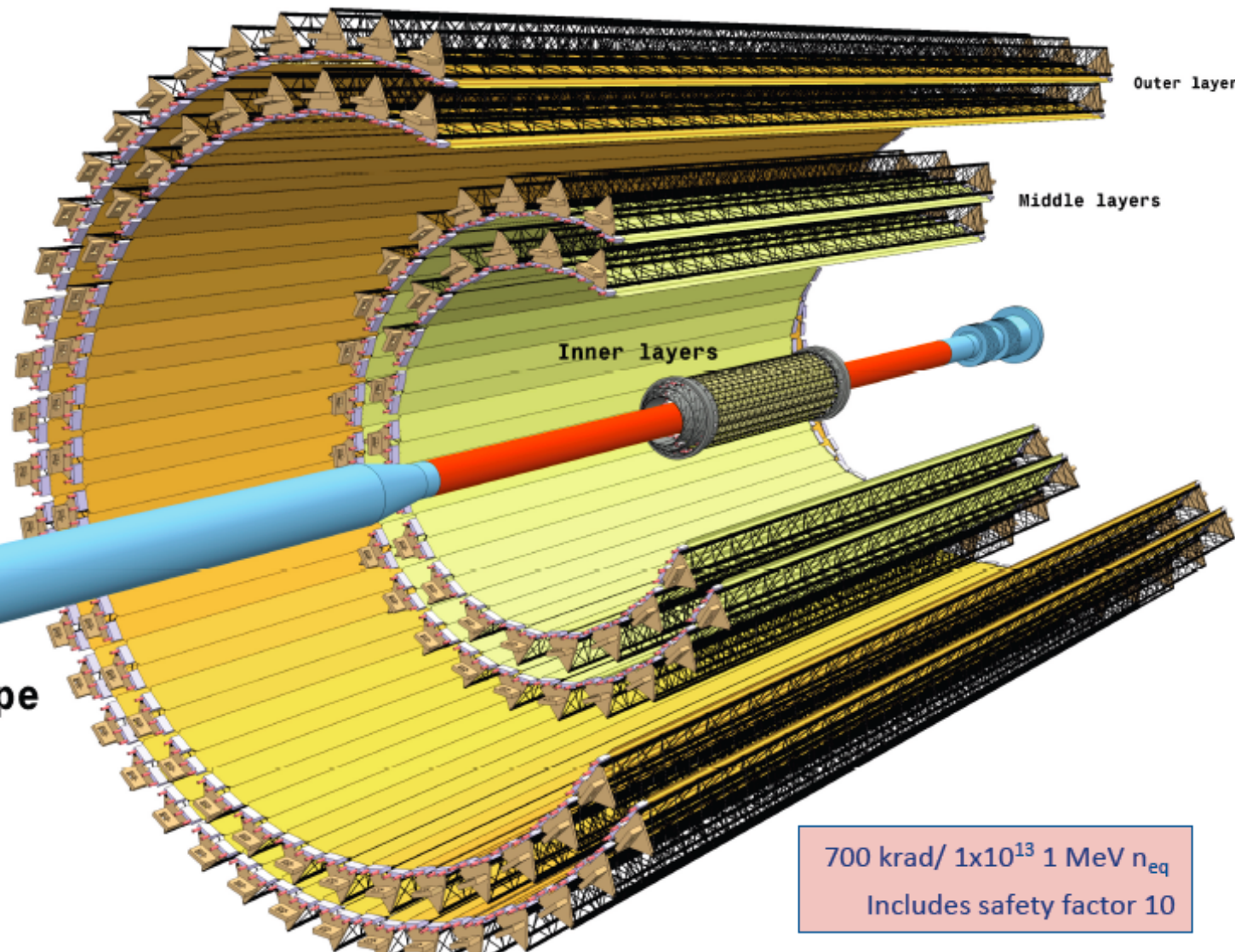


ITS TDR CERN-LHCC-2013-024

7 layers of MAPS

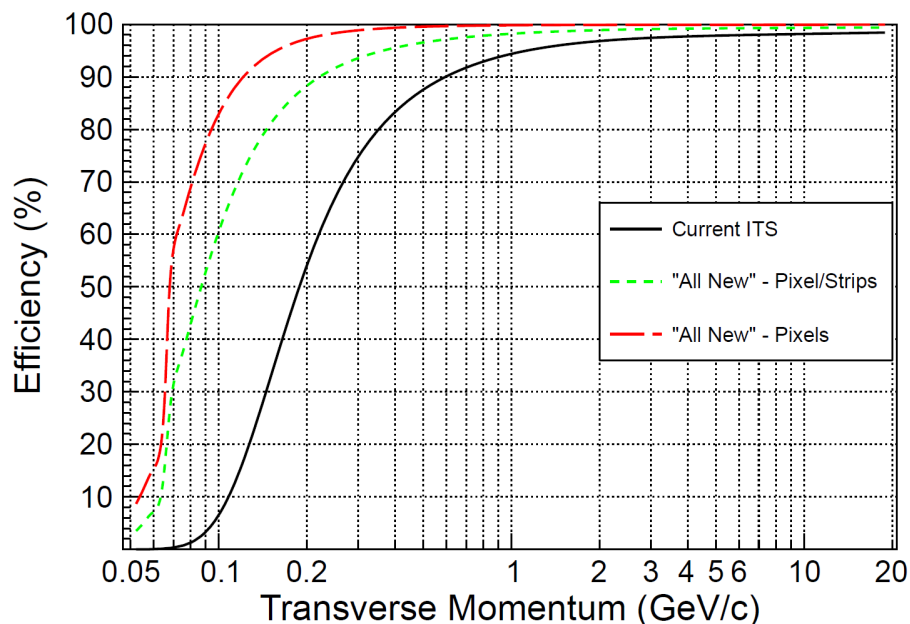
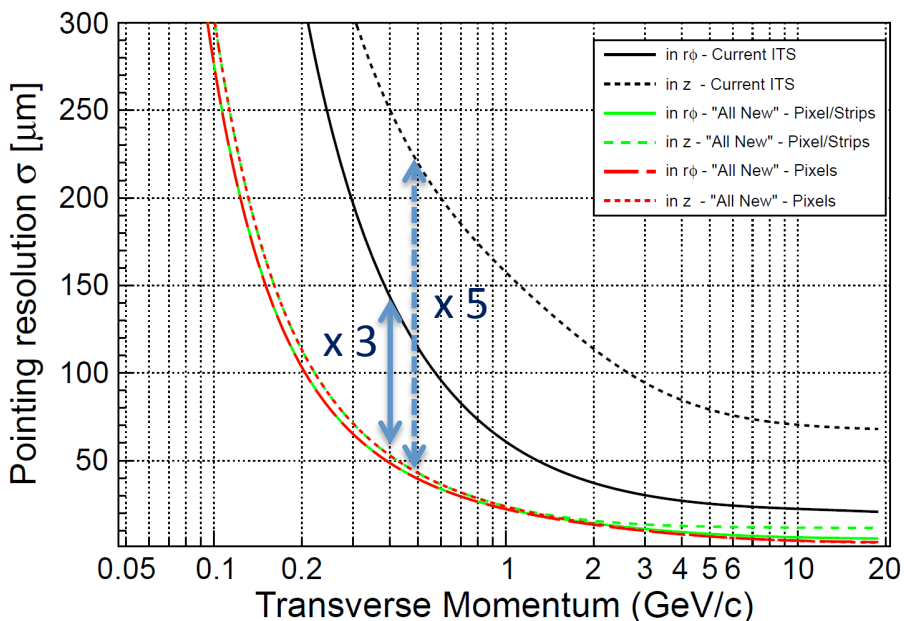
Beam pipe

Radial coverage
22 – 406 mm



700 krad/ 1×10^{13} 1 MeV n_{eq}
Includes safety factor 10

Improvement of impact parameter resolution and tracking efficiency



Simulation layout

7 pixel layers

- Resolutions: $\sigma_{r\phi} = 4 \mu\text{m}$, $\sigma_z = 4 \mu\text{m}$ for all layers
- Material budget: $X/X_0 = 0.3\%$ for all layers

radial positions (cm):

2.2, 2.8, 3.6, 20, 22, 41, 43

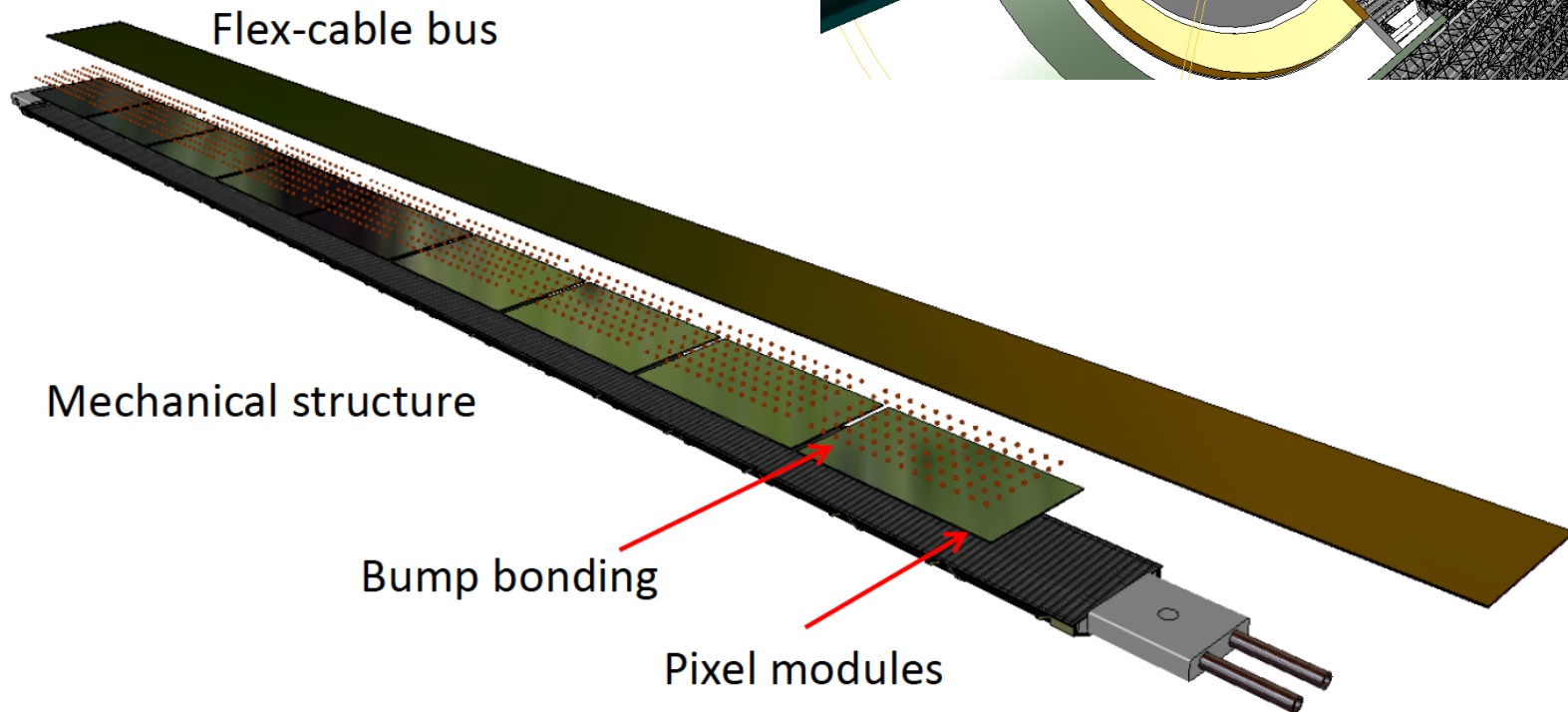
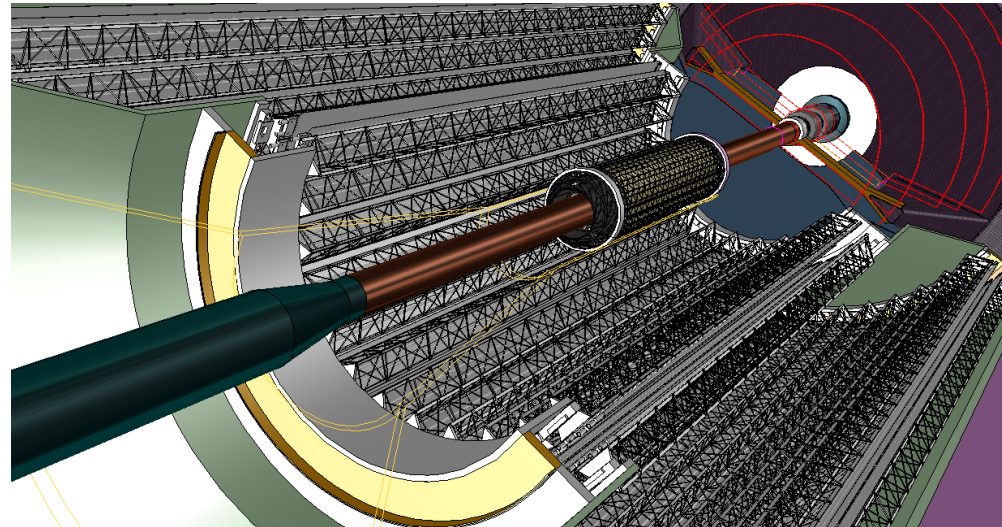
New ITS (baseline)

Inner Barrel: 3 layers

Outer Barrel: 4 layers

Detector module (Stave) consists of

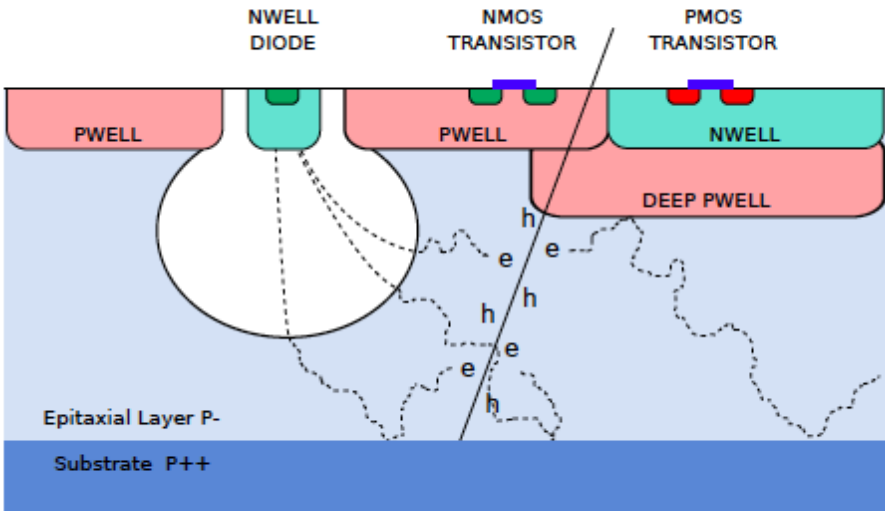
- Carbon fiber mechanical support
- Cooling unit
- Polyimide printed circuit board
- Silicon chips (CMOS sensors)



PIXEL Chip - technology

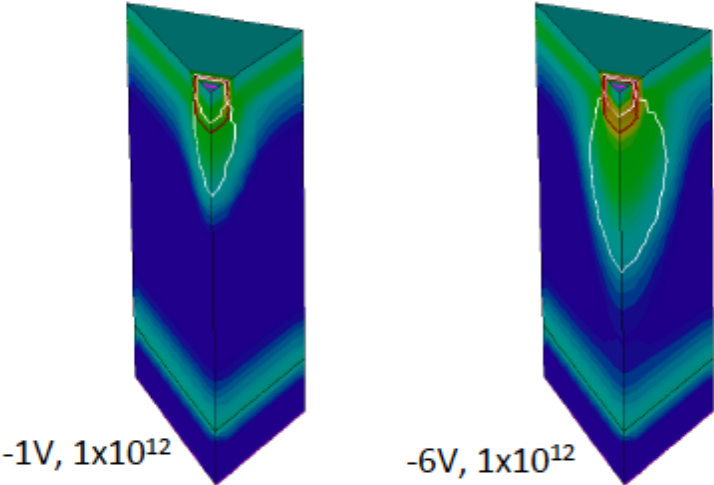
Monolithic PIXEL chip using Tower/Jazz 0.18 μm technology

- feature size 180 nm
- gate oxide < 4nm
- metal layers 6
- high resistivity epi-layer
 - thickness 18-40 μm
 - resistivity 1-6 $\text{k}\Omega\times\text{cm}$
- “special” deep p-well layer to shield PMOS transistors (allows in-pixel truly CMOS circuitry)
- Possibility to build single-die circuit larger than reticle size



Schematic cross-section of CMOS pixel sensor (ALICE ITS Upgrade TDR)

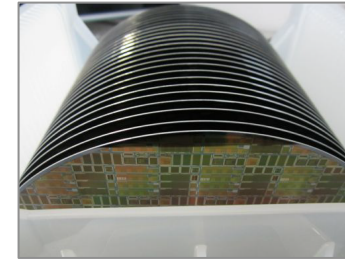
TCAD simulation of total diode reverse bias (ALICE ITS Upgrade TDR)



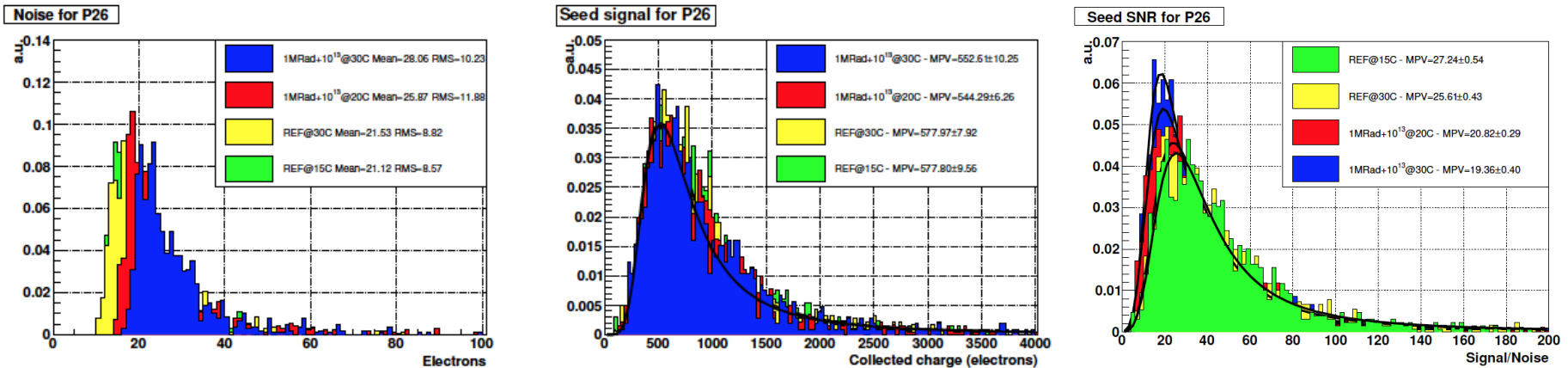
diode 3 μm x 3 μm square n-well with 0.5 μm spacing to p-well white line: boundaries of depletion region

Pixel chip - R&D with TowerJazz technology

- R&D with TowerJazz CIS process in 2011-2013
- What has been established so far
 - Adequate radiation hardness
 - Excellent charge collection efficiency for pixel $O(20-30)\mu\text{m}$
 - Excellent detection efficiency
 - Prototypes of different readout architectures have been built and fully characterized



Example of experimental results



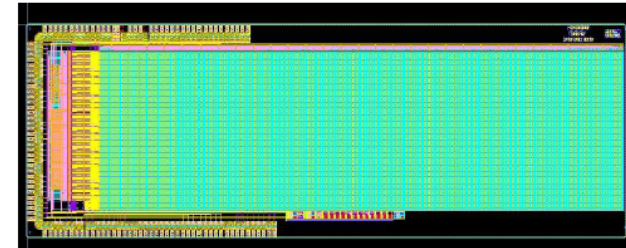
MIMOSA-32ter (IPHC), test-beam results

Towards a full-scale Chip

Prototype circuits

MISTRAL (IPHC-IRFU)

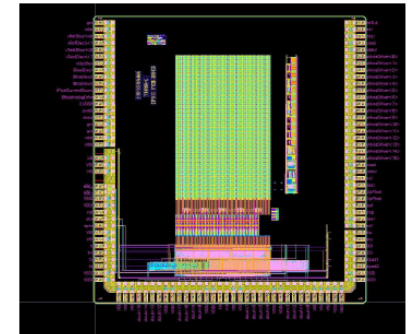
- Built on the experience from the STAR-PXL detector
- 350 rows x 1300 columns (pixel size: $22\mu\text{m} \times 33\mu\text{m}$)
- Frame integration/readout time $\sim 30\ \mu\text{s}$
- Power consumption $\sim 300\text{mW} / \text{cm}^2$



MIMOSA-22 THRa

ASTRAL (IPHC-IRFU)

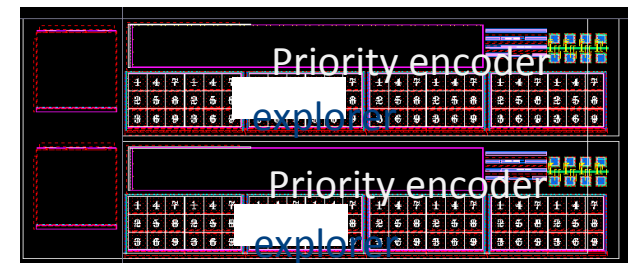
- Signal discrimination embedded in each pixel
- Integration time 15 (10) μs
- Power consumption 150 (200) mW



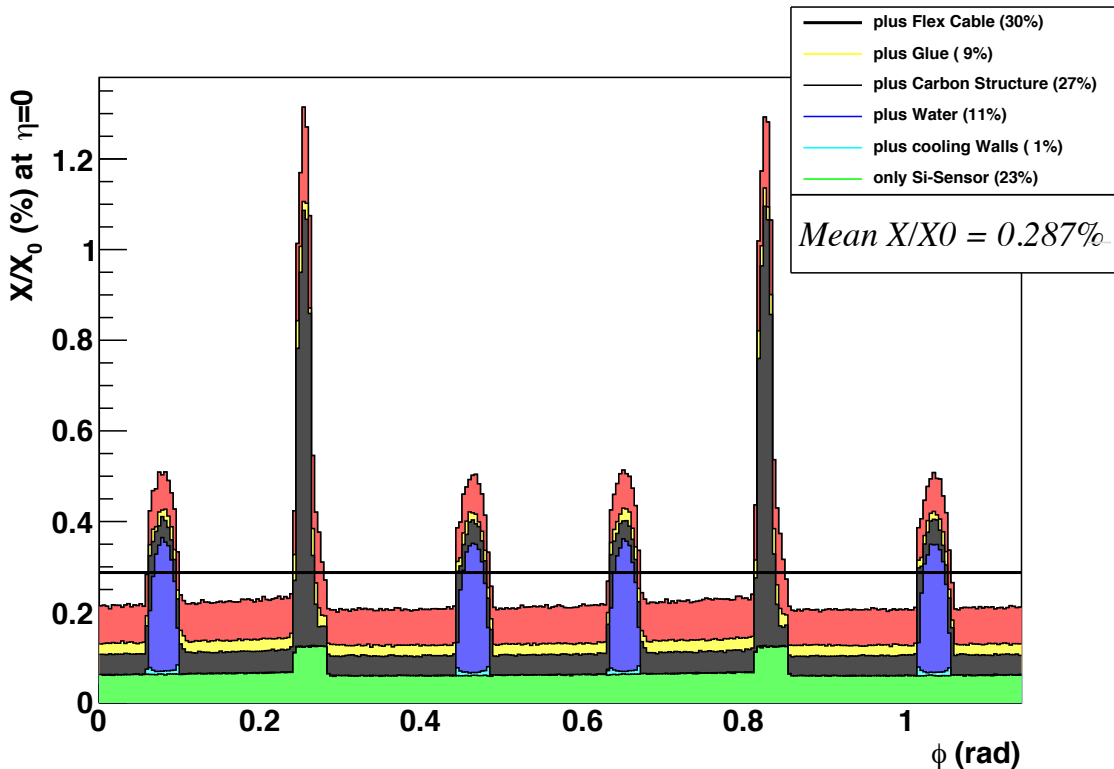
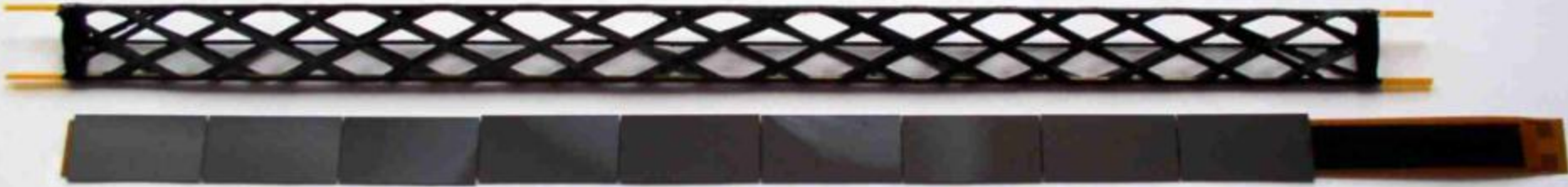
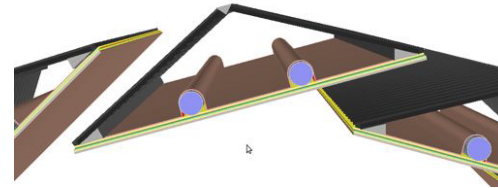
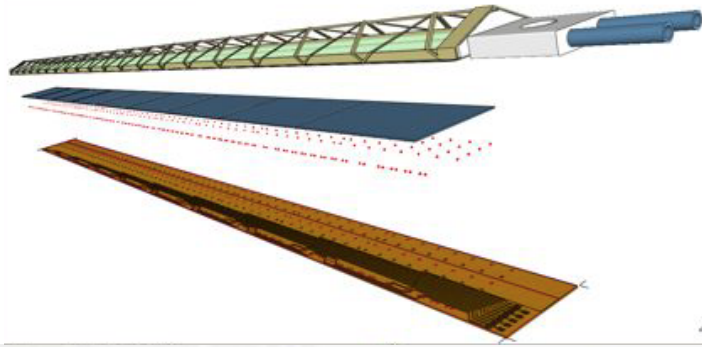
MIMOSA-22 THRb

ALPIDE Chip (CERN – INFN – CCNU)

- Signal discriminator inside the pixel
- Integration (\sim readout time) $\sim 4\ \mu\text{s}$
- pixel size: $28\mu\text{m} \times 28\mu\text{m}$
- Power consumption $< 100\text{mW} / \text{cm}^2$

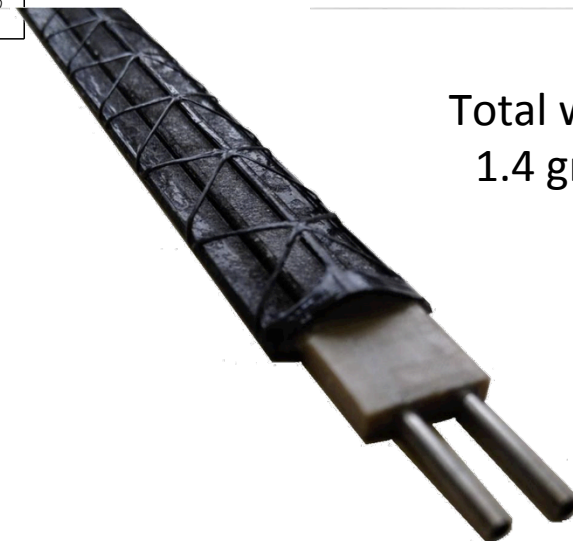


Inner Barrel Detector Stave



MECHANICS & COOLING

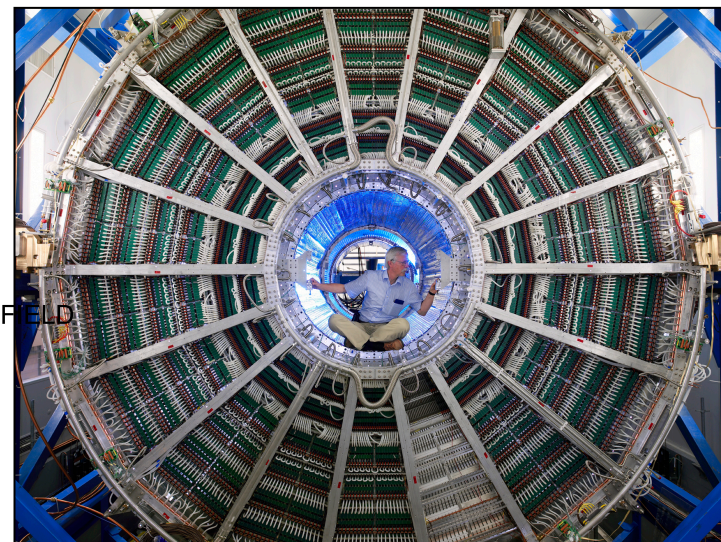
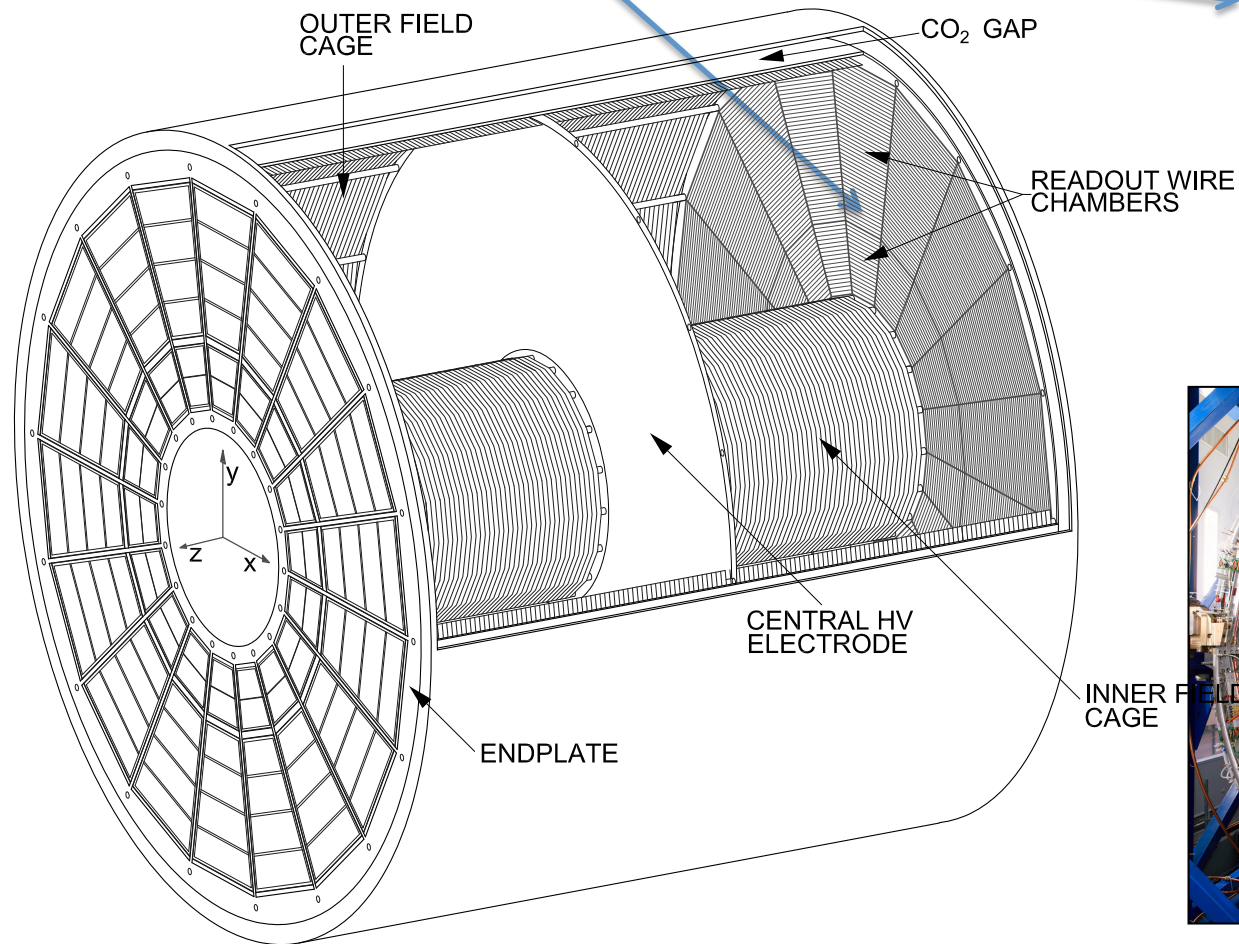
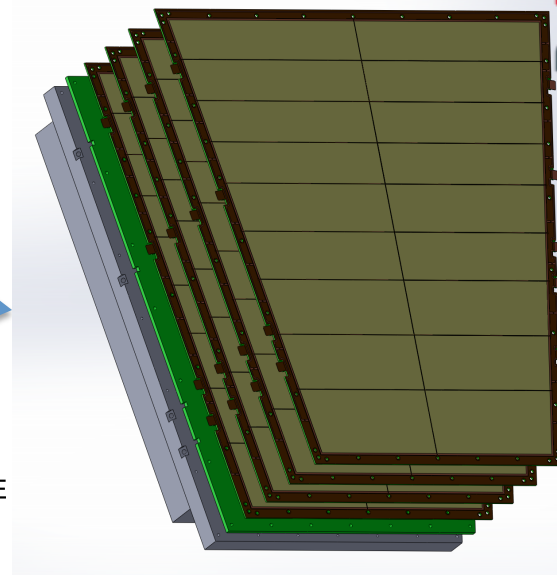
✓ Design optimization for material budget reduction



Total weight
1.4 grams

TPC Upgrade with GEMs

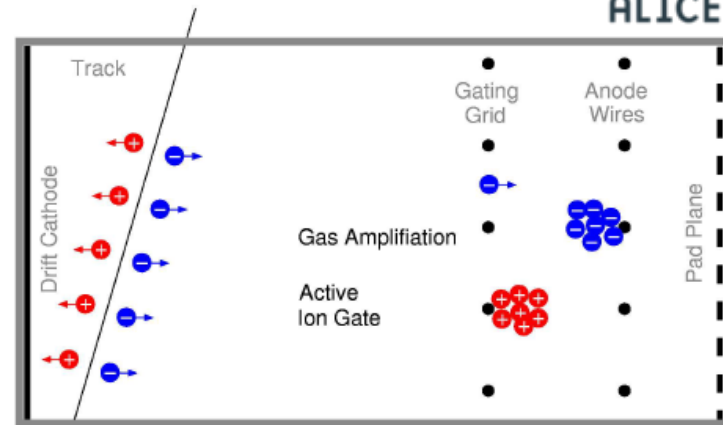
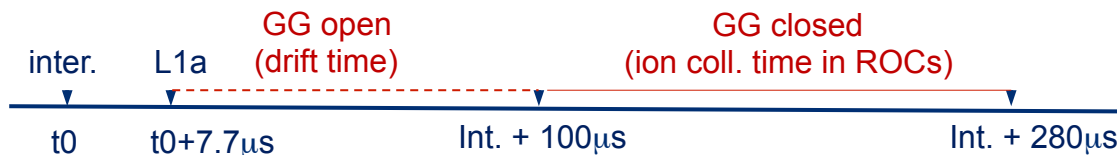
Replace wire chambers
With quadruple-GEM chambers



TPC upgrade – Why?



ROC ion feedback (λ_{int} and λ_{readout} dependent)



○ Space charge (no ion feedback from triggering interaction)

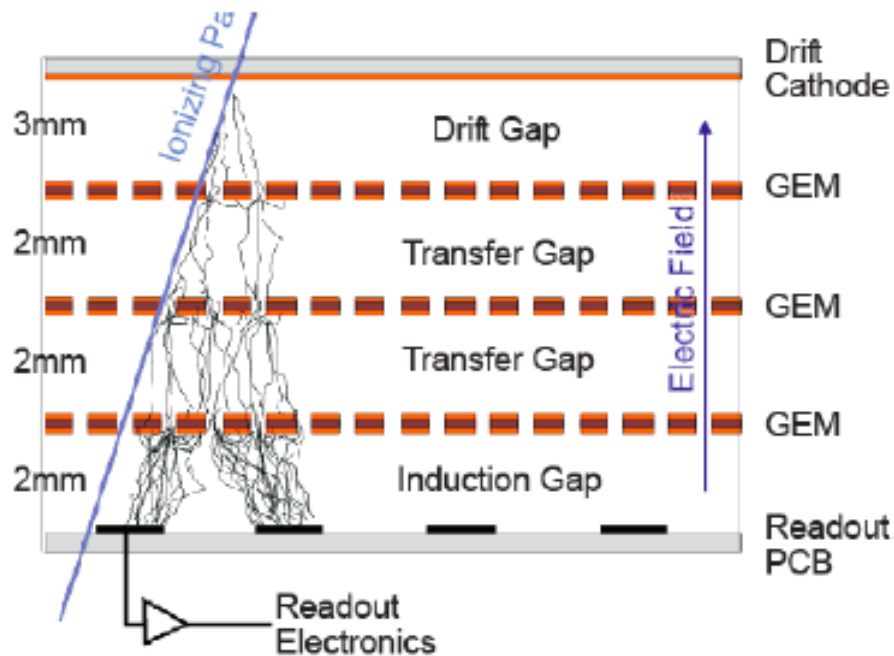
- GG open [$t_0, t_0+100\mu\text{s}$], $t_0 \equiv$ interaction that triggers TPC
- GG closed [$t_0+100\mu\text{s}, t_0+280\mu\text{s}$]
- Effective dead time $\sim 280\mu\text{s} \rightarrow$ max readout rate ~ 3.5 kHz
- Maximum distortions for $\lambda_{\text{int}}=50\text{kHz}$ and $L1=3.5\text{kHz}$: $\Delta r \sim 1.2\text{mm}$ (STAR TPC distortions $\sim 1\text{cm}$)

○ Space charge for continuous readout (GG always open)

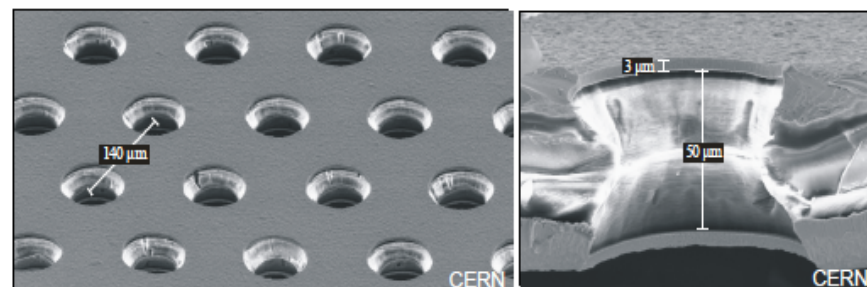
- gain $\sim 6 \times 10^3$
- 20% ion feedback if GG always open \rightarrow ion feedback $\sim 10^3$ x ions generated in drift volume
- Max distortions for 50kHz $\sim 100\text{cm}$

MWPC not compatible with 50 kHz operation

Triple-GEM principle of operation

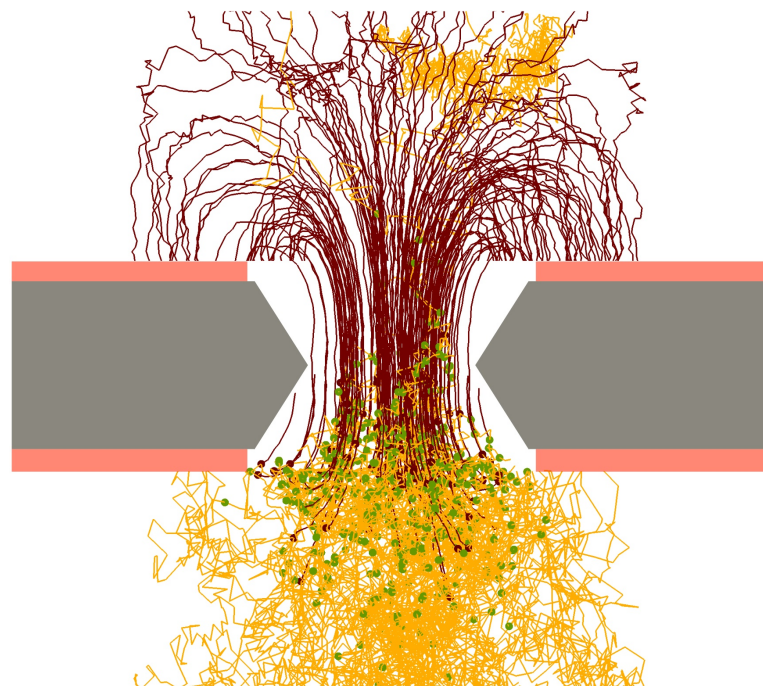


GEMs are made of a copper-kapton-copper sandwich, with holes etched into it



Electron microscope photograph of a GEM foil

- Fast **electron** signal (polarity!)
 - no “ion tail”
 - No “coupling to other electrods”
- ➔ Gas gain about a factor 3 lower than in MWPC

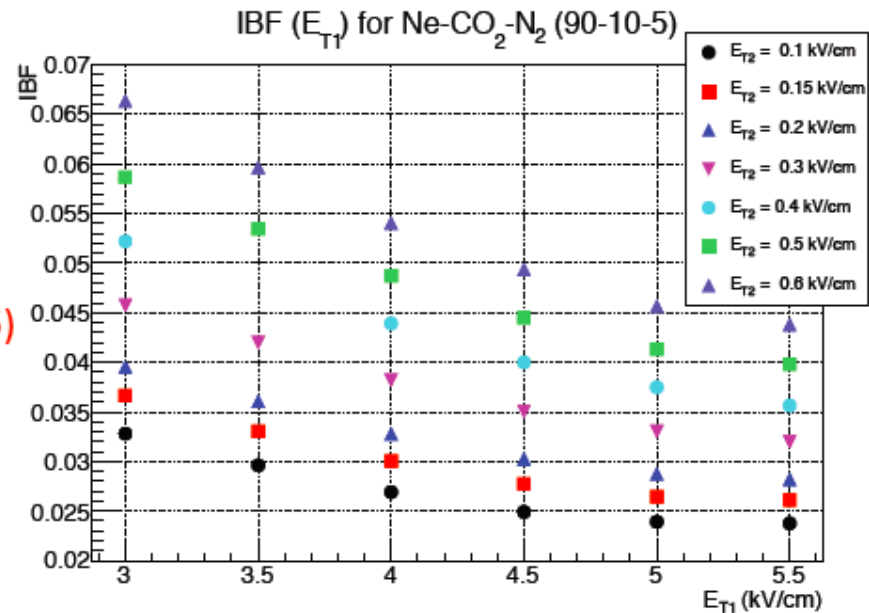


Ion Backflow in triple GEMs

- ion space-charge density:
 $\sim n_{\text{prim}} * \text{gain} * IBF * 1/v_{\text{ion}}$

→ baseline mixture **Ne-CO₂-N₂ (90-10-5)**

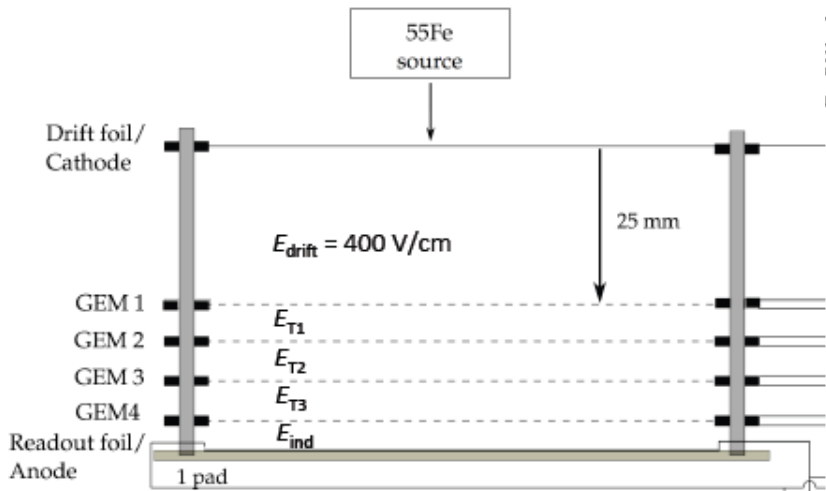
- requirement: $IBF \leq 1\%$,
 i.e. $\epsilon = \text{gain} * IBF < 20$
 at gain = 2000



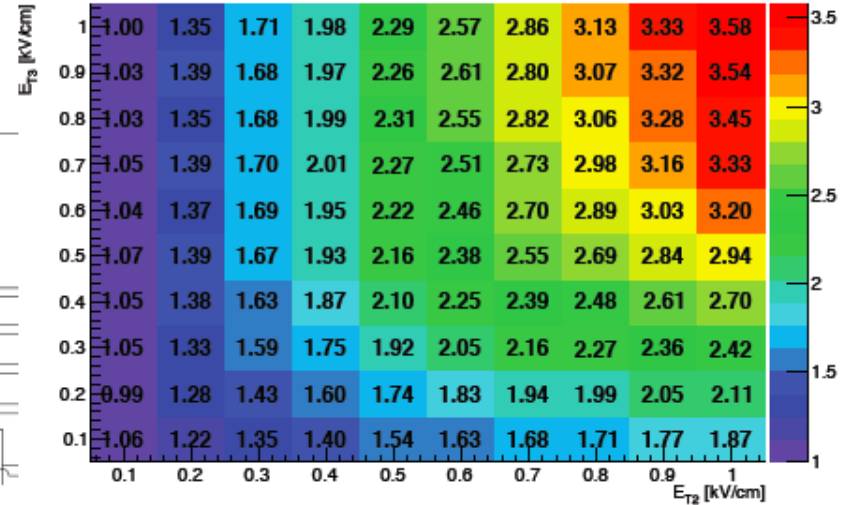
Comprehensive study of triple standard GEM system (gas mixture, E_{T1} , E_{T2})

→ IBF requirement **not achieved with triple GEMs**

Ion Backflow in quadruple GEMs



Ne-CO₂-N₂ (90-10-5) (S-S-S-S)



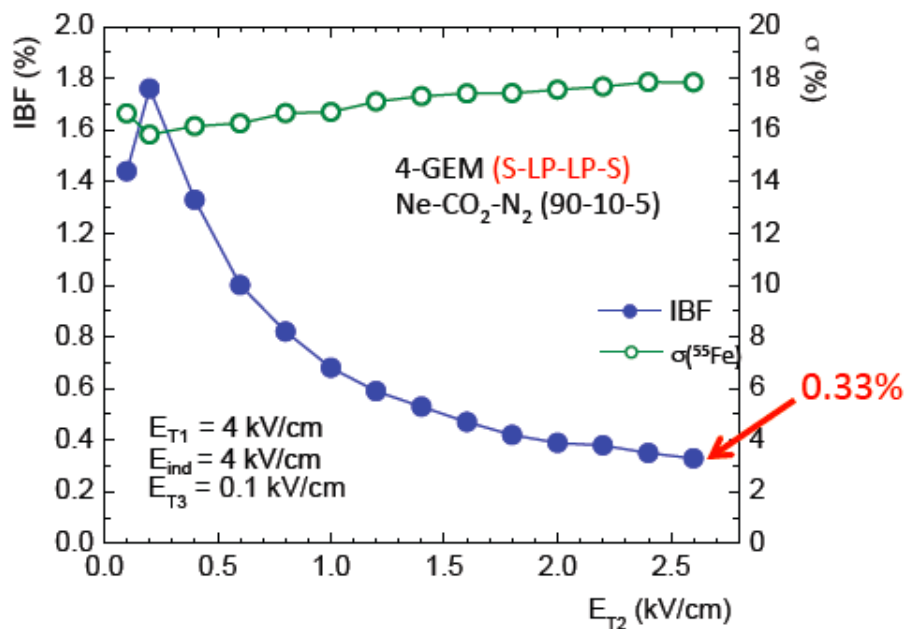
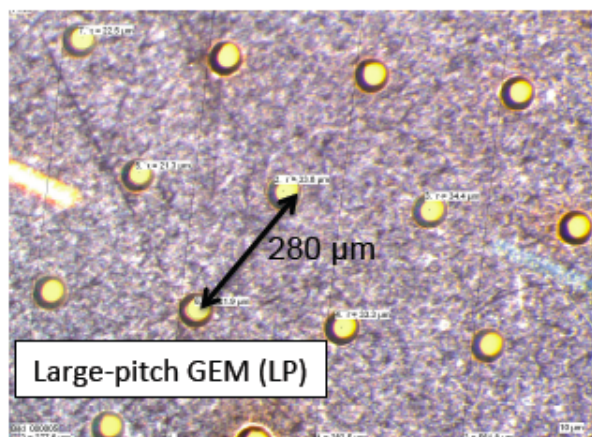
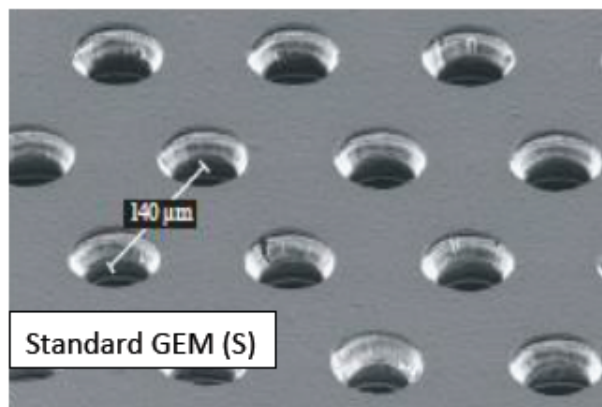
→ reduction of IBF in standard 4-GEM system (S-S-S-S):

- $IBF \approx 1\% \rightarrow \epsilon \approx 20$ at gas gain 2000 in Ne-CO₂-N₂ (90-10-5)

R&D status with quadruple GEMs

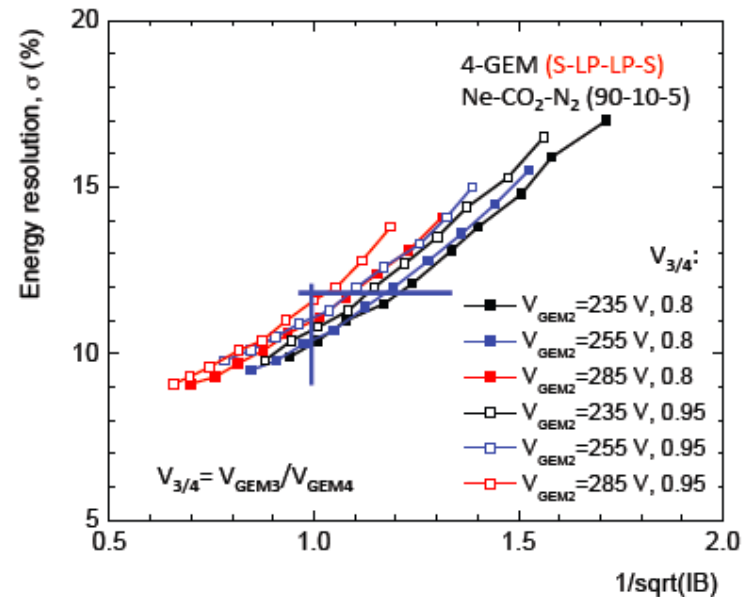
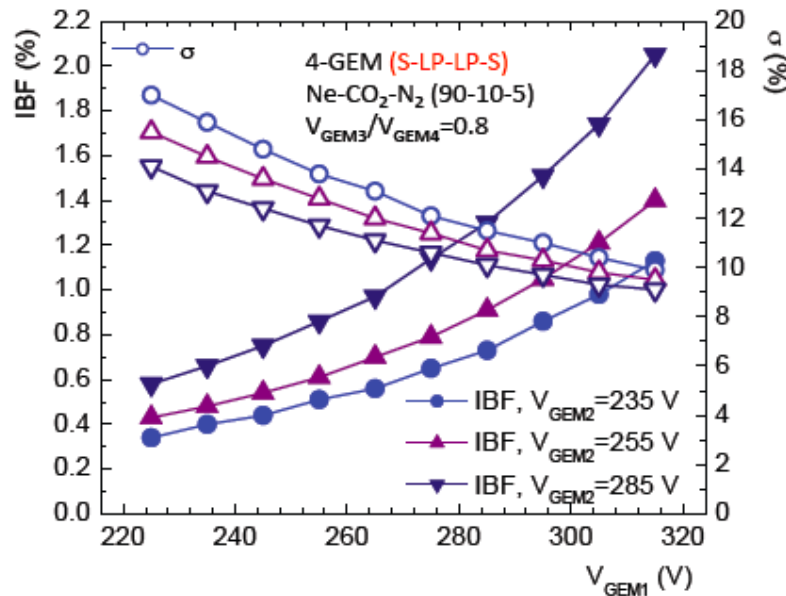


ALICE



- further reduction of IBF in 4-GEM system with **large-pitch** GEMs (S-LP-LP-S)
- consideration of **energy resolution** is important: dE/dx performance requires $\alpha(^{55}\text{Fe}) \leq 12\%$

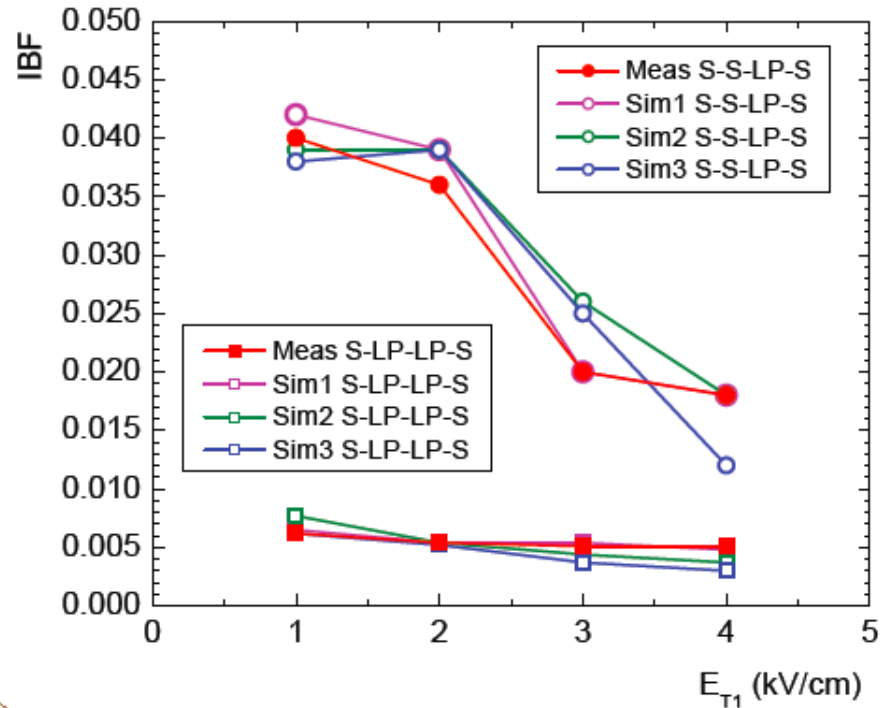
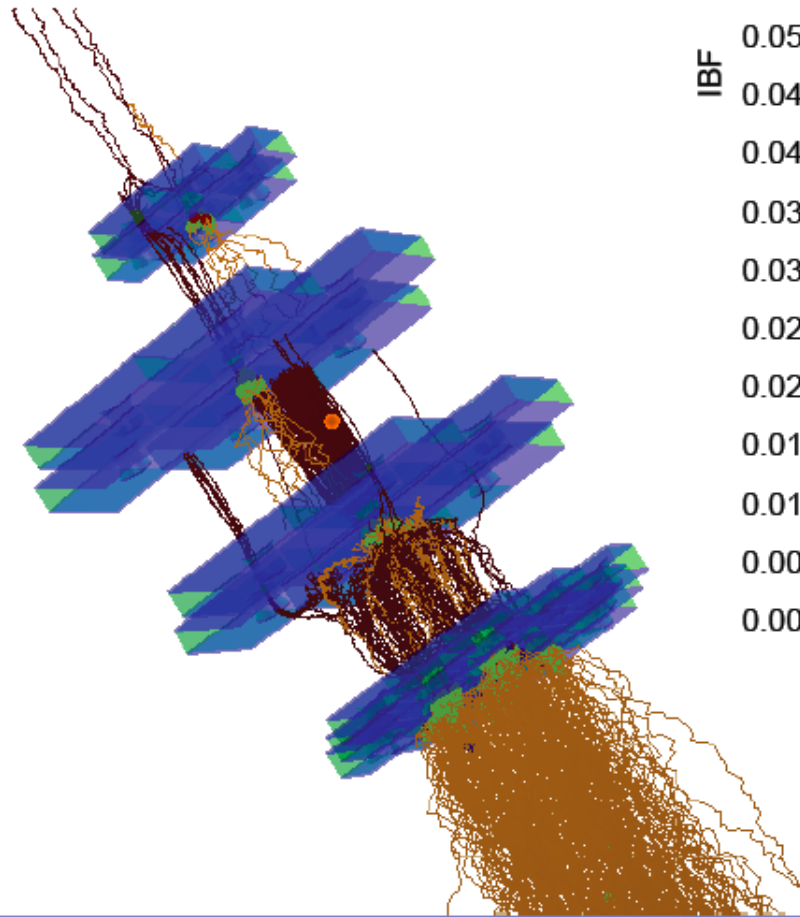
further optimization: IBF vs. energy resolution



- Comprehensive voltage scan establishes **operational point with IBF < 1% and energy resolution $\sigma(^{55}\text{Fe}) < 12\%$**

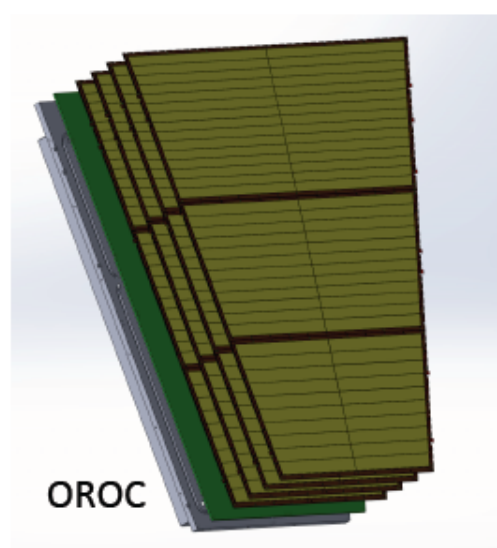
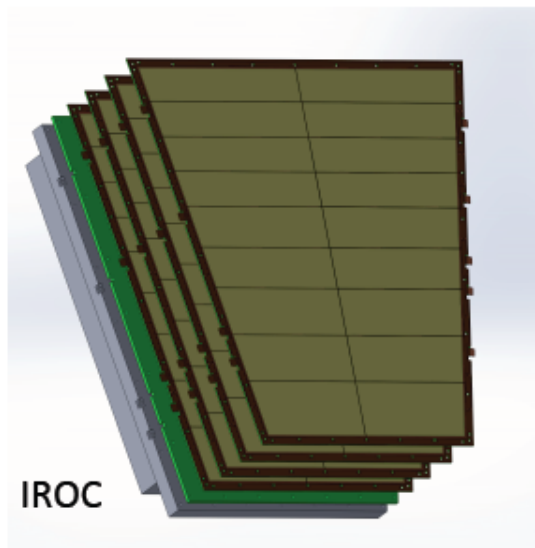
→ All performance studies are for IBF = 1% at gain = 2000, i.e. **$\epsilon = 20$**

simulation: IBF in 4-GEM systems

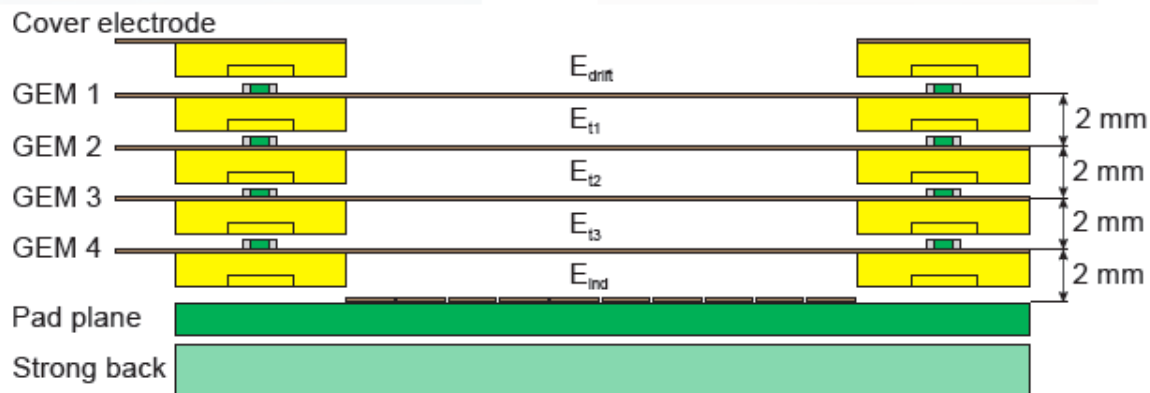


- IBF quantitatively well described by **simulation based on Garfield++**

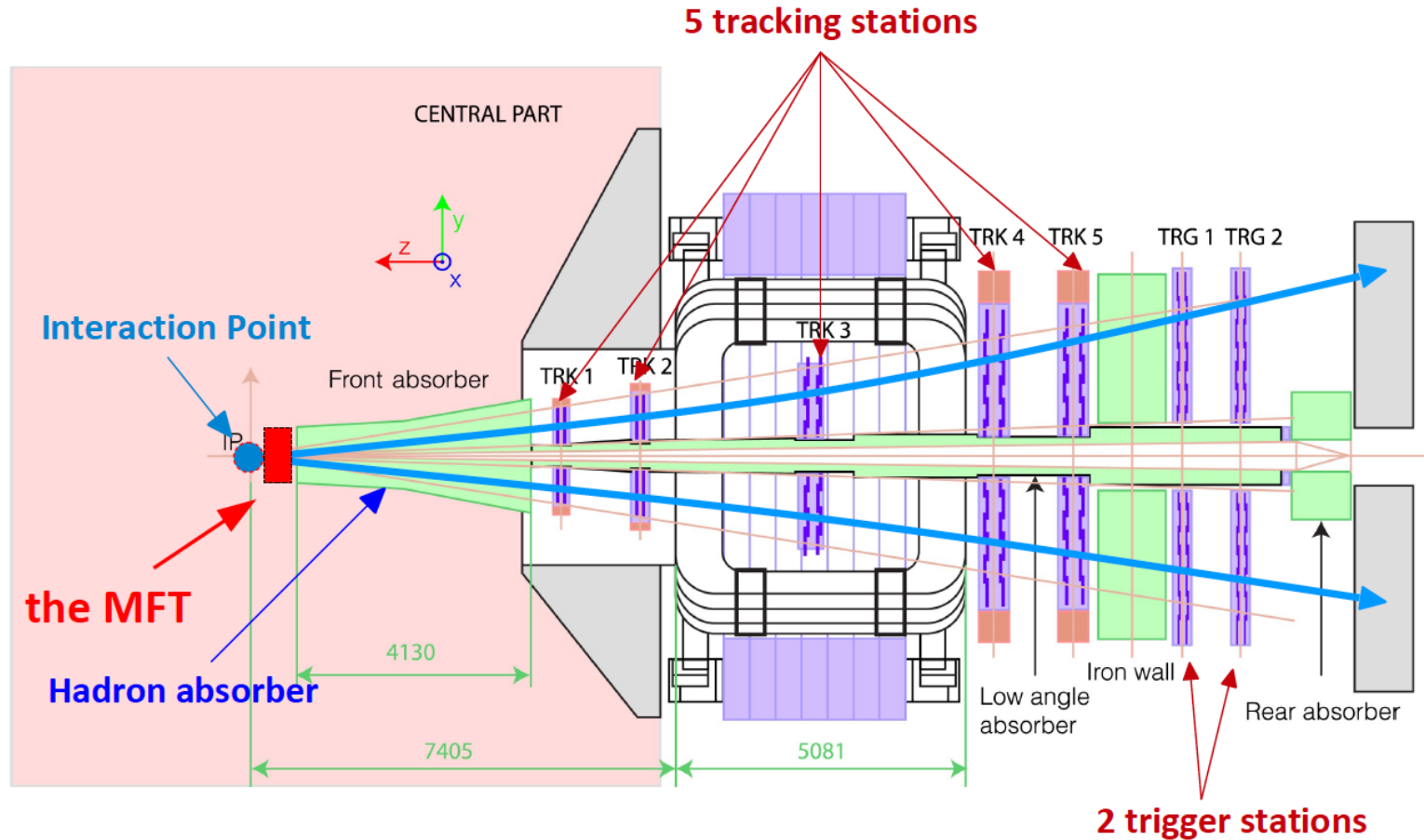
TDR baseline solution: 4-GEM system



- large-size single-mask GEM foils
- one (three) per layer in IROC (OROC)

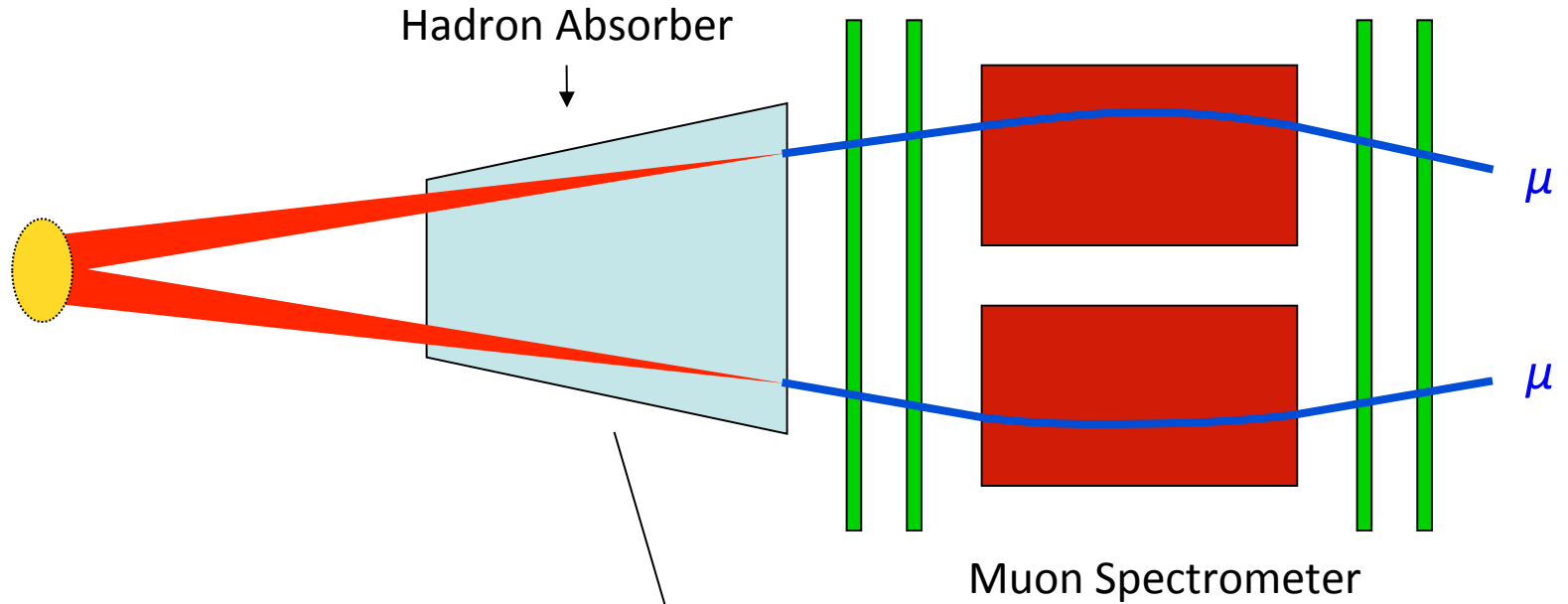


The MFT and the Muon-Spectrometer



Silicon pixel tracker in the acceptance of the Muon Spectrometer placed between the Interaction Point and the Hadron Absorber

The MFT Concept

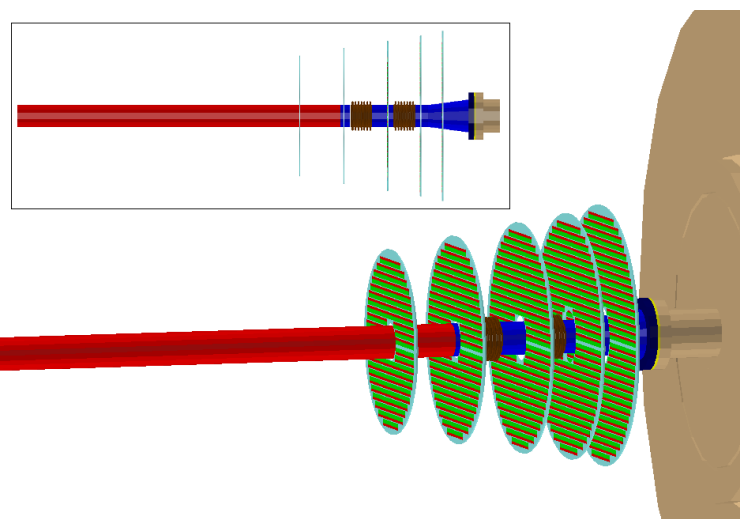
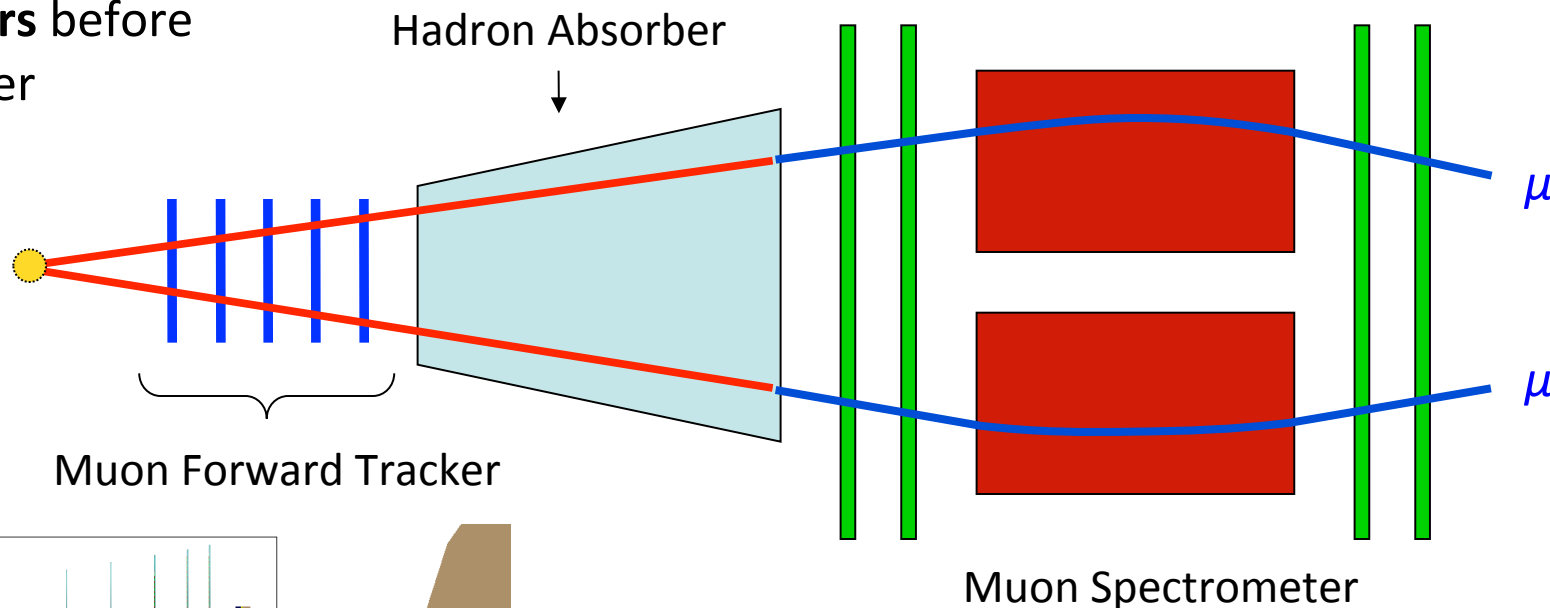


Extrapolating back to the vertex region
degrades the information on the kinematics

The MFT Concept

Muon tracks are extrapolated and “**matched**” to the **MFT clusters** before the absorber

High pointing accuracy gained by the muon tracks after matching with the MFT clusters



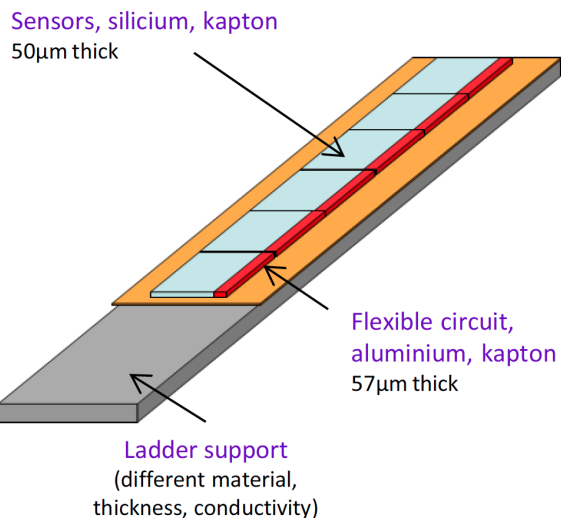
MFT baseline simulation set-up

Plane	Int. radius (cm)	Ext. radius (cm)	Z location (cm)	Pixel pitch (μm)	Thickness (% of X_0)
0	2.5	11.0	-50		
1	2.5	12.3	-58		
2	3.0	13.7	-66	25	0.4
3	3.5	14.6	-72		
4	3.5	15.5	-76		

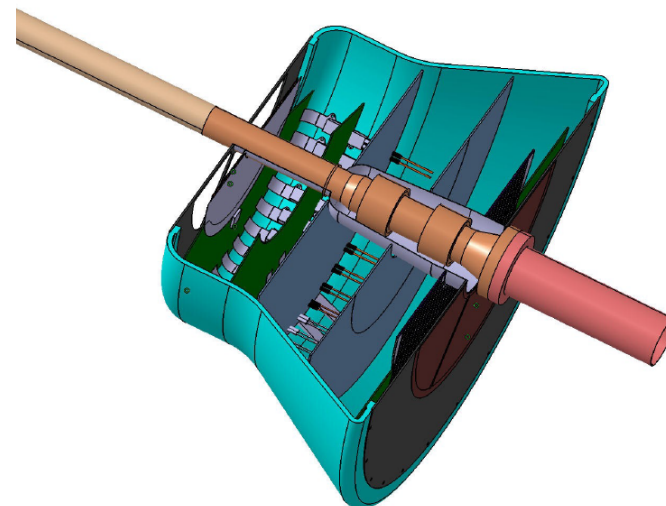
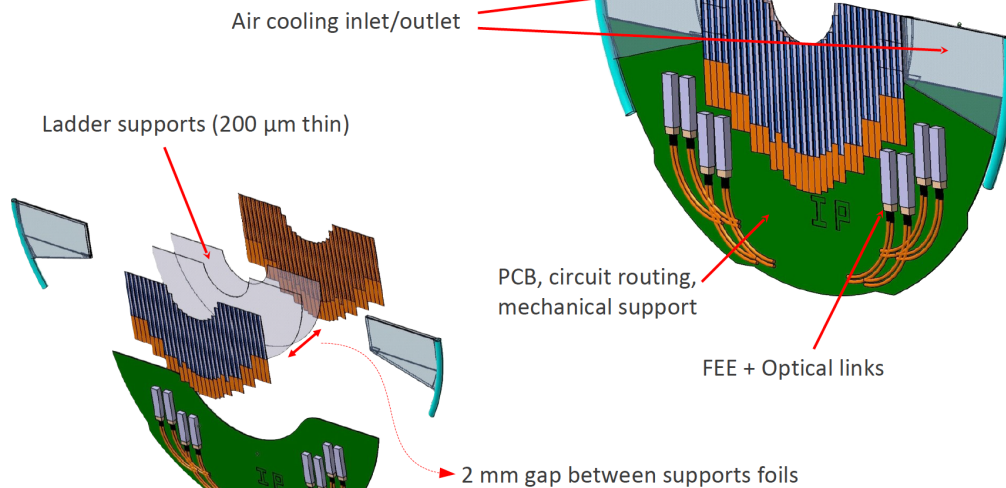
MFT Layout

Pixel chip: common development with ITS

Ladder: basic detector element



Structure of half disk



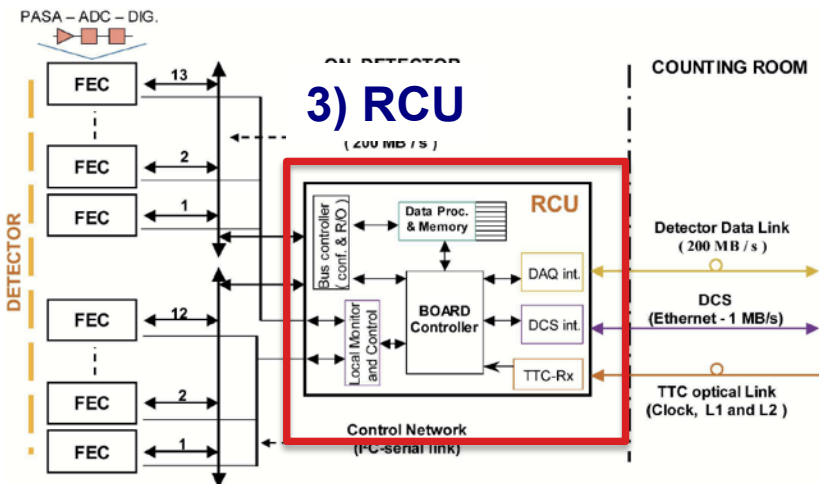
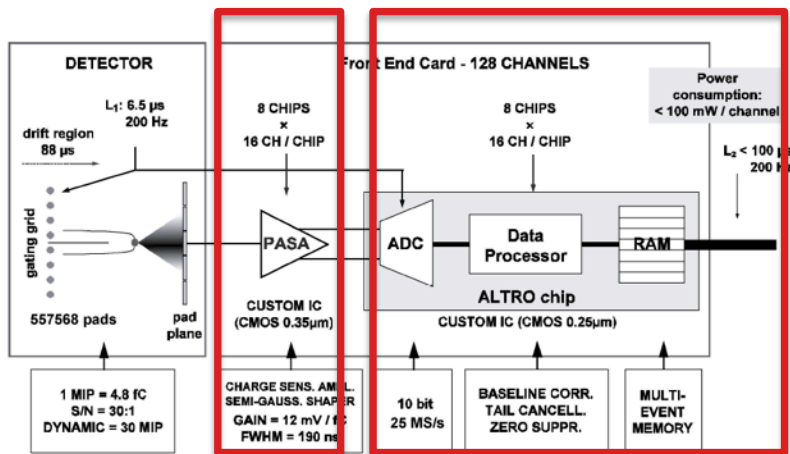
- MFT planes are ladder assemblies of active and (dead) readout zones
- Pixel sensors are mounted on both sides of the plane to guarantee hermeticity

Common FE Chip for TPC/Muon Tracker

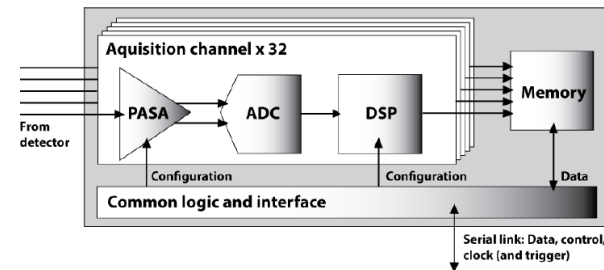
A Large Ion Collider Experiment



1) PASA 2) ALTRO



SAMPA Chip



32 Channels
Including the
PASA,
ALTRO,
RCU functionalities

Readout System

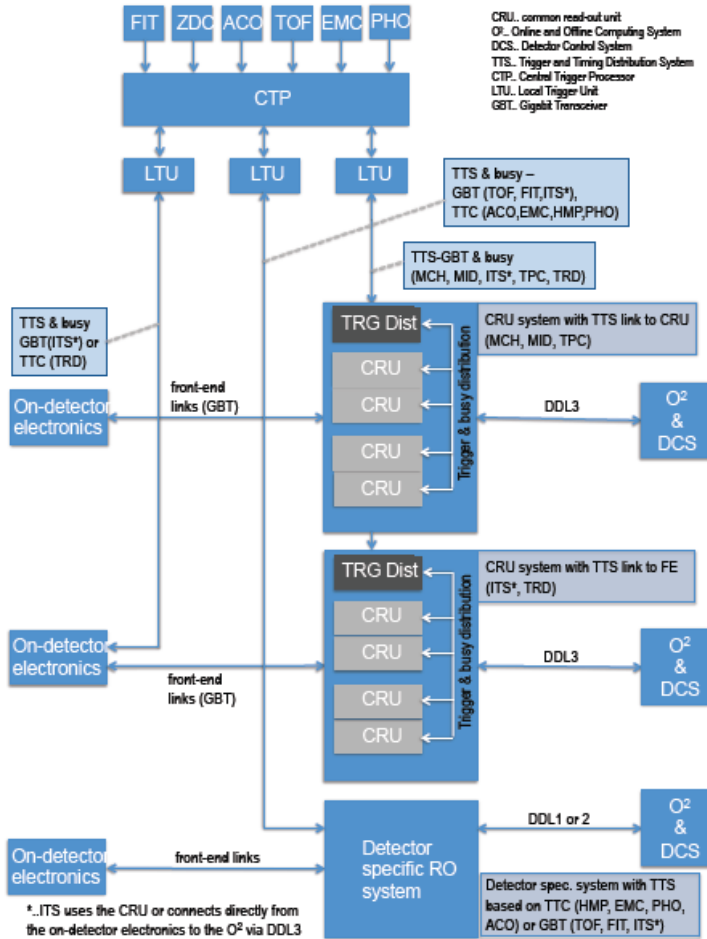


Figure 2.1: General ALICE system block diagram.

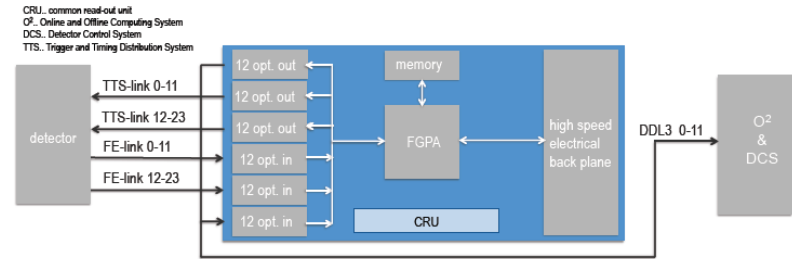


Figure 2.5: CRU block diagram.

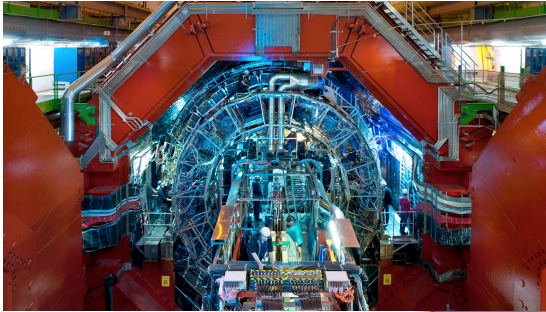


All data pushed to the online system at 50kHz PbPb interaction rat.

CRU possible common solution with LHCb/ Tell40.



O² Project



All data are written to tape.

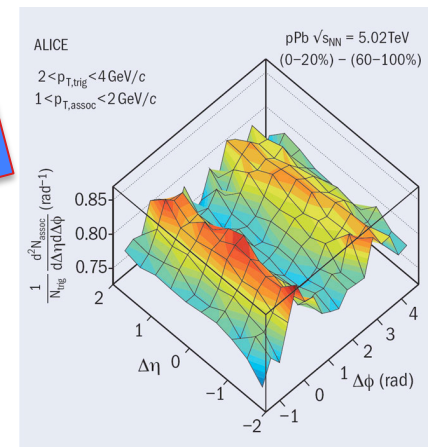
Writing raw data is not possible (factor 20 too large).

→ perform part of 'reconstruction' online.

→ Online/Offline boundary disappears → O²



From Detector Readout to Analysis:
What is the "optimal" computing architecture?



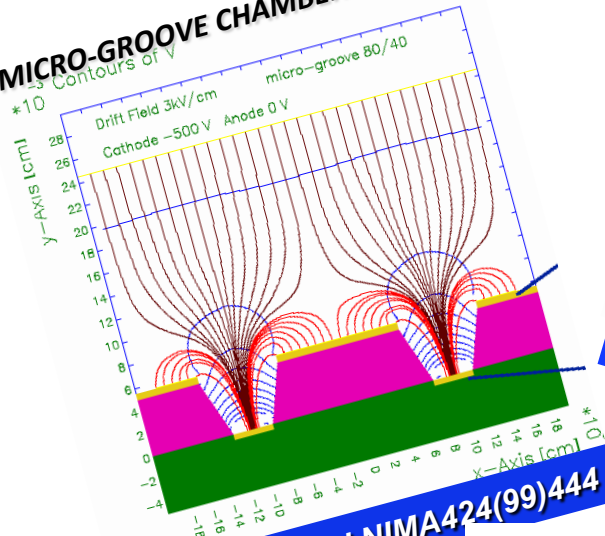
Summary

- Major upgrade of ALICE detector, for **installation in 2018/19**, to cope with Pb-Pb collisions at high rates and improve vertexing capabilities at low p_T
- The detectors will be modified to **inspect up to 50 kHz Pb-Pb collisions** shipping all data to the online systems either continuously or upon a **minimum-bias trigger**
- Key detector items of this upgrade programme are:
 - **New ITS (the largest HEP pixel detector ever, 7 layers, $\sim 11\text{m}^2$)**
 - Built on the experience from STAR PXL
 - Very low material thickness: 0.3% per layer
 - **Replacement of TPC endplates** with new readout based on quadruple-GEM detectors and new electronics for continuous readout
 - **New 5-plane muon silicon telescope**, based on MAPS, in front of hadron absorber in the acceptance of the Muon Spectrometer
 - **Readout rate upgrade**, of all other ALICE subdetectors
- Next Steps
 - Technical Design Reports

Excursion to Micropattern Gas Detectors

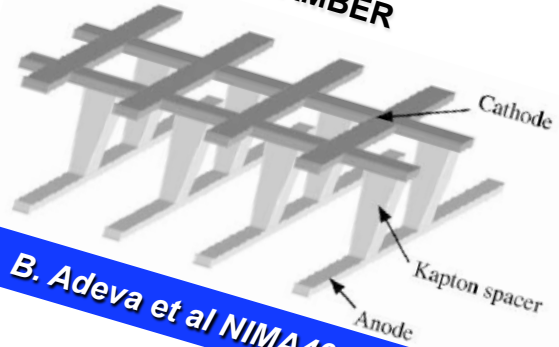
Trends for gaseous detectors: Micro Pattern Gas Detectors

MICRO-GROOVE CHAMBER



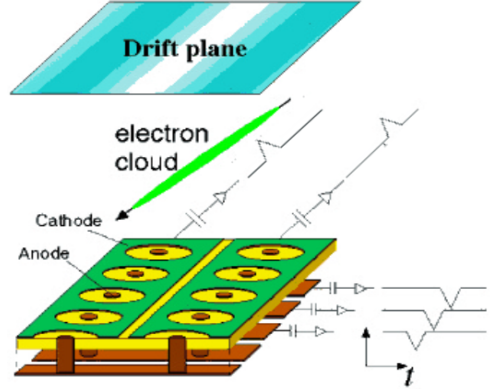
Bellazzini et al NIMA424(99)444

MICROWIRE CHAMBER



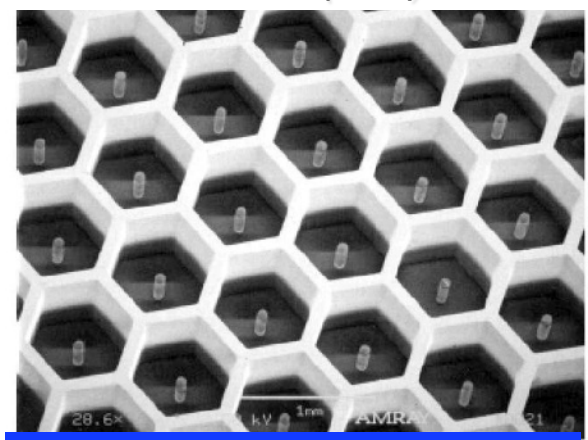
B. Adeva et al NIMA461(2001)33

MICRO-PIXEL CHAMBER



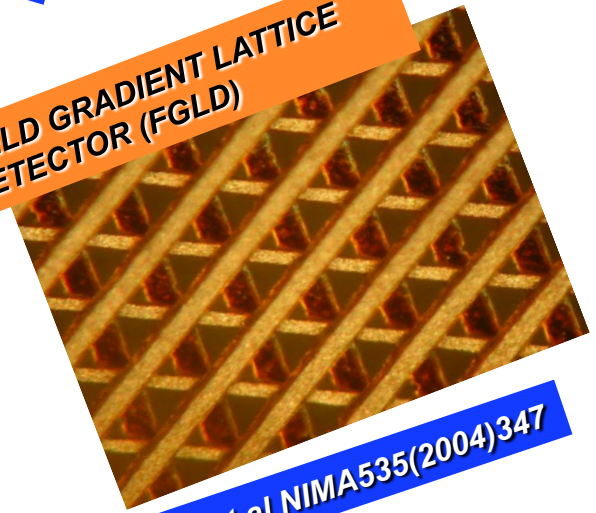
Ochi et al NIMA471(2001)264

MICRO-PIN ARRAY (MIPA)



P. Rehak et al TNS NS47(2000)1426

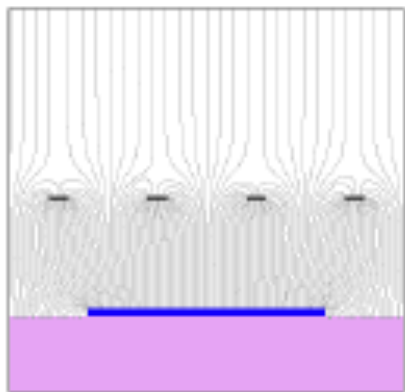
FIELD GRADIENT LATTICE DETECTOR (FGLD)



L.Dick et al NIMA535(2004)347

Trends for gaseous detectors: Micro Pattern Gas Detectors

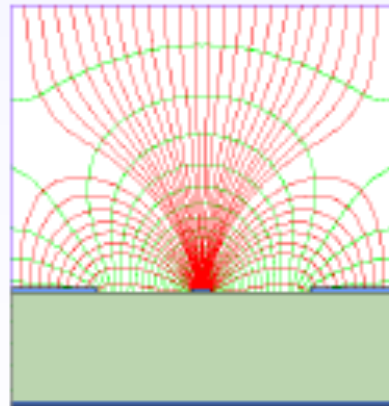
MICROMEGA



parallel plate

MicroMeshGasdetector

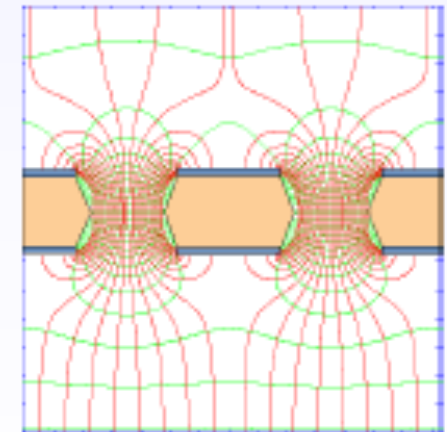
MSGC



strip

MicroStripGasChamber

GEM



hole

GasElectronMultiplier

Trends for gaseous detectors: Micro Pattern Gas Detectors

During the 1990s, Micro Strip Gas Chambers (MSGCs) were developed with the idea of producing affordable large area tracking systems. They were prominent candidates for the inner tracking system of the ATLAS and CMS experiments.

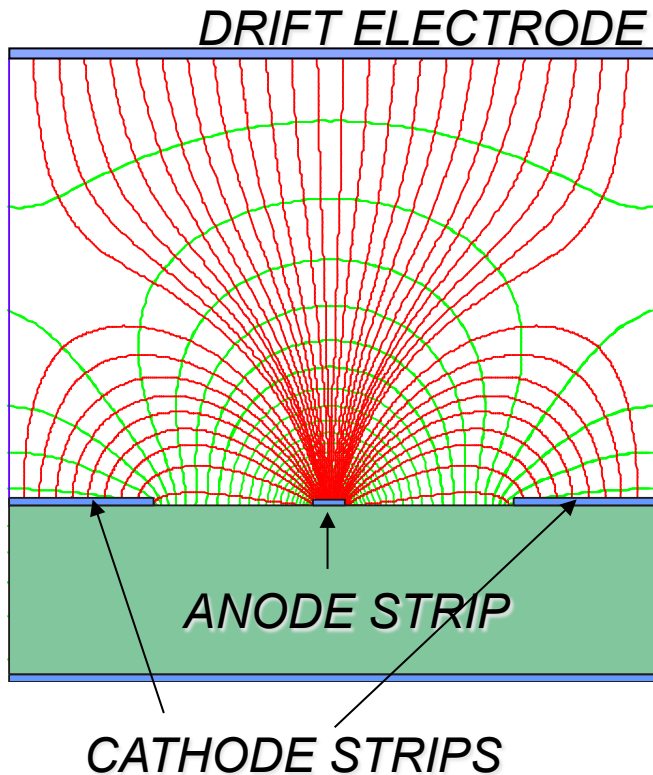
The falling cost of Silicon Detectors and increasing difficulties with MSGCs 'forced' the LHC community to abandon these detectors.

Out of the MSGC efforts there emerged however several new so called Micro Pattern Gas Detectors (MPGDs) which are starting to find their way into many experiments.

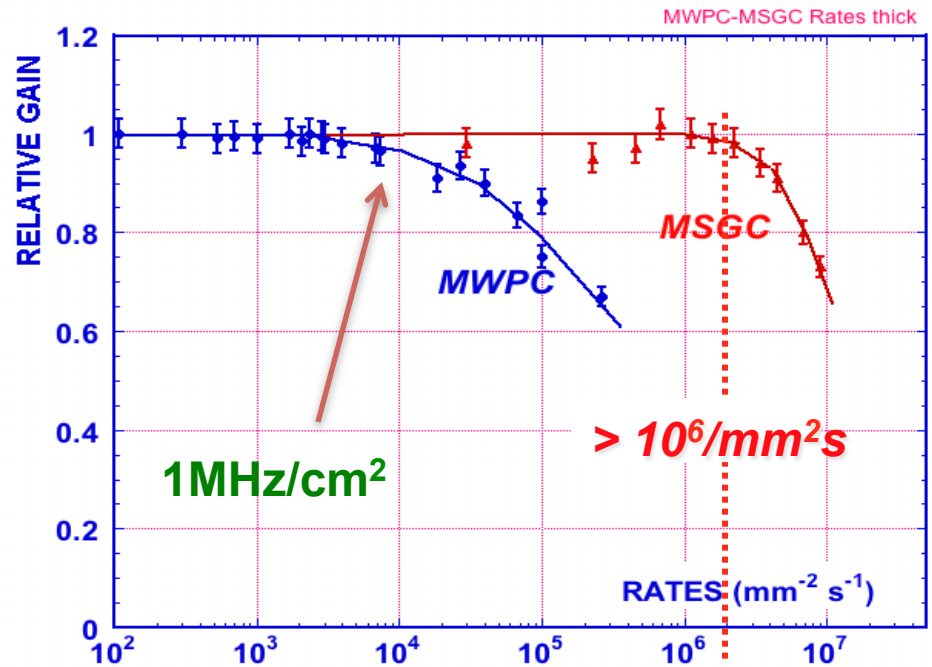
Micro Strip Gas Chambers (MSGCs)

Gas gain is provided not by wires but by metal strips on resistive electrodes.

Due to small pitch and fast ion collection MSGCs have very high rate capability.



A.Oed, *Nucl. Instr. and Meth. A263(1988)351*



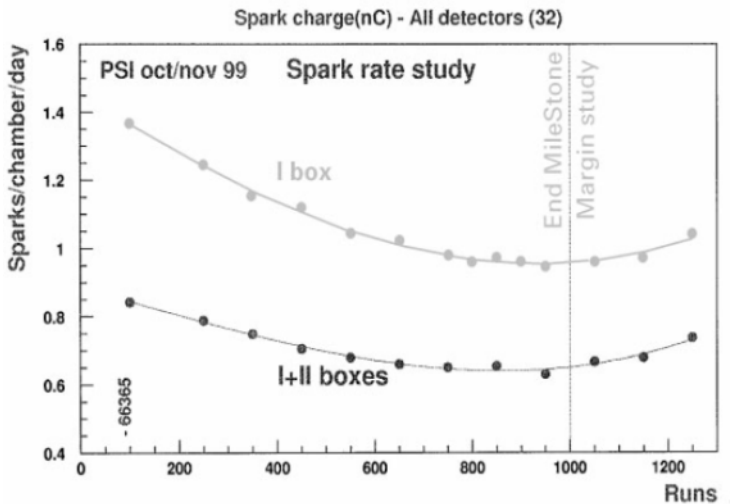
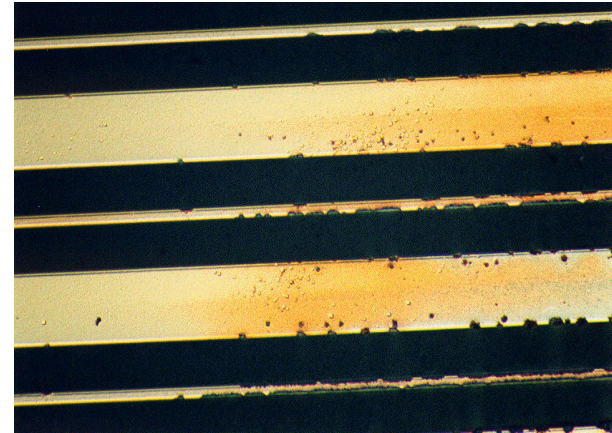
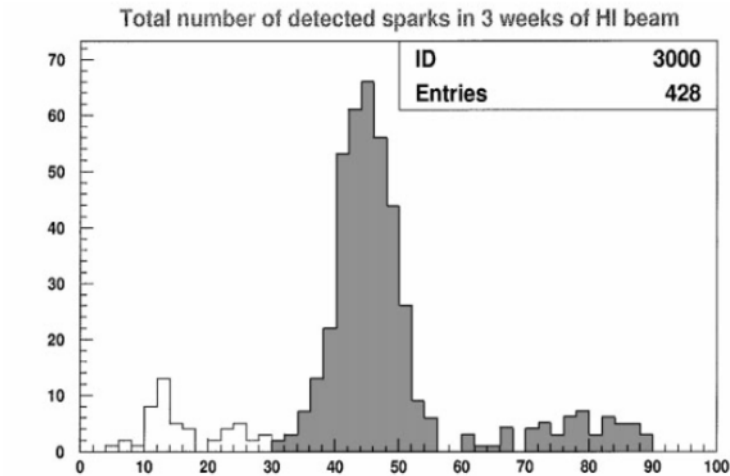
R. Bouclier et al, *Nucl. Instr. and Meth. A323(1992)240*

Micro Strip Gas Chambers (MSGCs)

Unfortunately MSGCs are rather prone to discharge, particularly in hostile environments.

Discharges measured in the CMD MSGC prototypes at PSI:

Strip damages due to Micro Discharges and heavy sparks:

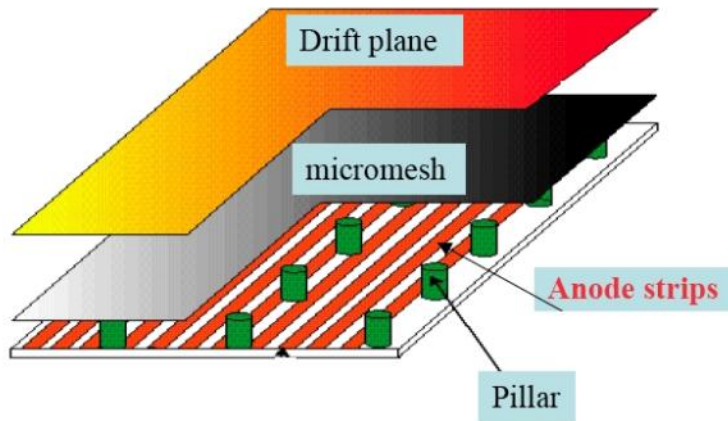
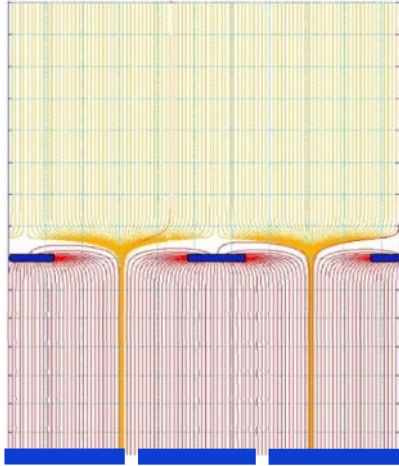


CERN-GDD

GEMs & MICROMEAS

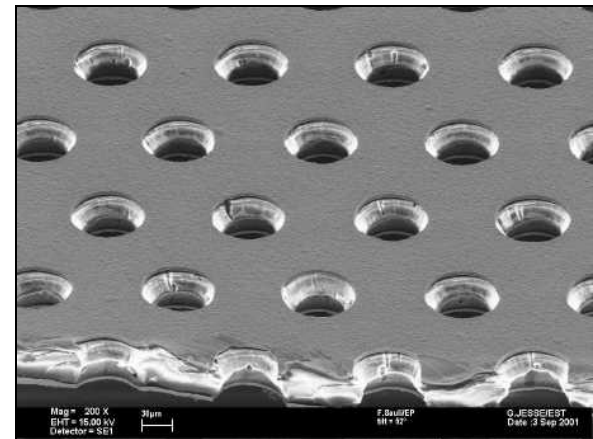
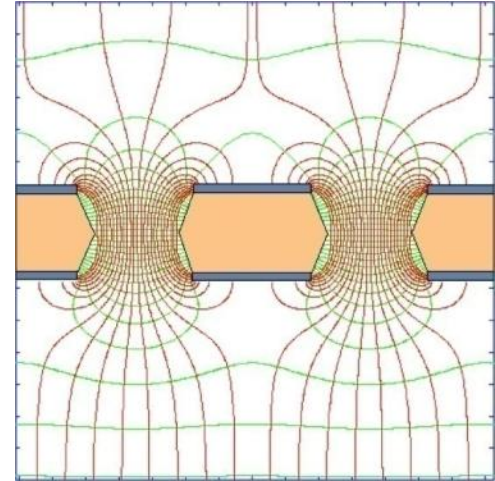
MICROMEAS

Narrow gap (50-100 μm) PPC with thin cathode mesh
Insulating gap-restoring wires or pillars



GEM

Thin metal-coated polymer foils
70 μm holes at 140 μm pitch

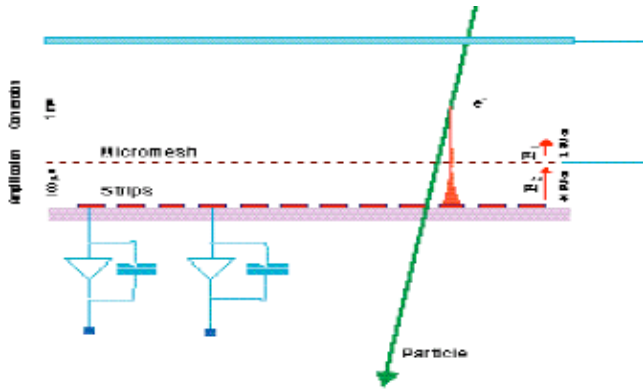


Y. Giomataris et al, Nucl. Instr. and Meth. A376(1996)239

F. Sauli, Nucl. Instr. and Methods A386(1997)531

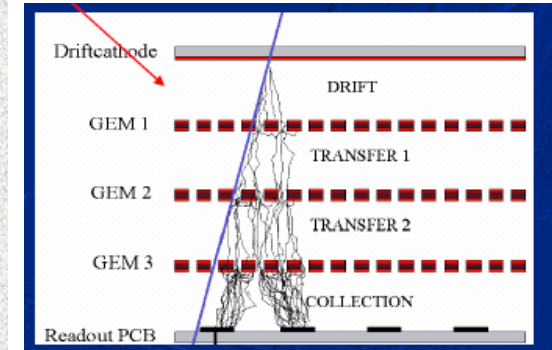
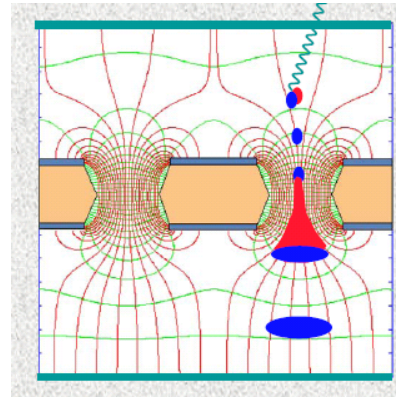
GEMs & MICROMEAS

MICROMEAS



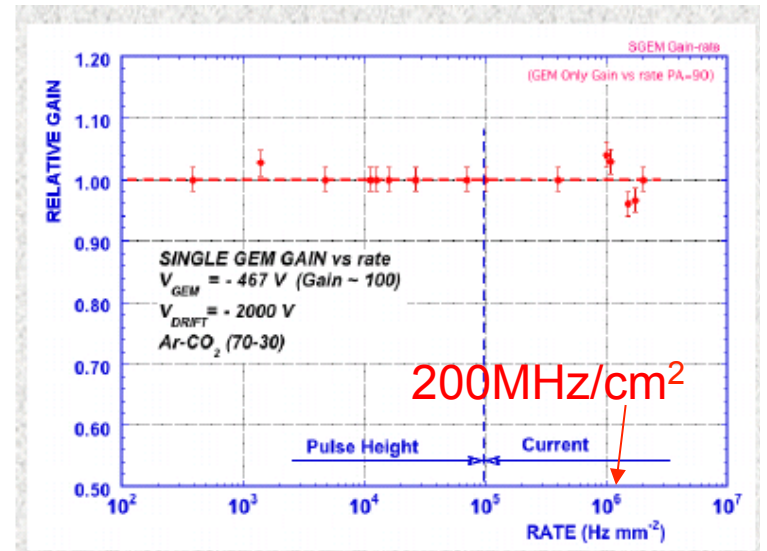
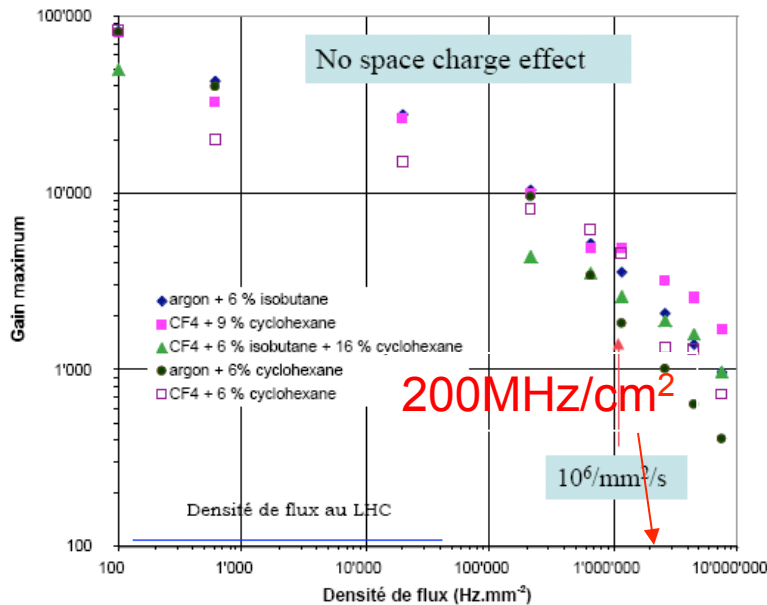
Micromegas use typical drift gaps of 1-3mm and avalanche multiplication gaps of 50-100um.

GEM

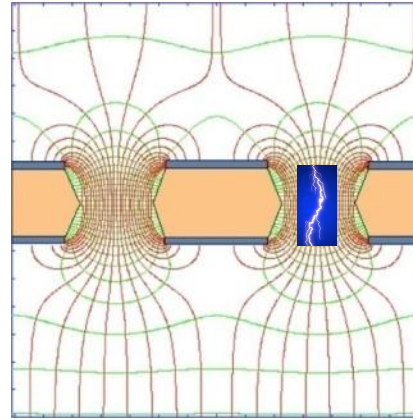
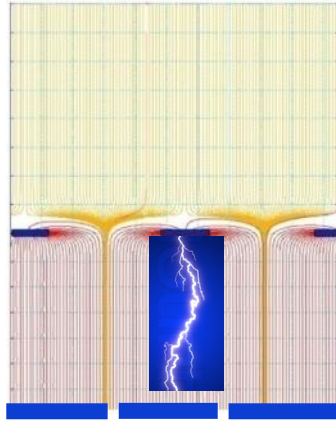


GEMs are typically cascaded in order to reduced the gain/stage and therefore the sparking probability.

GEM and MICROMEAS show intrinsic rate capabilities of up to 200MHz/cm²



Micropattern Gas Detectors, Sparks



Due to the presence of insulators and ‘undefined’ edges with high electric fields, MPGDs have initially been suffering from spark discharges that can either damage the detector, damage the electronics and cause dead time due to the recharging time of the electrodes.

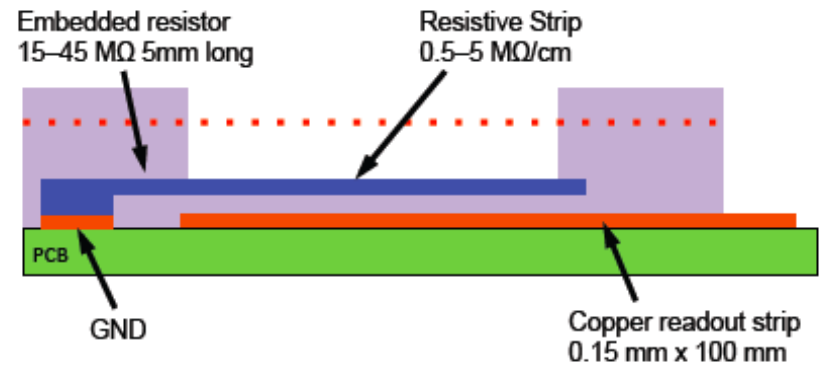
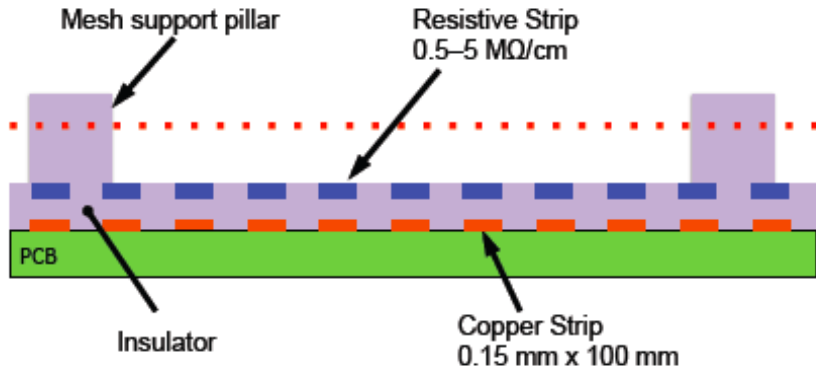
GEMs and MICROMEAS are ‘not’ damaged by sparks. The problem of dead-time is addressed by segmentation of the GEM foils of MICROMEGA meshes.

GEMs have strongly reduced the sparking problems due to cascading of GEM stages (Triple GEM).

MICROMEAS have reduced spark rates by technological improvements and are using resistive layers on the readout plane for protection of the electronics.

Resistive Micromega

ATLAS Phase1 small wheel upgrade

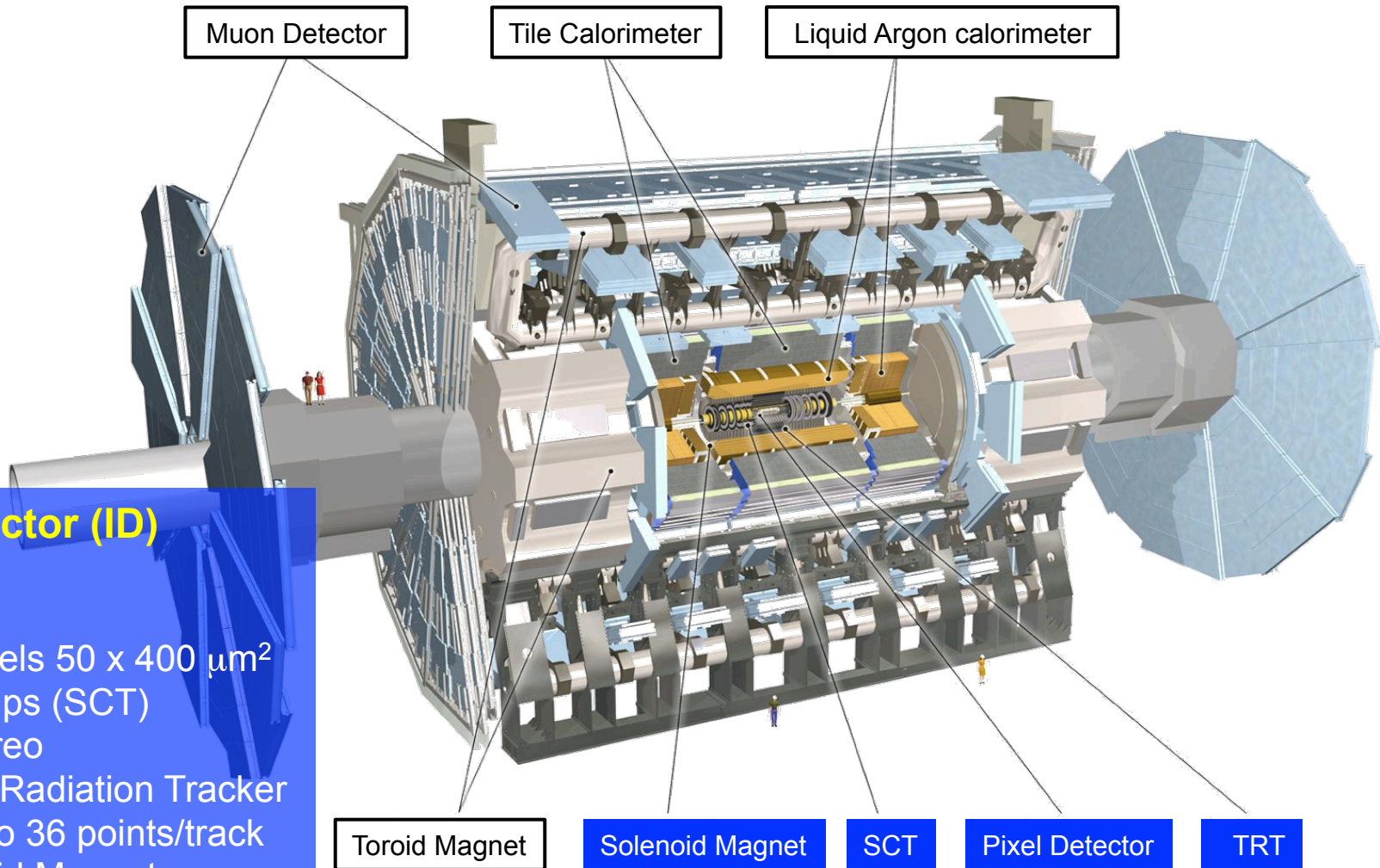


The ATLAS Experiment upgrade

The ATLAS Upgrade Programme

Thorsten Wengler
ECFA High Luminosity
LHC Experiments Workshop
1st – 3rd October 2013
Aix-les-Bains, France

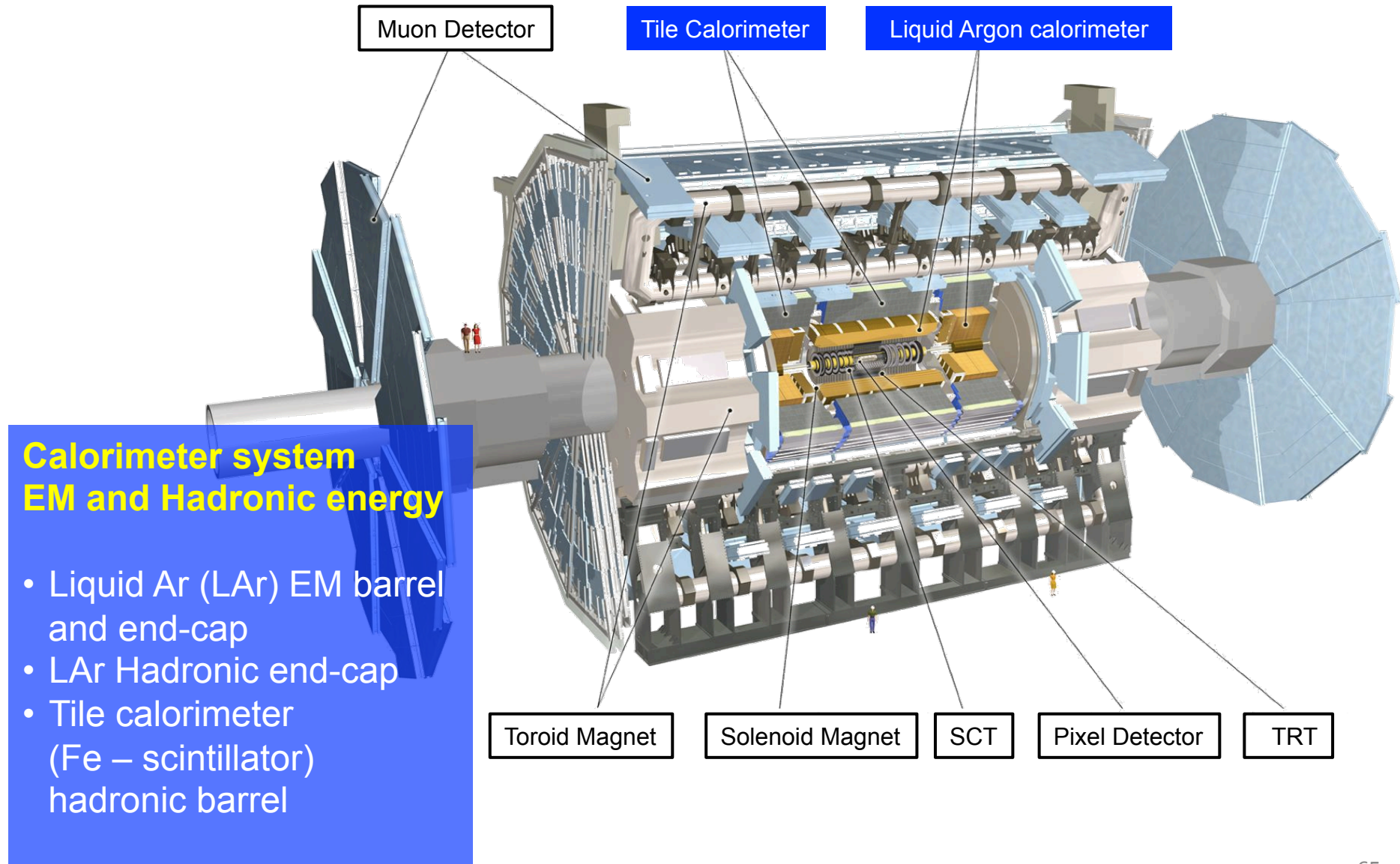
The ATLAS Detector



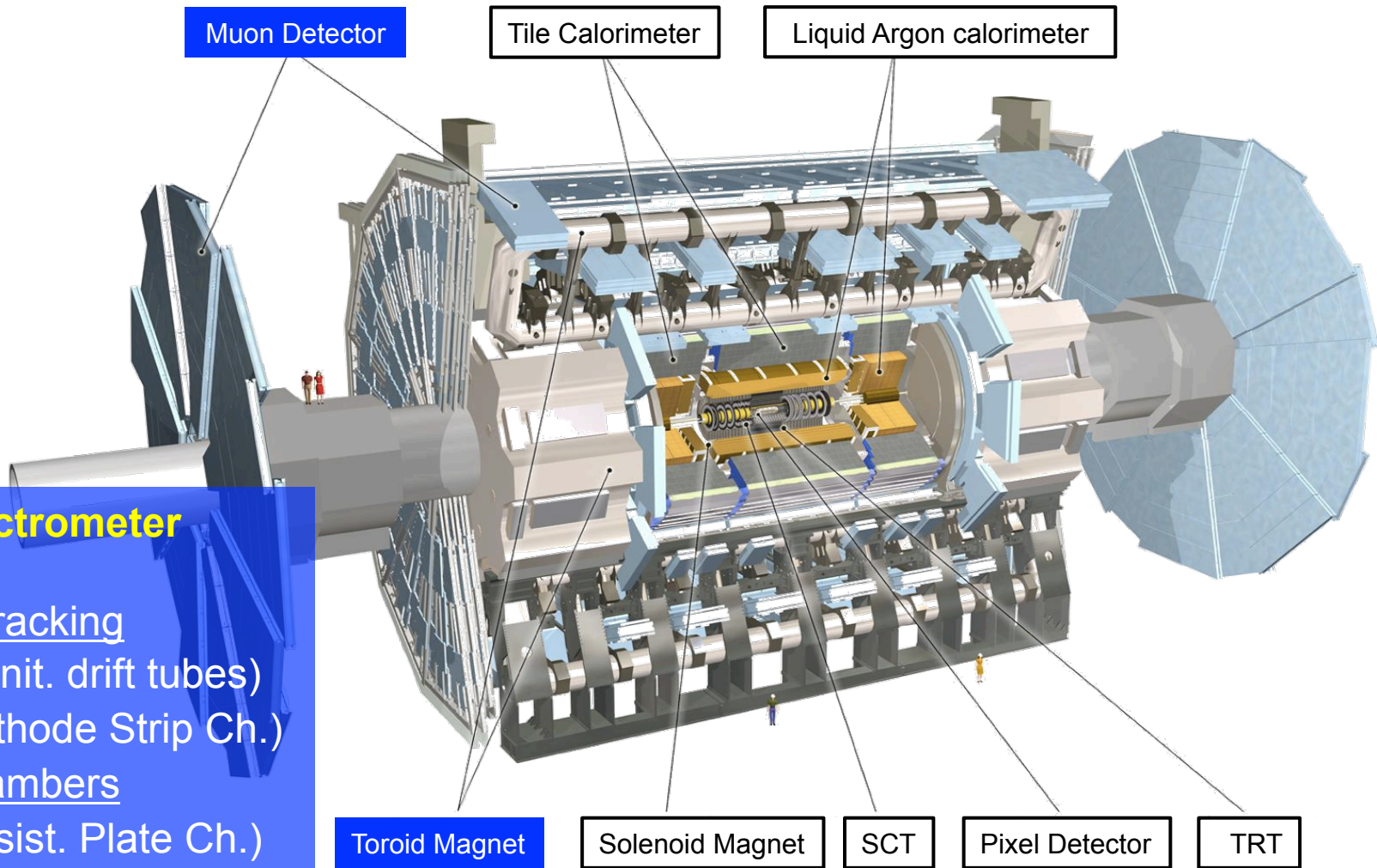
Inner Detector (ID) Tracking

- Silicon Pixels $50 \times 400 \mu\text{m}^2$
- Silicon Strips (SCT)
 $80 \mu\text{m}$ stereo
- Transition Radiation Tracker (TRT) up to 36 points/track
- 2T Solenoid Magnet

The ATLAS Detector



The ATLAS Detector



Muon spectrometer μ tracking

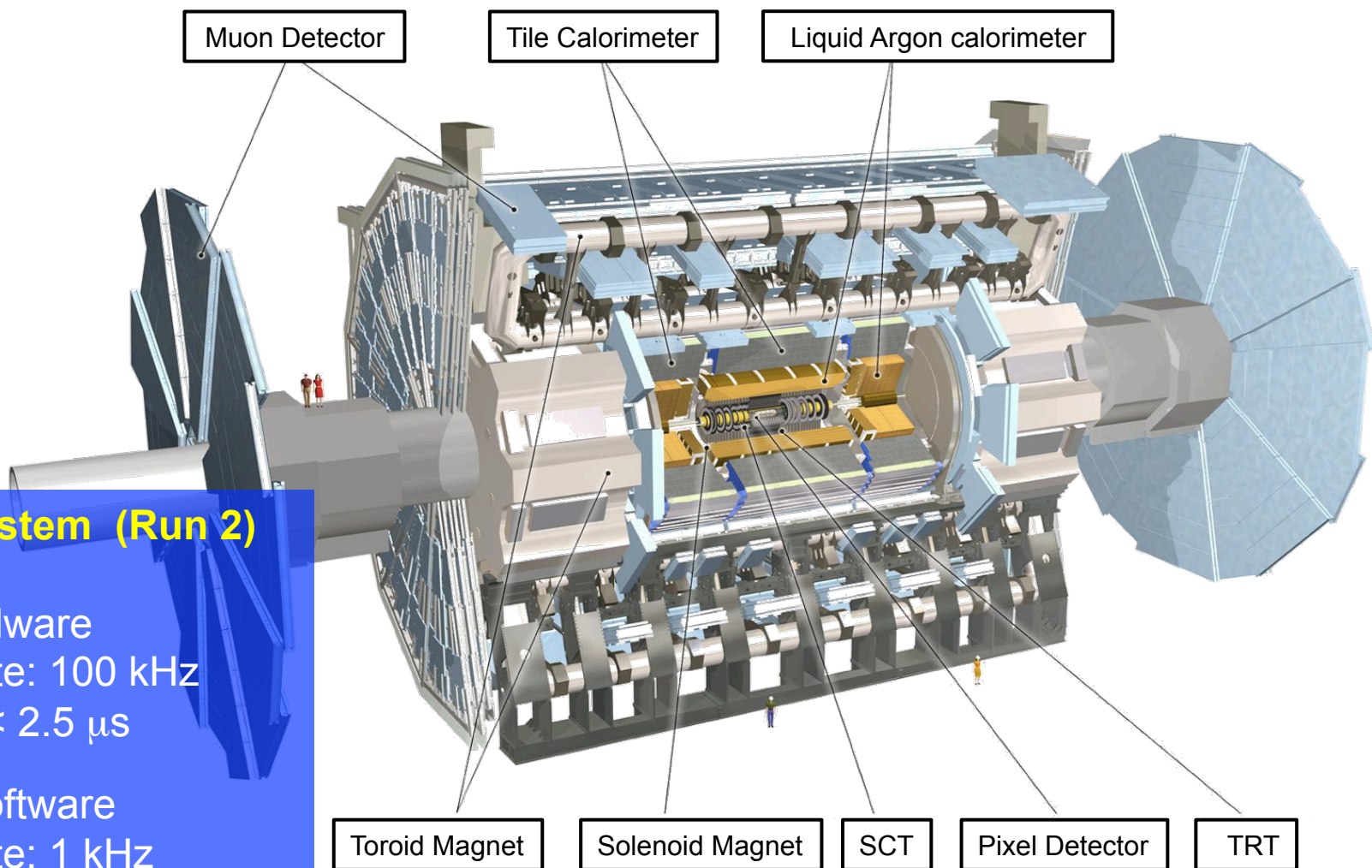
Precision tracking

- MDT (Monit. drift tubes)
- CSC (Cathode Strip Ch.)

Trigger chambers

- RPC (Resist. Plate Ch.)
- TGC (Thin Gap Ch.)
- Toroid Magnet

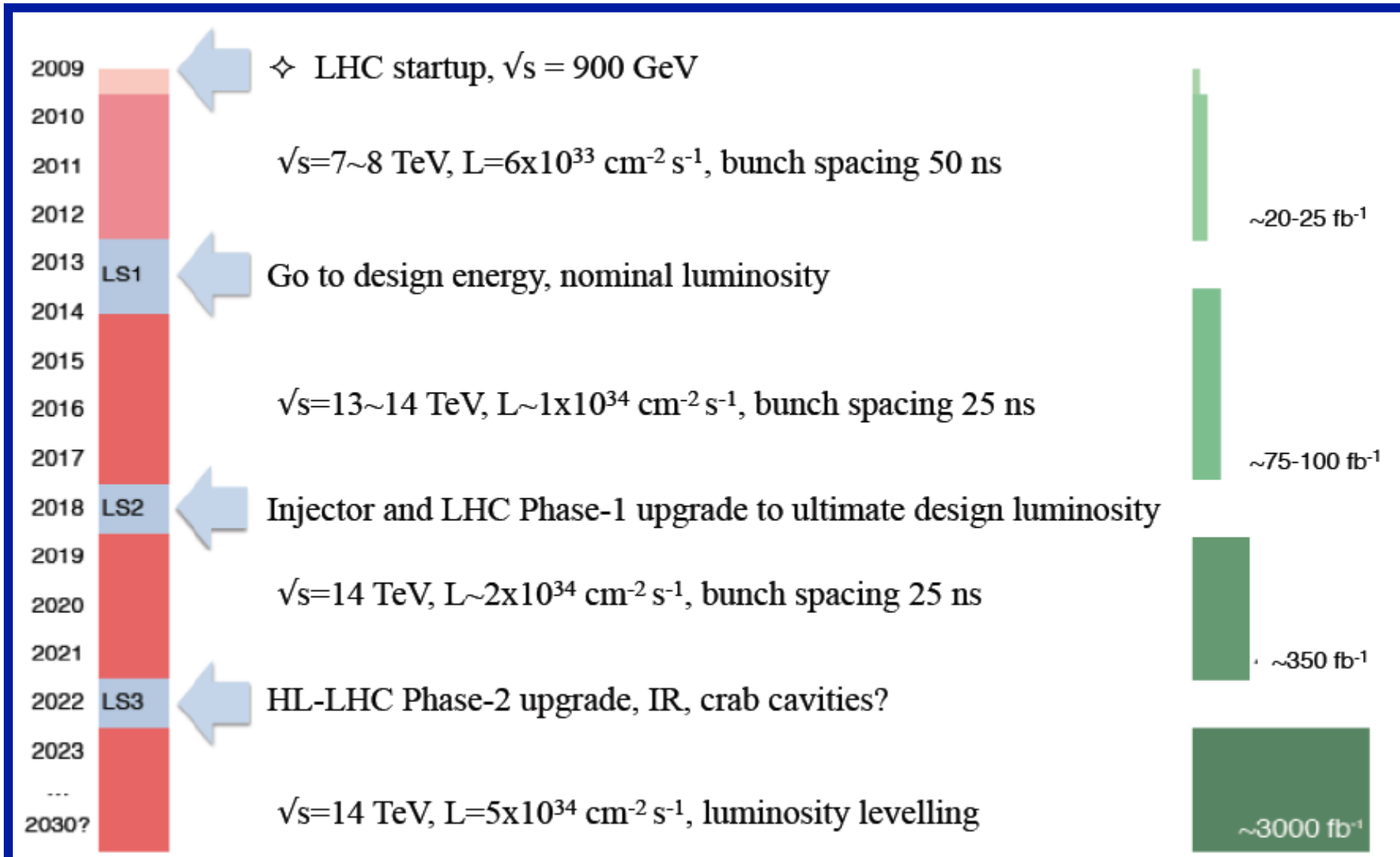
The ATLAS Detector



Trigger system (Run 2)

- L1 – hardware
output rate: 100 kHz
latency: $< 2.5 \mu\text{s}$
- HLT – software
output rate: 1 kHz
proc. time: $\sim 550 \text{ ms}$

The LHC roadmap



The ATLAS upgrade programme



CERN-LHCC-2011-012
LHCC-I-020
December, 2011

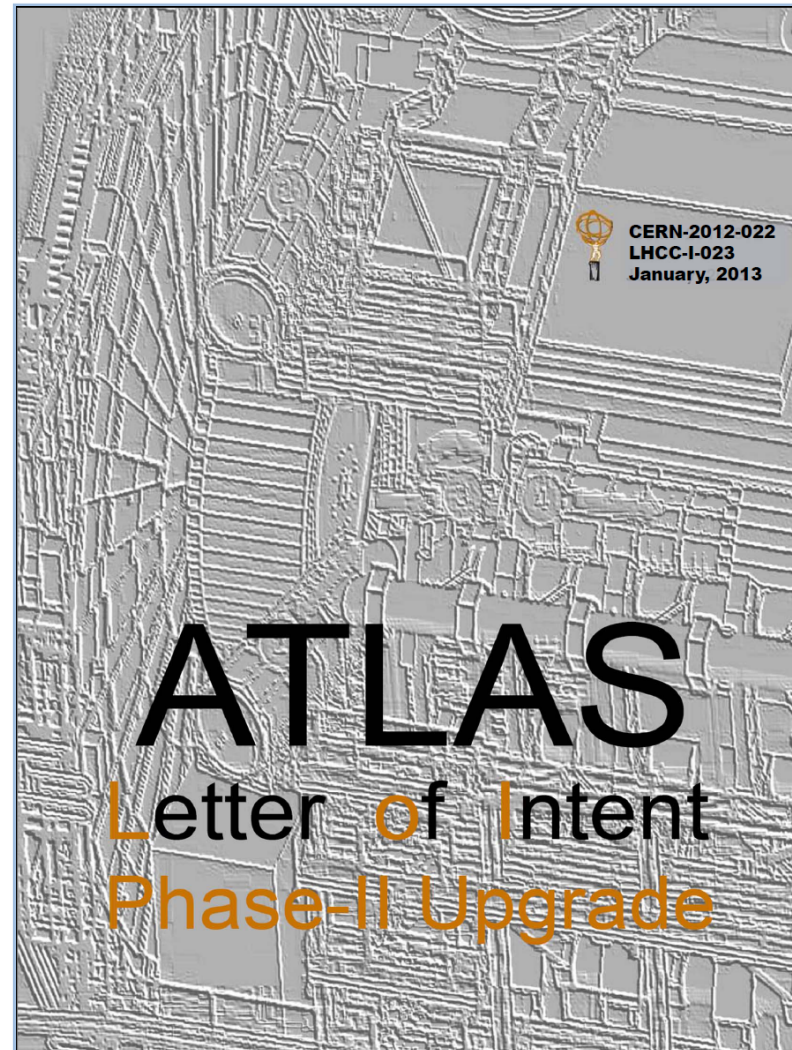
TDRs approved by LHCC

- New Small Wheel
- Fast Track Trigger

TDRs submitted to LHCC

- Trigger/DAQ
- LAr Trigger

ATLAS
Letter of Intent
Phase-I Upgrade

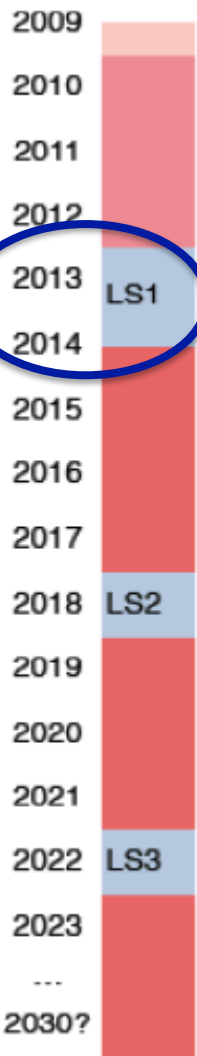


CERN-2012-022
LHCC-I-023
January, 2013

ATLAS
Letter of Intent
Phase-II Upgrade

+ TDR of Insertable B-Layer (Phase-0)

ATLAS Upgrade Plan



$\sqrt{s} = 13\sim 14$ TeV, 25ns bunch spacing
 $L_{\text{inst}} \approx 1 \times 10^{34} \text{ cm}^{-2}\text{s}^{-1}$ ($\mu=27.5$)
 $\int L_{\text{inst}} \approx 50 \text{ fb}^{-1}$

- New Insertable pixel b-layer (IBL) and pixel services
- New Al/Be beam pipe
- New ID cooling
- Upgrades to L1 Central Trigger
- Detector consolidation (e.g. calorimeter power supplies)
- Add specific neutron shielding
- Finish installation of EE muon chambers staged in 2003
- Upgrade magnet cryogenics

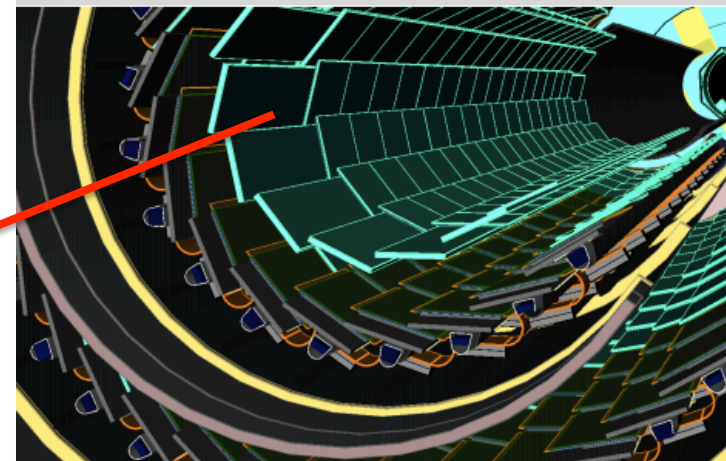
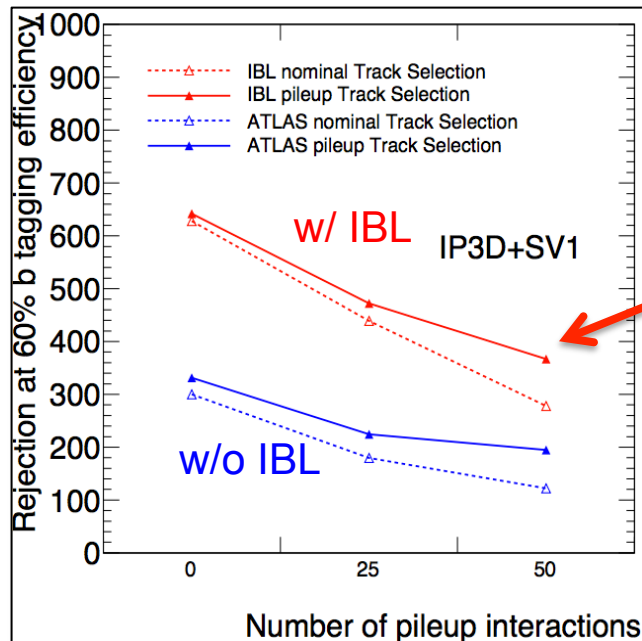
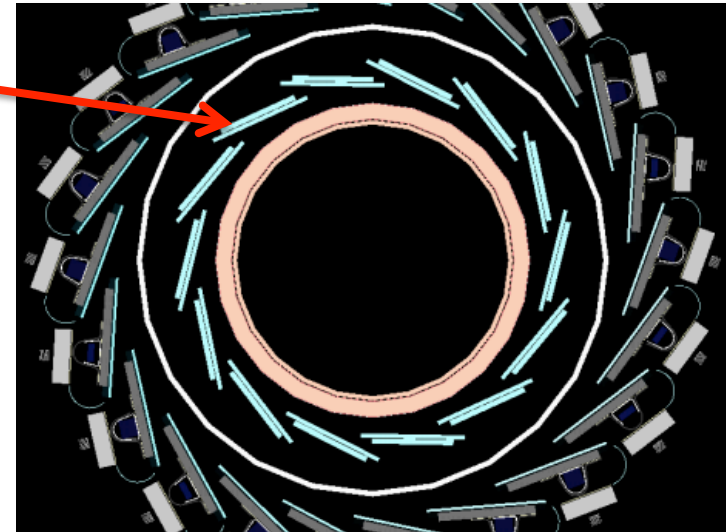
Phase-0

New inner pixel layer
Detector consolidation

Ongoing: Phase-0 upgrades (LS-1)

- **Insertable B-Layer**

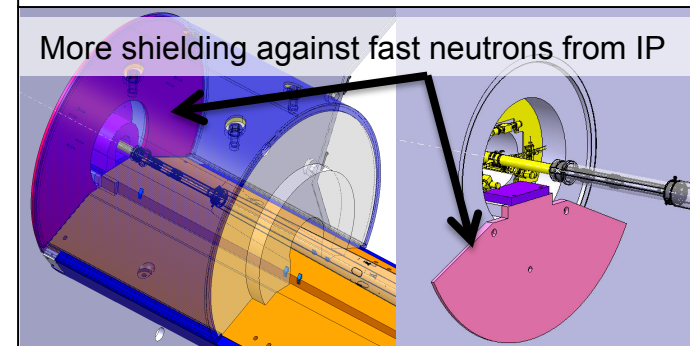
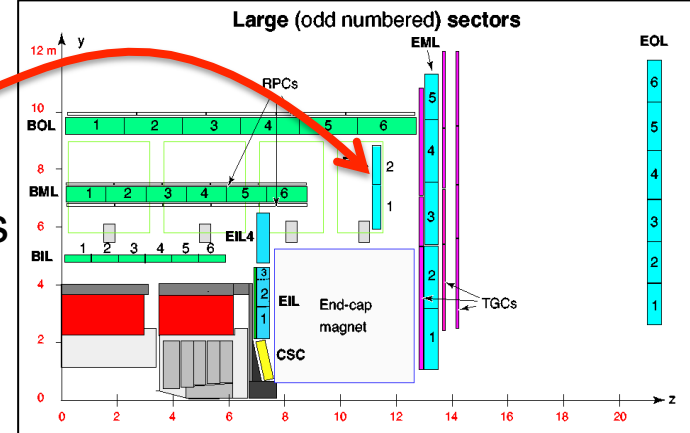
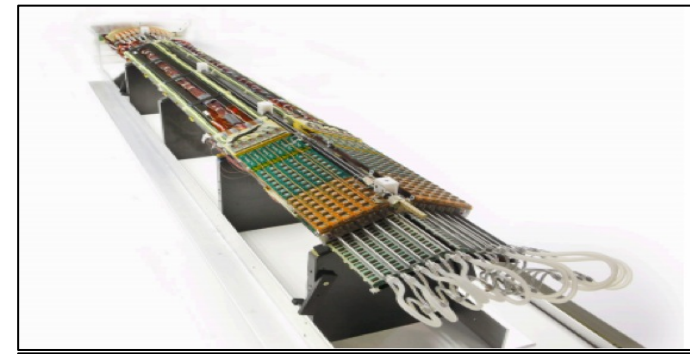
- Production/Integration on schedule
- Installation of IBL in the pixel detector, in the pit: March 2014
- Important ingredient for low mass, rad-hard construction: 2 cm x 2 cm FE-I4 Pixel Chip, 130 nm CMOS process
- Will stay until Phase-II



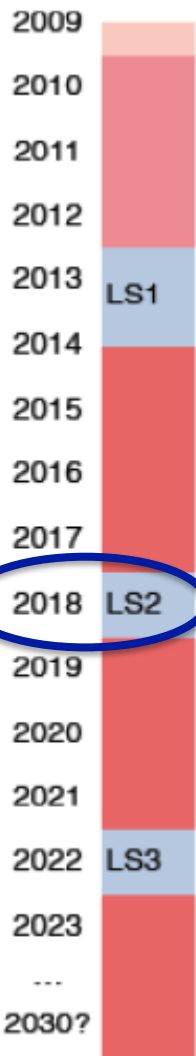
b-tagging rejection vs pile-up

Ongoing: Phase-0 upgrades (LS1)

- Pixel Detector
 - new service panels – recover malfunctioning channels, better access, more bandwidth
- Pixel + SCT Detectors
 - New thermoshipon cooling system, keeping evaporative cooling system as backup
- Muon spectrometer
 - Install Muon End-cap Extension (EE) chambers to improve coverage at $1.0 < |n| < 1.3$
- Add specific neutron shielding
- Detector consolidation
 - Calorimeter power supplies
 - Optical readout elements, ...
 - Magnet cryogenics



ATLAS Upgrade Plan



ultimate luminosity
 $L_{\text{inst}} \approx 2-3 \times 10^{34} \text{ cm}^{-2}\text{s}^{-1}$ ($\mu \approx 55-81$)
 $\int L_{\text{inst}} \gtrsim 350 \text{ fb}^{-1}$

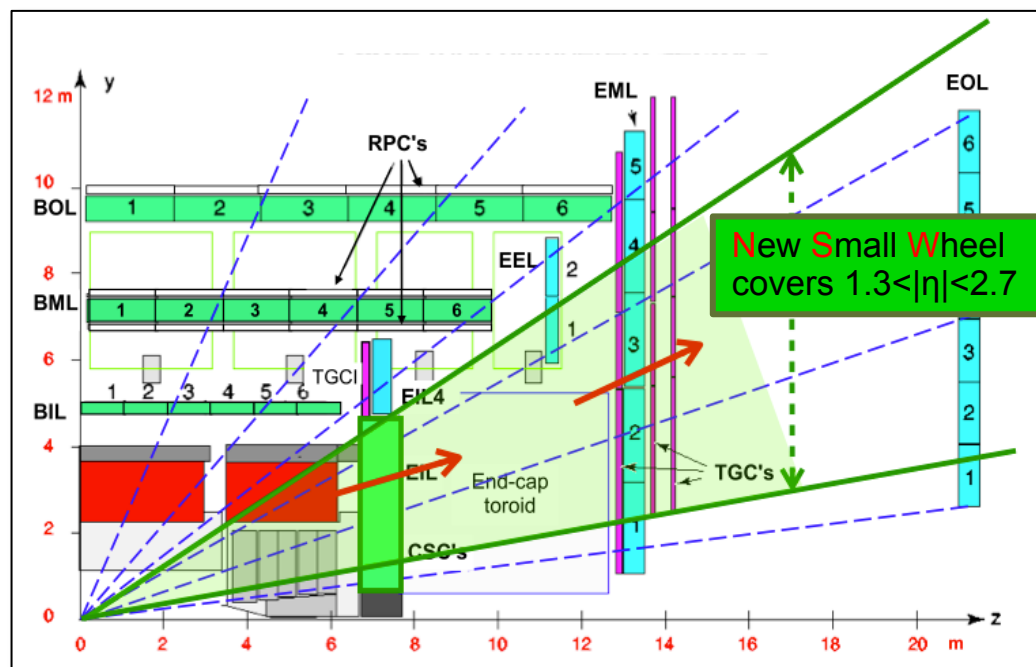
- New Small Wheel (NSW) for the forward muon Spectrometer
- High Precision Calorimeter Trigger at Level-1
- Fast Tracking (FTK) for the Level-2 trigger
- Topological Level-1 trigger processors
- Other Trigger and DAQ upgrades, e.g. Muon Trigger interface (MuCTPI)
- ATLAS Forward Physics (AFP), proton det. at $\pm 210 \text{ m}$

Phase-1

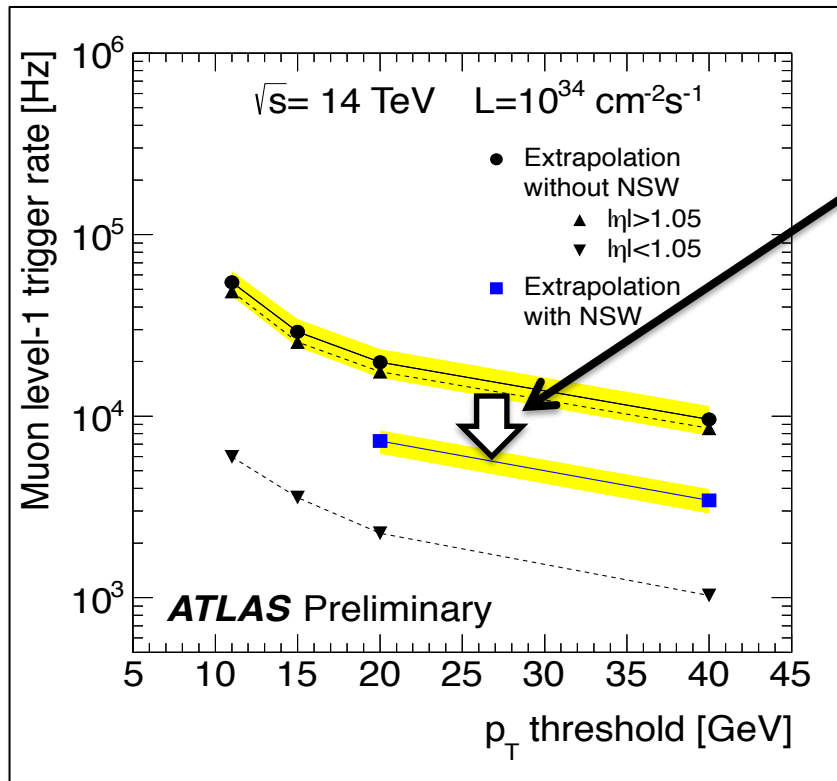
Improve L1 Trigger capabilities to cope with higher rates

Muons: New Small Wheel

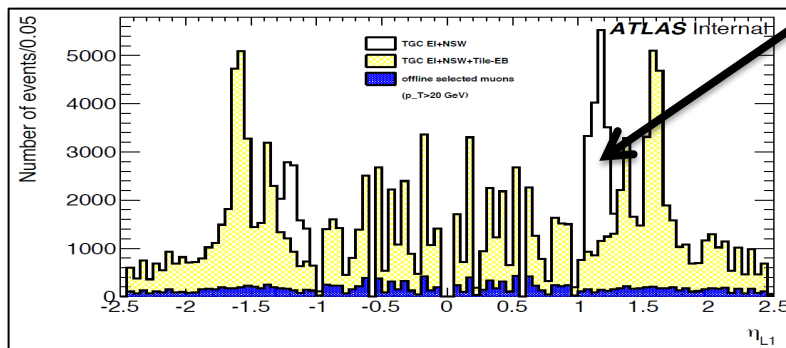
- Consequences of luminosity rising beyond design values for forward muon wheels
 - degradation of the tracking performance (efficiency / resolution)
 - L1 muon trigger bandwidth exceeded unless thresholds are raised
- Replace Muon Small Wheels with **New Muon Small Wheels**
 - improved tracking and trigger capabilities
 - position resolution $< 100 \mu\text{m}$
 - IP-pointing segment in NSW with $\sigma_\theta \sim 1 \text{ mrad}$
 - Meets Phase-II requirements
 - compatible with $\langle \mu \rangle = 200$, up to $L \sim 7 \times 10^{34} \text{ cm}^{-2}\text{s}^{-1}$
 - Technology: MicroMegas and sTGCs



Muons: New Small Wheel cont.



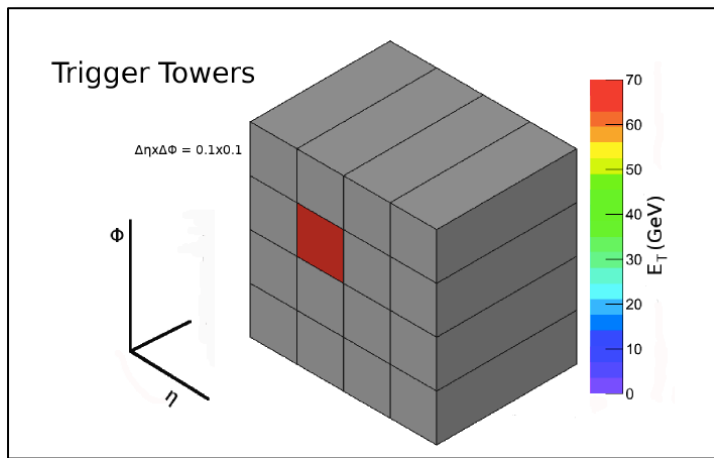
- Strong reduction of muon L1 trigger rate in forward direction
 - Dominated by fakes
- Vital for running at high luminosity
- In addition smaller improvements during phase-0
 - Additional muon chambers in barrel/end-cap overlap region
 - Coincidences with outer layers of Tile Calorimeter removes peak of muon fakes



Level-1 calorimeter trigger

Run-1 calorimeter trigger input:
Trigger Towers $\Delta\eta \times \Delta\phi = 0.1 \times 0.1$

- Used to calculate core energy, isolation



Run-1 trigger menu
at $L_{inst} = 3 \times 10^{34} \text{ cm}^{-2}\text{s}^{-1}$



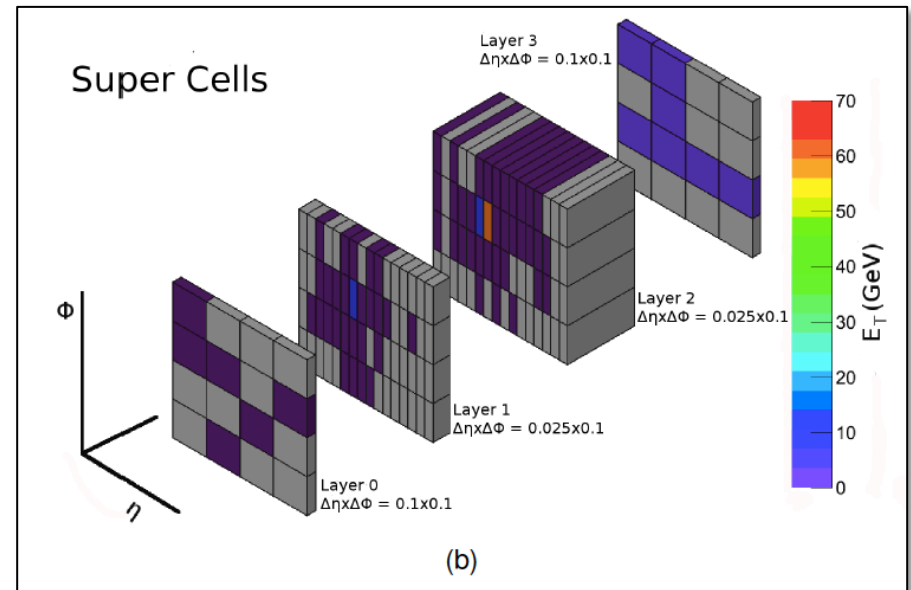
Total rate for EM triggers
would be **270 kHz!**
(Total L1 bandwidth is 100kHz)



maintain lower thresholds
at an acceptable rate



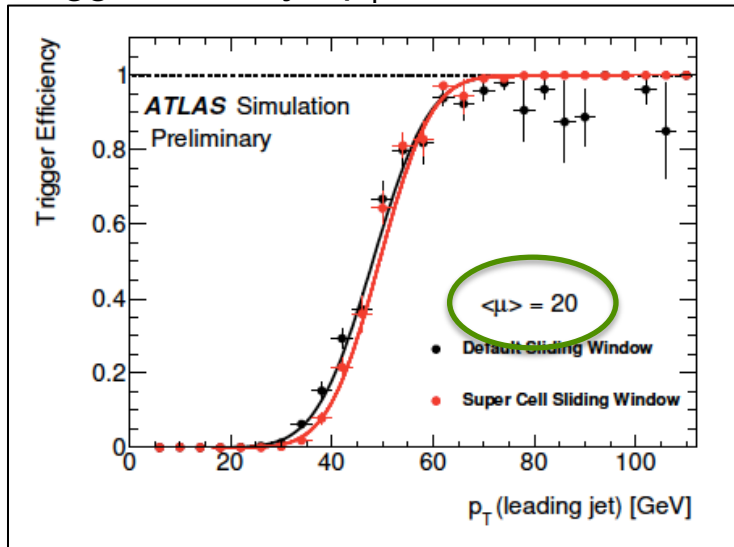
Provide better granularity
and better energy resolution



Complemented by new L1Calo
trigger processors eFEX and jFEX

Level-1 calorimeter trigger cont.

Trigger eff. vs jet p_T



Significant degradation of the turn-on curve with pile up ($\langle \mu \rangle = 80$)

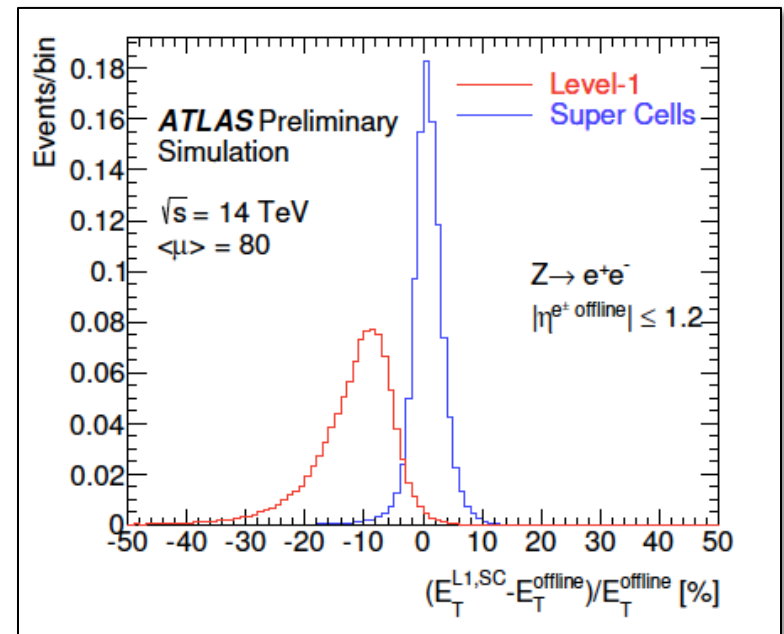
- requiring much higher offline threshold (black curve)
- recovered through introduction of super-cells (red curve)

EM Triggers

- Better shower shape discrimination
→ lower EM threshold by ~ 7 GeV at same rate
- In addition significantly improved resolution
→ lower EM threshold by another few GeV at same rate

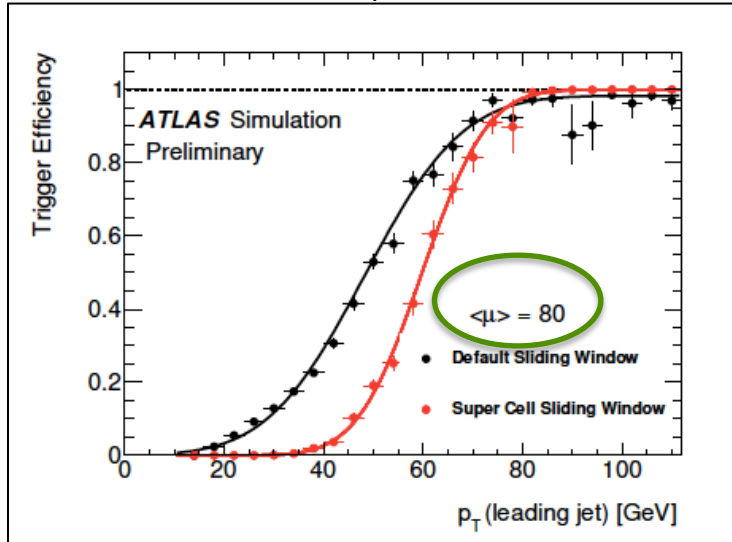
Topological triggering

- Will feed calorimeter trigger input to L1 topological processor (already in Phase-0)



Level-1 calorimeter trigger cont.

Trigger eff. vs jet p_T



Significant degradation of the turn-on curve with pile up ($\langle\mu\rangle=80$)

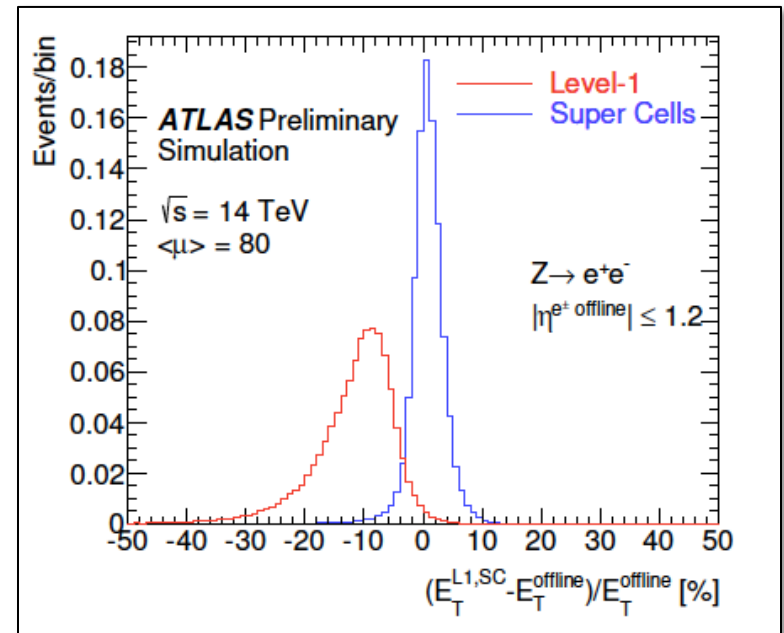
- requiring much higher offline threshold (black curve)
- recovered through introduction of super-cells (red curve)

EM Triggers

- Better shower shape discrimination
→ lower EM threshold by ~ 7 GeV at same rate
- In addition significantly improved resolution
→ lower EM threshold by another few GeV at same rate

Topological triggering

- Will feed calorimeter trigger input to L1 topological processor (already in Phase-0)



Fast Track Trigger (FTK)

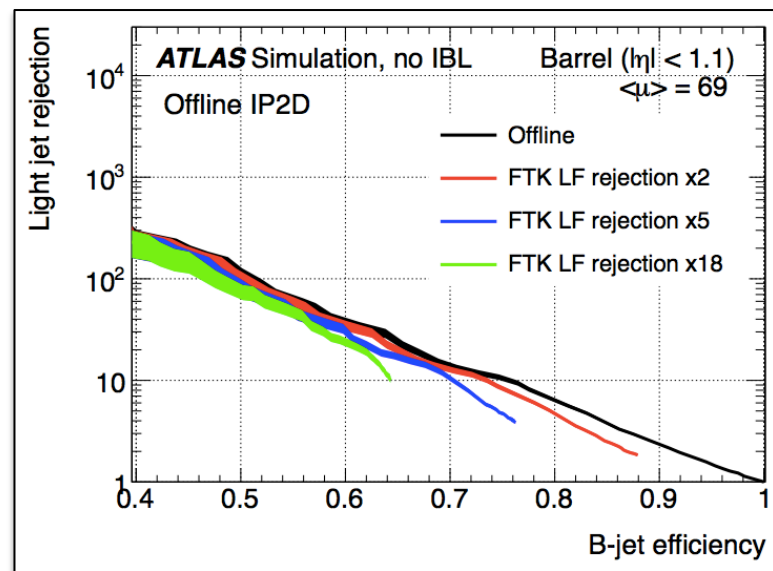
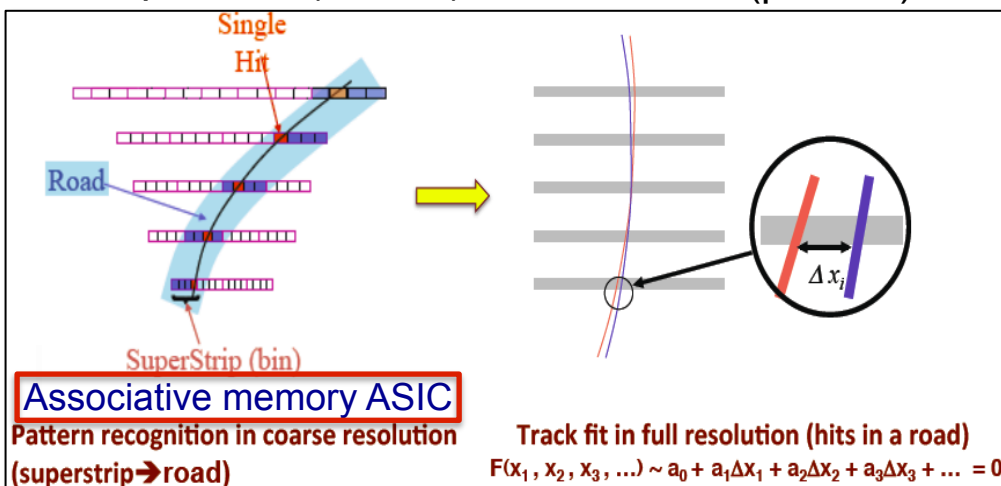
- Dedicated, hardware-based track finder
 - Runs after L1, on duplicated Si-detector read-out links
 - Provides tracking input for L2 for the full event
 - not feasible with software tracking at L2
 - Finds and fits tracks ($\sim 25 \mu\text{s}$) in the ID silicon layers at an “offline precision”

- Processing performed in two steps



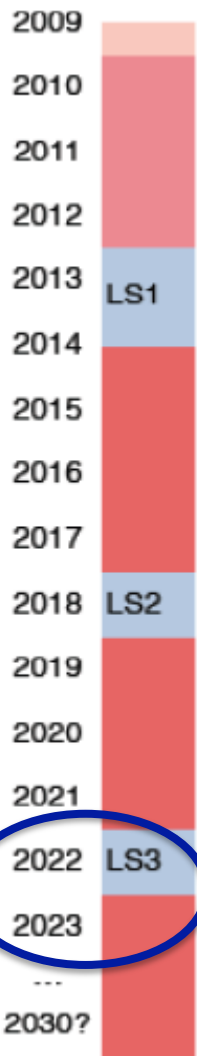
hit pattern matching to pre-stored patterns (coarse)

subsequent linear fitting in FPGAs (precise)



Light jet rejection using FTK compared to offline reconstruction (further improved by addition of IBL)

ATLAS Upgrade Plan



$L_{\text{inst}} \approx 5 \times 10^{34} \text{ cm}^{-2}\text{s}^{-1}$ ($\mu \approx 140$) w. level.
 $\approx 6-7 \times 10^{34} \text{ cm}^{-2}\text{s}^{-1}$ ($\mu \approx 192$) no level.
 $\int L_{\text{inst}} \approx 3000 \text{ fb}^{-1}$

- All new Tracking Detector
- Calorimeter electronics upgrades
- Upgrade muon trigger system
- Possible Level-1 track trigger
- Possible changes to the forward calorimeters

Phase-2

Prepare for $\langle \mu \rangle = 200$
Replace Inner Tracker
New L0/L1 trigger scheme
Upgrade muon/calorimeter electronics

New Tracking detector

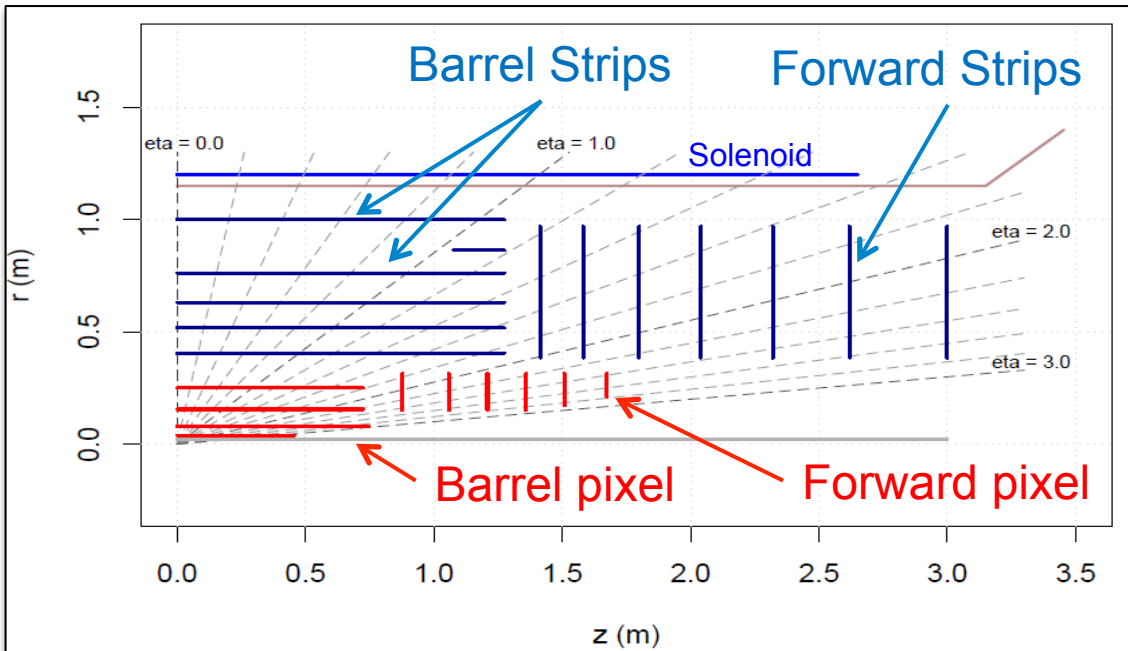
- **Current Inner Detector (ID)**

- Designed to operate for 10 years at $L=1 \times 10^{34} \text{ cm}^{-2}\text{s}^{-1}$ with $\langle \mu \rangle = 23$, @25ns, L1=100kHz

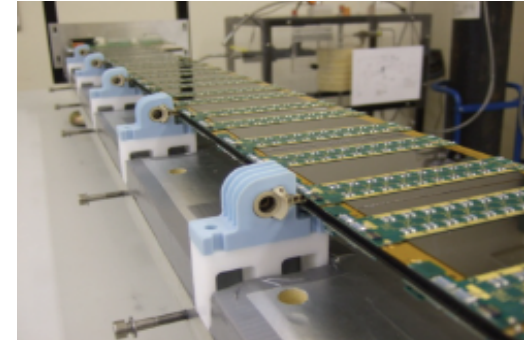
- **Limiting factors at HL-LHC**

- Bandwidth saturation (Pixels, SCT)
- Too high occupancies (TRT, SCT)
- Radiation damage (Pixels (SCT) designed for 400 (700) fb^{-1})

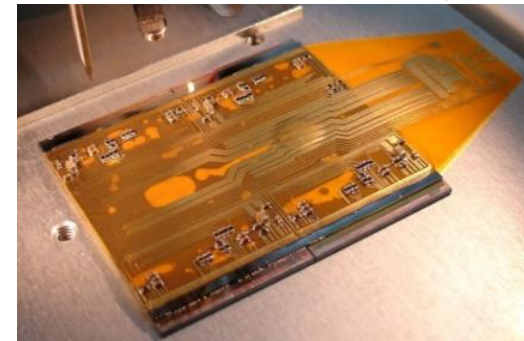
Lol layout new (all Si) ATLAS Inner Tracker for HL-LHC



Microstrip Stave Prototype



Quad Pixel Module Prototype



New 130nm prototype strip ASICs in production

- incorporates L0/L1 logic

Sensors compatible with 256 channel ASIC being delivered

New Tracking detector cont.

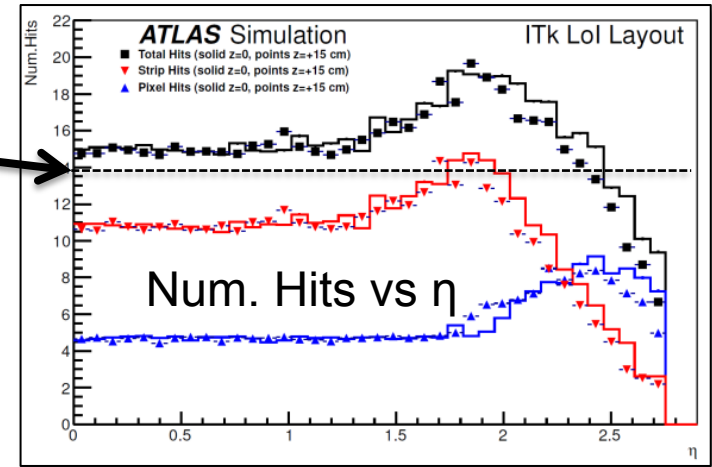
- Studies with LOI layout

- Robust tracking (14 layers)
- Occupancy <math><\mu>=200</math>
- Reduced material wrt current ID
- Comparable / better tracking performance at <math><\mu>=200</math> as current ID at <math><\mu>=0</math>

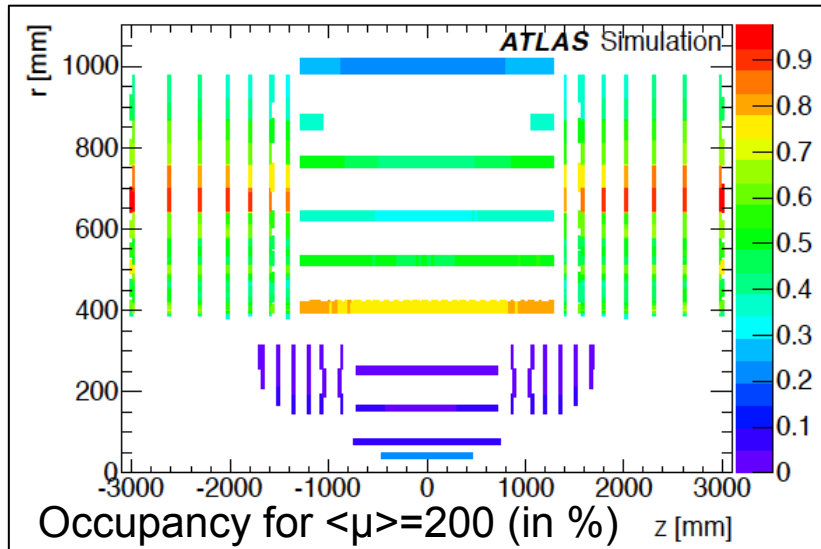
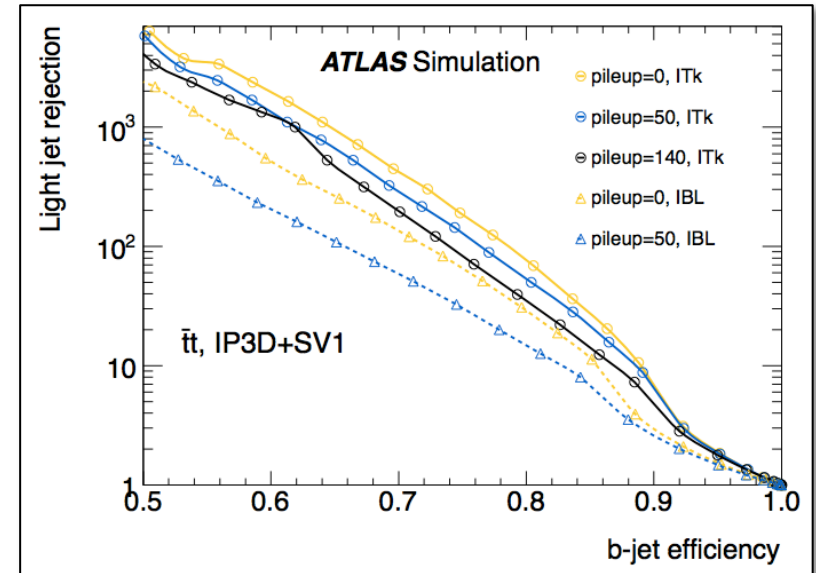
- Prototypes tested to 2x HL-LHC flux

- Solid baseline design

- working on optimisation

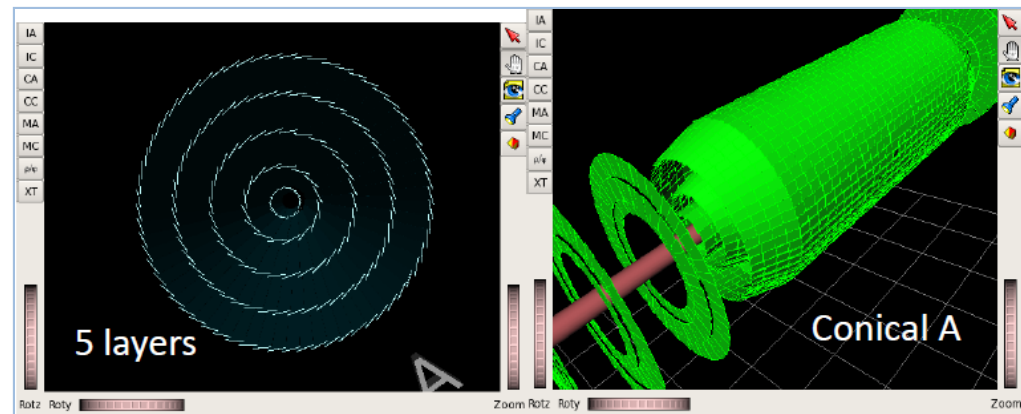


Light jet rejection, ID (w/IBL) and ITk



New Tracking detector cont.

- Many topics still to be addressed
 - How can the layout still be optimised?
 - Can all assemblies/components be qualified to the required radiation hardness?
 - How critical is the luminous beam-spot extent in z ?
 - Are there physics reasons to significantly extent the coverage in η ?
 - Cost / material optimisations with current technologies?
 - Alternative technologies?
- Addressing these questions now is very timely
 - note TDR of current ID was written in 1997 ...



Alternative layouts being considered which include either a further pixel layer or inclined pixel

Trigger system architecture

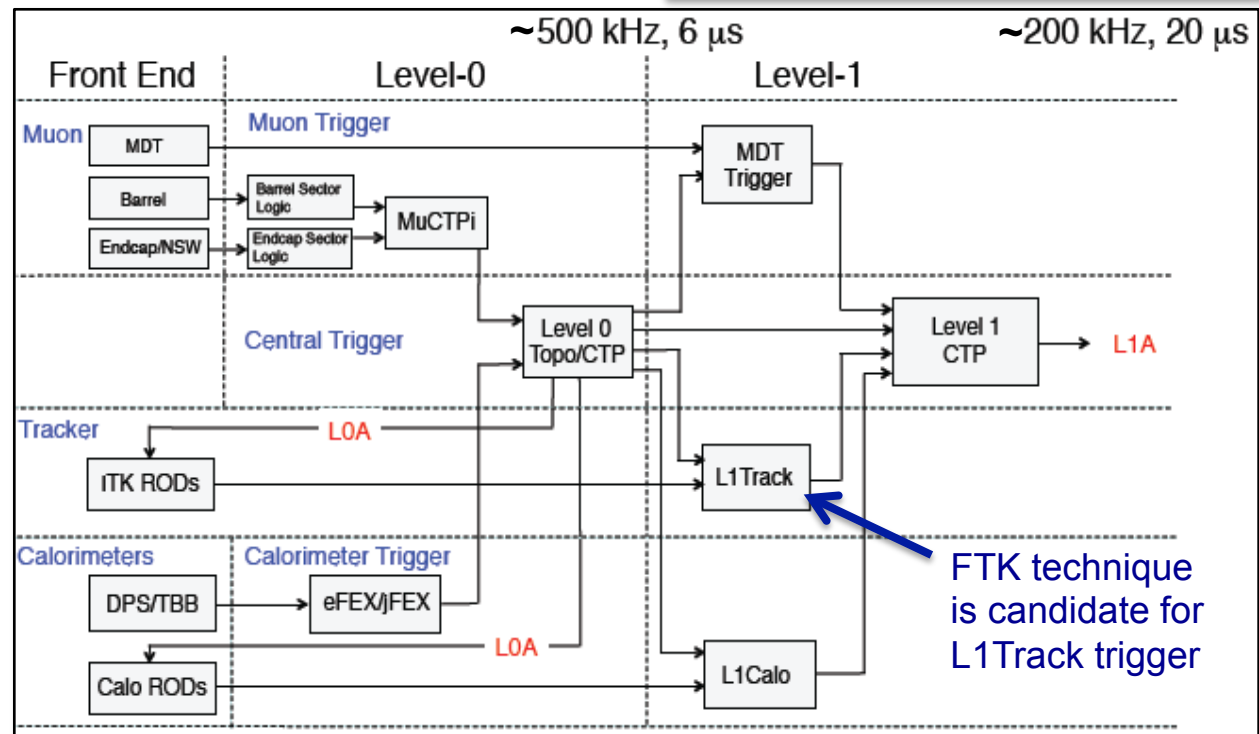
- New design for Phase II

- 2-level system, Phase-I L1 becomes Phase-II L0, new L1 includes tracking
- Make use of improvements made in Phase 1 (NSW, L1Calo) in L0
- Introduce precision muon and inner tracking information in L1
 - Better muon pT resolution
 - Track matching for electrons,...
- Requires changes to detector FE electronics feeding trigger system

Will also have new timing/control links and LHC interface system

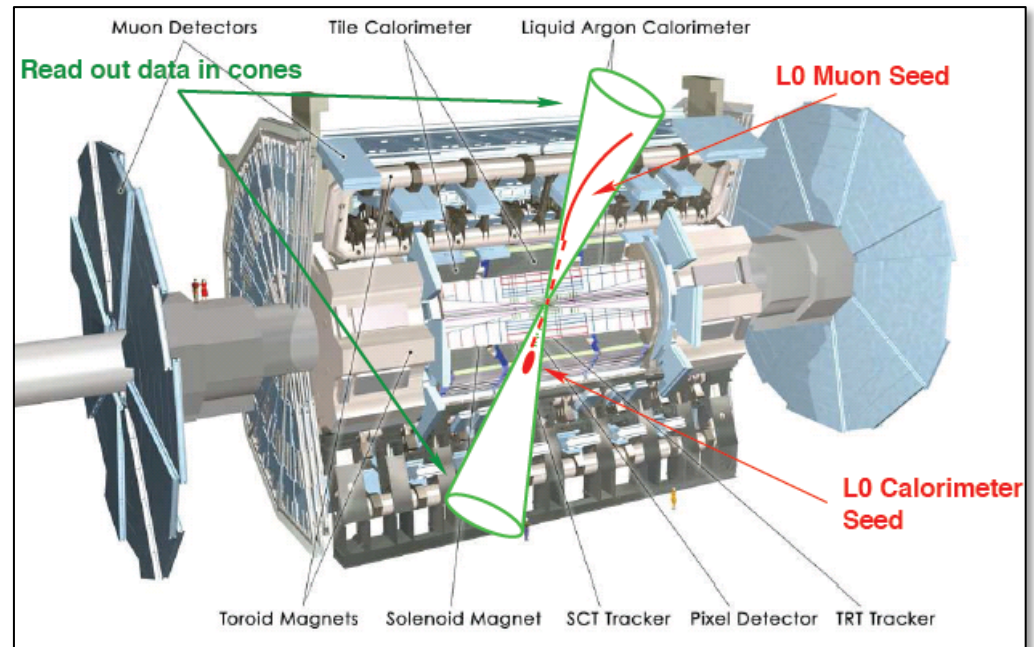
Level-0
 Rate ~ 500 kHz, Lat. ~6 μ s
 Muon + Calo

Level-1
 Rate ~200 kHz, Lat. ~20 μ s
 Muon + Calo + Tracks



L1Track Trigger

- Adding tracking information at Level-1 (L1)
 - Move part of High Level Trigger (HLT) reconstruction into L1
 - Goal: keep thresholds on p_T of triggering leptons and L1 trigger rates low
- Triggering sequence
 - L0 trigger (Calo/Muon) reduces rate within $\sim 6 \mu\text{s}$ to $\geq 500 \text{ kHz}$ and defines Rols
 - L1 track trigger extracts tracking info inside Rols from detector FEs
- Challenge
 - Finish processing within the latency constraints



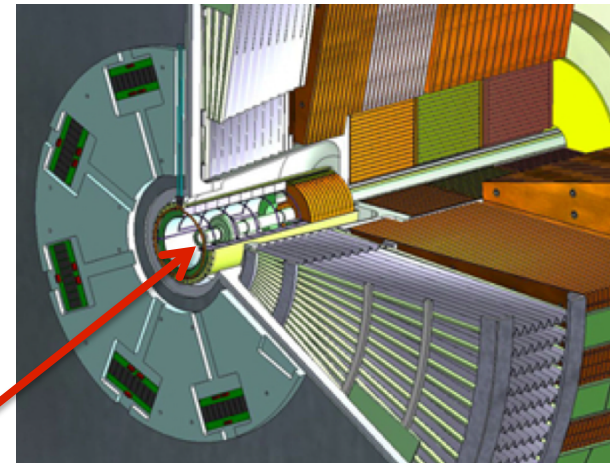
Calorimeter electronics

- **Tile Calorimeters**

- No change to detector needed
- Full replacement of FE and BE electronics
 - New read-out architecture: Full digitisation of data at 40MHz and transmission to off-detector system, digital information to L1/L0 trigger

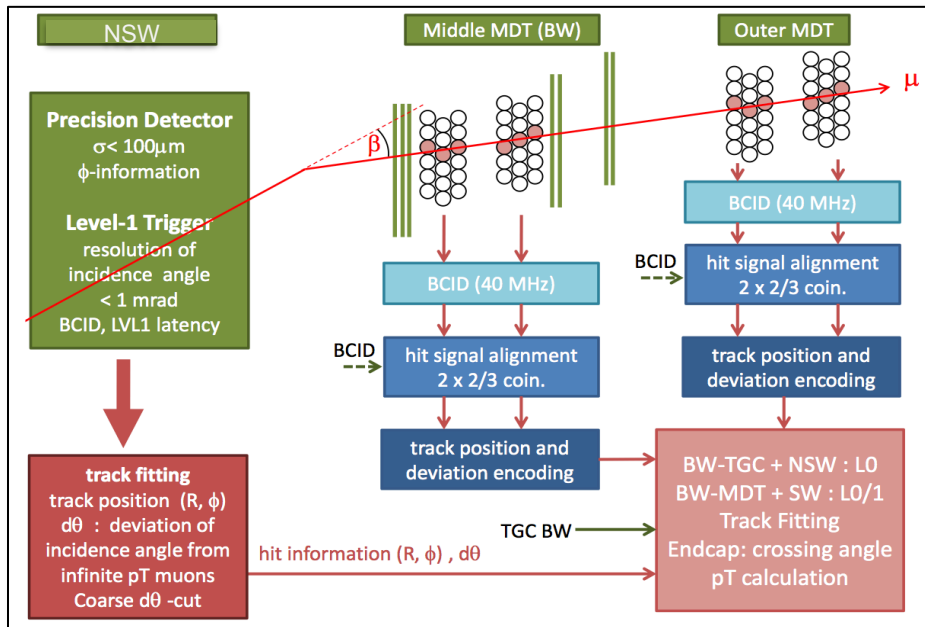
- **LAr Calorimeter**

- Replace FE and BE electronics
 - Aging, radiation limits
 - 40 MHz digitisation, inputs to L0/L1
 - Natural evolution of Phase-I trigger boards
- Replace HEC cold preamps if required
 - i.e. if significant degradation in performance
- Replace Forward calorimeter (FCal) if required
 - Install new sFCAL in cryostat or miniFCAL in front of cryostat if significant degradation in current FCAL

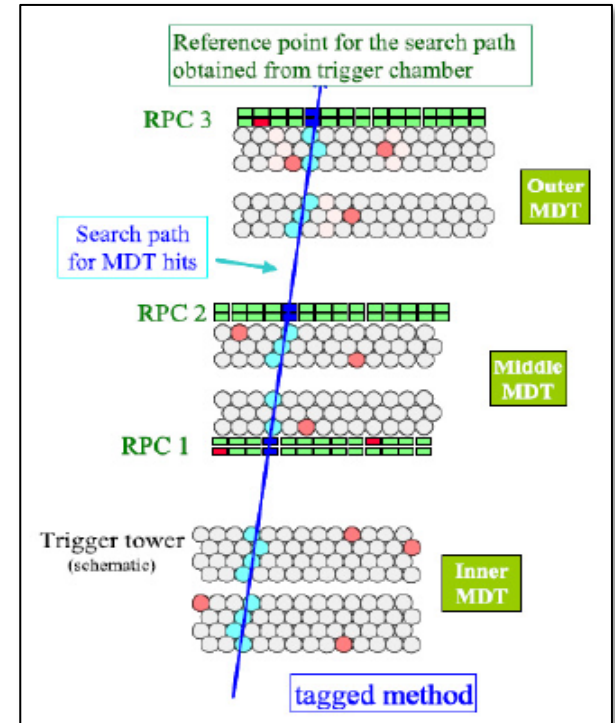


Muon system upgrade

- Upgrade FE electronics
 - accommodate L0/L1 scheme parameters
- Improve L1 p_T resolution
 - Use MDT information possibly seeded by trigger chambers ROIs (RPC/TGC)
 - Another option: add higher precision RPC layer at inner MDT station



Match angle measurement in end-cap MDTs to precision measurement in NSW

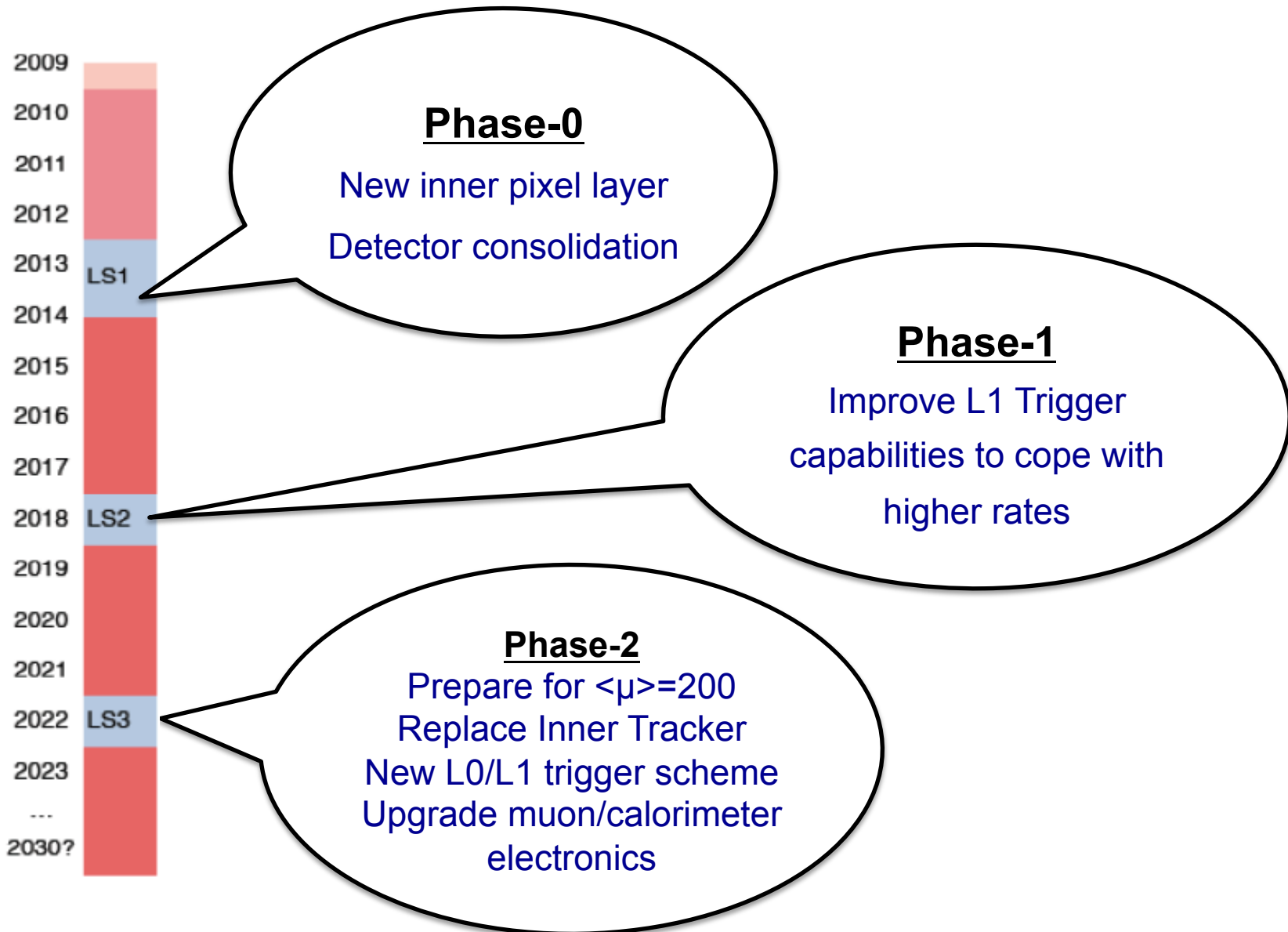


Role of high- p_T track used as a search road for MDT hits of the candidate track

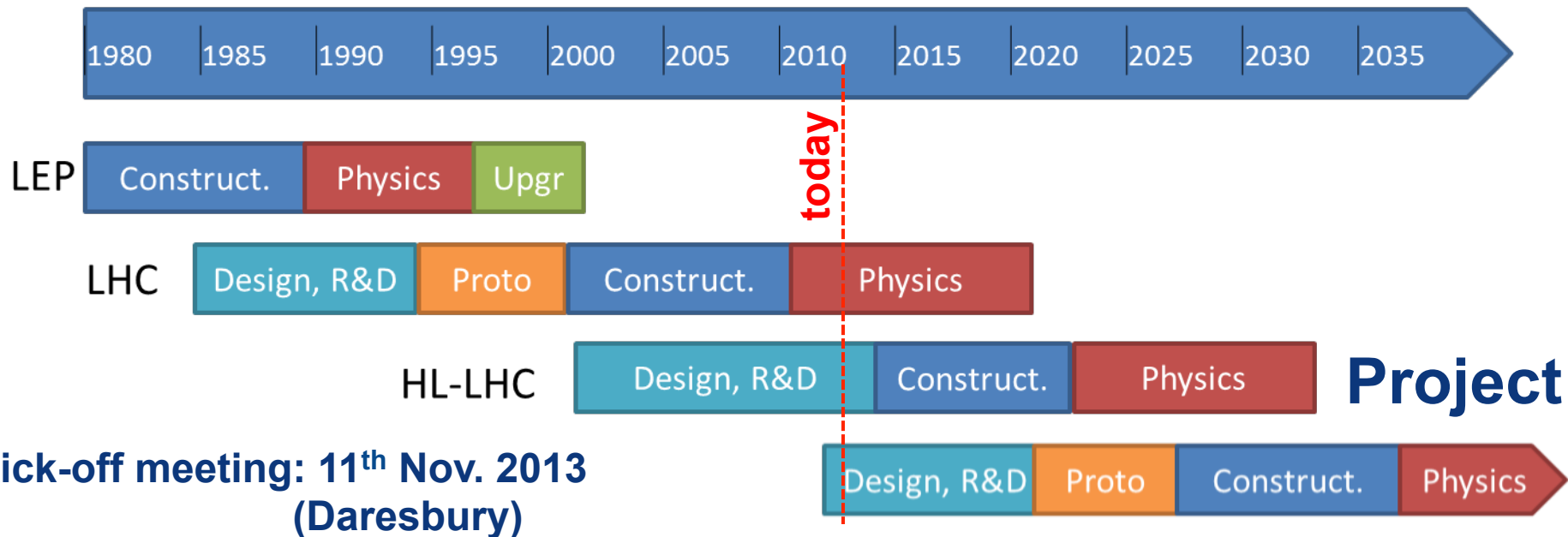


Combine track segments of several MDTs to give precise p_T estimate

Summary



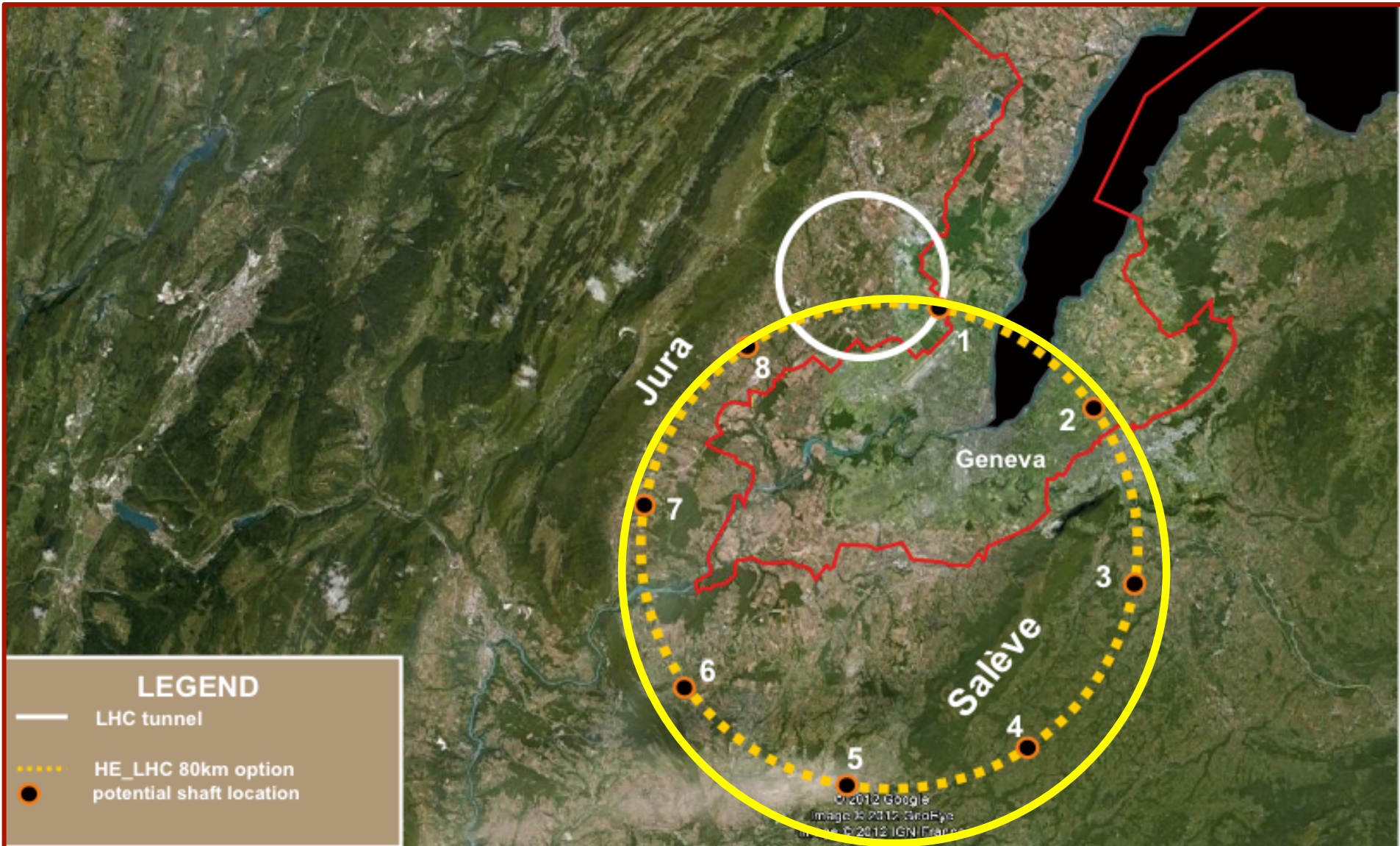
*“CERN should undertake design studies for accelerator projects in a global context, with emphasis on **proton-proton** and electron-positron **high-energy frontier machines**.”*



FCC Study : p-p towards 100 TeV
Kick-off meeting: mid-February 2014

FCC: Future Circular Colliders

Future Circular Colliders





UNIVERSITÉ
DE GENÈVE



Future Circular Colliders Study Kickoff Meeting



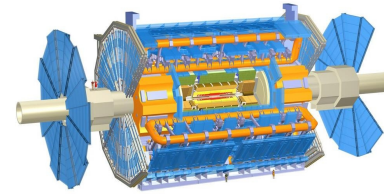
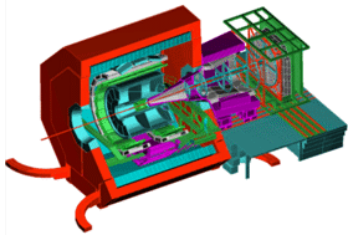
12-15 February 2014
University of Geneva,
Geneva

Europe/Zurich timezone

Webcast: Please note that this event will be available live via the Webcast Service.

Future Circular Collider Kickoff Meeting

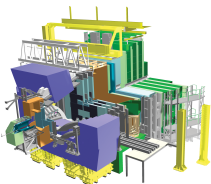
This meeting is the starting point of a five-year international design study called “Future Circular Colliders” (FCC) with emphasis on a hadron collider with a centre-of-mass energy of the order of 100 TeV in a new 80-100 km tunnel as a long-term goal. The design study includes a 90-400 GeV lepton collider, seen as a potential intermediate step. It also examines a lepton-hadron collider option. The international kick-off meeting for the FCC design study will be held at the University of Geneva, Unimail site, on 12–15 February 2014. The scope of this meeting will be to discuss the main study topics and to prepare the groundwork for the establishment of international collaborations and future studies. The formal part of the meeting will start at noon on Wednesday 12 February and last until noon on Friday 14 February. It will be followed by break-out sessions on the various parts of the project on the Friday afternoon, with summary sessions until noon on Saturday 15 February.



LHC → HL-LHC → FCC

Lot's of exciting stuff !

Thanks for your Attention



W. Riegler, CERN

